ABSTRACT

HAFIZ, FAEZA. Stochastic Optimization of Energy Management for Residential Systems with Distributed Energy Resources (Under the direction of Dr. Iqbal Husain and Dr. David Lubkeman).

This dissertation presents energy management and capacity sizing strategies for residential and community based distributed systems with PV-panel, energy storage, and plug-in electric vehicle (PEV). It also includes demand response (DR) along with the energy management of the PV- storage hybrid unit and PEV storages to help the grid for distribution service restoration (DSR) following a natural disaster.

For residential systems, PV panels and energy storage integration requires proper sizing for homeowners to get adequate economic benefits. In this research, a PV-panel and storage sizing method following deterministic energy management based on dynamic programming (DP) and net present value (NPV) has been developed. A method of load variance control is also considered to help the electricity service providers to avoid "duck-belly" curve type problems. As DP faces the 'curse of dimensionality' problem, dynamic programming successive algorithm (DPSA) is applied in this work.

Load and solar generation always deviate from the forecasted values in the real scenario. Uncertainty consideration and correlation between them need to be considered for energy management of the storage devices in the PV-storage hybrid unit and the PEV. In this research, multi-stage stochastic models are formulated with the objective of daily electricity purchase cost minimization including solar generation and load demand uncertainties. These models are solved with stochastic dual dynamic programming (SDDP). After consideration of standalone control of the PV-storage and PEV-storage units for a residential application, a novel coordinated energy management method is formulated in this work. For this method, both the load and solar generation

uncertainties and correlation between them are considered for optimal charge/discharge scheduling of PV-storage and PEV-storage to minimize the daily electricity purchase cost.

From the literature review, it has been found that a central storage is favorable instead of individual energy storage for a solar deployed community. However, the issues of location and the ownership of the central energy storage were not considered. In this work, a novel framework for central energy management of storages in a solar integrated community is proposed to avoid the issues. In this proposed framework, individual energy storages are controlled through a shared energy management (SEM) strategy where uncertainties of load and solar generation are considered.

With the energy management of the storage devices, DR is also included to improve the grid resiliency. In this research, DR is applied for DSR using the microgrid concept. With the help of three-step optimization method, the proposed framework helps the grid to restore power. This proposed method also helps to find out the optimal location for applying DR based control in a distribution system.

To implement the SDDP based optimal strategy in a real-time system, this research also focuses on an online based energy management algorithm for PV-storage hybrid unit control at the residential level. Deep learning method is used for load and solar forecasting with rolling horizon to reduce the variance. The forecasted values are applied to obtain the optimal decision from SDDP considering uncertainties after a certain interval. Utilizing this optimal decision, a rule-based method is developed to obtain the dynamic energy storage charge/discharge command.

Stochastic Optimization of Energy Management for Residential Systems
with Distributed Energy Resources

by
Faeza Hafiz

A dissertation submitted to the Graduate Faculty of
North Carolina State University
in partial fulfillment of the
requirements for the degree of
Doctor of Philosophy

Electrical Engineering

Raleigh, North Carolina
2019

APPROVED BY:

_____	_____
Dr. Iqbal Husain Co-Committee Chair	Dr. David Lubkeman Co-Committee Chair
_____	_____
Dr. Mesut Baran	Dr. Anderson Rodrigo DeQueiroz

DEDICATION

To: My Ammu, Selina Akhter.

BIOGRAPHY

Faeza Hafiz received her B.Sc. and M. Sc. Degrees from Bangladesh University of Engineering and Technology (BUET), Dhaka, Bangladesh in Electrical and Electronic Engineering in 2009 and 2013, respectively. She received her Ph.D. degree from the Department of Electrical and Computer Engineering at North Carolina State University in 2018.

She worked as an Assistant Engineer in Bangladesh Power Development Board from 2010-2013. She was a summer intern at National Renewable Energy Laboratory and research aide (technical) at Argonne National Laboratory during the year 2017 and 2018, respectively. Her current research interests are power system optimization, mathematical modeling, energy management of the hybrid system, smart grid resiliency, machine learning, and data analysis.

ACKNOWLEDGMENTS

My foremost and sincere gratitude goes to my advisor, Dr. Iqbal Husain. The guidance and encouragement from Dr. Husain helped me to overcome many difficulties during my years of research. I have learnt new things to improve my capability of conducting independent research.

I also like to thank my co-advisor, Dr. David Lubkeman. His critical remarks always helped me to enhance my professional skills.

I am thankful to my committee members, Dr. Mesut Baran, Dr. Joseph DeCarolis, and Dr. Anderson Rodrigo de Queiroz for their valuable time, comments and suggestions to improve my this research work.

I would like to acknowledge Dr. Chen Chen and Dr. Bo Chen from Argonne National Laboratory, and Dr. Poria Fajri from University of Nevada Reno for their technical suggestion.

I am grateful to my labmates MA Awal, Dhrubo Rahman, Sariful Islam, Landon Mackey, Kristen Booth, Rifat Kaiser Raachi, Siddhart Mehta, Hui Yu, Ashfanoor Kabir, Chandan Sikder, Ali Safayet, Moyeen-ul huq, and Mehnaz Akter Khan for their support and friendship along my path towards the degree. Special thanks to Karen Autry for always cheering us for research.

Finally, I would like to thank my parents Selina Akhter and Hafiz Ahmed Bhuiyan, my sisters Faeqa Hafiz and Fahmida Hafiz, and my husband Mirza Mohammad Monzure Elahi, for their continuous inspiration during all these years to chase my dream.

TABLE OF CONTENTS

LIST OF TABLES

LIST OF FIGURES

CHAPTER 1

PV Generation and Energy Storage in Power System

1.1. Solar Generation Deployment and Challenges to the Grid

There is an overarching effort around the world to integrate more renewable generation sources, such as hydro, solar, wind, geothermal, and wave energy resources, into the power system to meet the increased global demand for energy. Among these renewable resources, solar photovoltaic (PV) generation has gained much popularity due to the rapid cost reduction of PV panels, easier accessibility, and reduction of carbon emissions. Rapid cost-reduction of PV over the last decade has made utility-scale PV installations commercially viable and this trend is expected to continue in the long term. According to the Solar Energy Industry Association (SEIA), 2,227 MW rooftop solar was installed in 2017 in the U.S. Based on the research from the National Renewable Energy Laboratory (NREL), rooftop solar could produce almost 40% of our required electricity usage. Figure 1.1 presents the additional part of electricity sales that could be met with rooftop solar electricity. It illustrates that 26 states saw an increase of more than 10%, a further 16 states saw an increase of 0-10%. Estimates for just 4 states fell or remained the same [1]. The research report stated that there are over 8 billion square meters of suitable roofs in the USA. It is possible to generate about 1,400 TWh of electricity each year and two-thirds of this amount would come from small residential buildings. But excess generation on a distribution feeder from such installation has severe consequences for the existing infrastructure. The conventional distribution network and protection system are not capable of handling power flowing upstream from distributed generation resources. As the penetration level of such distributed generation sources grows, the conventional unidirectional distribution system is

expected to face quite a number of operational, structural and service challenges, which are elaborated in the following subsections.

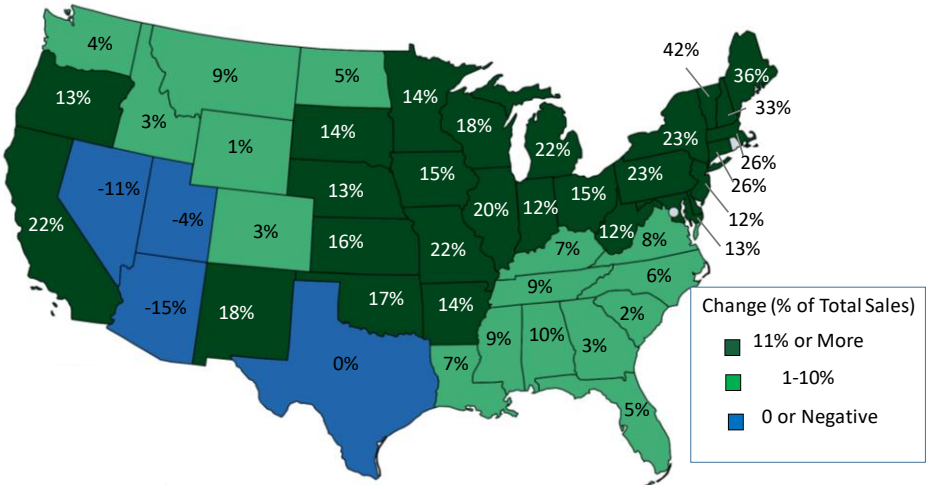

Figure 1.1. Potential change of rooftop solar from the year 2008 – 2016 [1].

1.1.1. Impacts on System Operation

(i) Voltage variability

For steady-state operation, typically voltage regulation at different points of the distribution network is achieved with the help of coordination among existing voltage regulators and by switching capacitor banks. However, PV output is directly impacted by solar irradiance. Due to changing weather conditions and variable cloud shadows, PV generation introduces huge variability in distribution feeders which consequently makes the task complex for voltage regulation [2], [3], [4].

(ii) Harmonics injection

To interface the DC output of PV to the AC grid, power electronic converters are used in current control mode. Typical solar inverters are switched at few kHz to tens of kHz which essentially injects a finite amount of switching harmonics into the grid. Moreover, these inverters

may also inject near-synchronous, e.g. 3rd or 5th , harmonics. In the worst case, they may lead to harmonic resonances at higher but sub-switching frequencies, i.e. up to a few kHz. These generated harmonics deteriorates power quality, reliability, and robustness of the system [5]. High level of harmonics injection may even disrupt the stable operation of the whole system [6].

(iii) Loss of system inertia

PV generation is non-dispatchable and it also does not provide inertial response to the grid like a conventional synchronous generator. Therefore, a higher level of PV penetration essentially implies a loss of system inertia. In [7], the impact of reduced inertia due to high PV penetration on the steady-state and transient stability of power system was addressed. The presence of solar PV generation also affects the wide-area behavior of a system, i.e. intra-area and inter-area modes of oscillation [8].

(iv) Phase imbalance

Most residential PV installations are interfaced with single phase [9]. Variability among the generation of different units as well as the imperfect distribution of such generation resources among different phases may lead to voltage imbalance among phases[10].

(v) Increased line loss

Distributed PV generation brings the source closer to the load, seemingly which should reduce the line losses. However, reverse power flowing upstream due to excess PV generation may offset the loss-reduction or even increase the loss [11].

1.1.2. Impacts on the Power System Structure

The introduction of large-scale photovoltaic power generation converts the distribution grid from traditional single-supply grid to multiport grid. It changes the direction of the fault current that can affect the feeder protection system. It may lead to malfunction of circuit breakers,

loss of selectivity of the fuse, change in the operating characteristics of relay protection, loss of ability to quickly restore transient faults of automatic recloser, and impact on the inverter or other equipments of the photovoltaic grid-connected system [12], [13].

1.1.3. Impacts on Services

(i) Introduction of "Duck-belly" curve

PV generation reaches its peak at midday, whereas total demand is the lowest at that time. As a result, electricity demand drops that constitutes the belly of the so-called "duck curve", e.g. CAISO duck curve shown in Figure 1.2. In the late afternoon, most working people head back home. A steep ramp-up in electricity demand starts then and extends till evening. Moreover, PV generation drops rapidly as the sun goes down. This opposite trend in generation and demand, makes the situation exceedingly difficult for the electricity service providers to maintain stability by increasing the power output of dispatchable generation sources at a very rapid rate [14]. Although curtailment of PV generation offers a relatively simple solution, the sub-optimal operation of PV fails to leverage the full potential of PV generation [15].

(ii) Impact on ramp-rate limited generation sources

Fast and frequent variation of PV output due to transient cloud shadows lead to uncertainties in supply and demand side, which pose new challenges for utilities and system operators. The presence of variable solar generation can cause coal or natural gas-fired plants to turn on and off more often or to change their output levels more frequently. This frequent change may lead to increased wear-and-tear of the units and decrease in efficiency, particularly from thermal stresses on equipment [16].

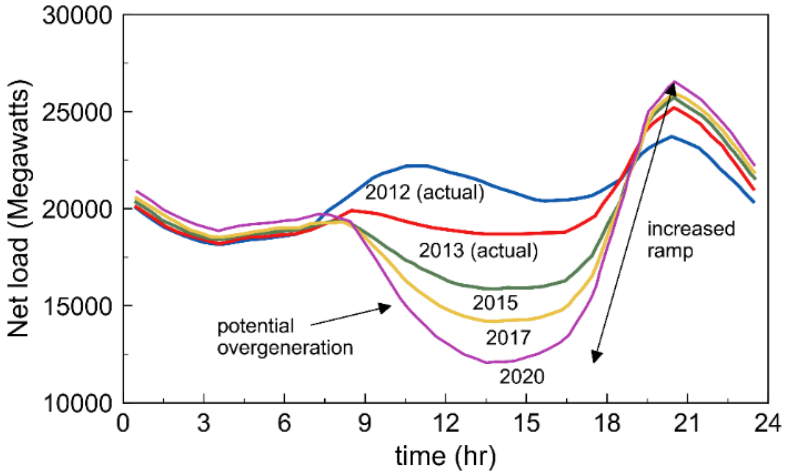

Figure 1.2. CAISO Duck-Curve [14].

1.2. Storage Deployment: A friend to the Smart Grid

The issues discussed earlier starts to arise if PV penetration level scaled up above a specific level. To avoid these issues, restricting new PV installation and curtailment of PV generation from installed units are probable solution. If the penetration level of PV rises above certain level, curtailment of PV generation becomes mandatory for the utility companies to maintain grid reliability and supply-demand balance [17]. This curtailment reduces the acceptance and popularity of PV installation. Therefore, raising PV penetration level without generation-curtailment as well as without compromising reliable grid operation necessitates energy storage technology to play a grid-friendly role.

Recent deployment of energy storage in power system has drawn a lot of attention due to the introduction of distributed energy resources in the system. Rapid reduction of production costs of lithium-ion battery technology leads to the increased utilization of storage which is shown in Figure 1.3 (a) based on the battery surveys by Bloomberg new energy finance [18]. According to Navigant Research, the expectation of residential and community storage deployment will reach 14,000 MW within the year of 2024 in U.S.A, which is shown in Figure 1.3 (b). Energy storages

are considered to be integrated at the generation, transmission, distribution, and residential levels, shown in Figure 1.3 (c), to address different problems. The application of energy storage to solve different problems at the three different levels of the power system are discussed below.

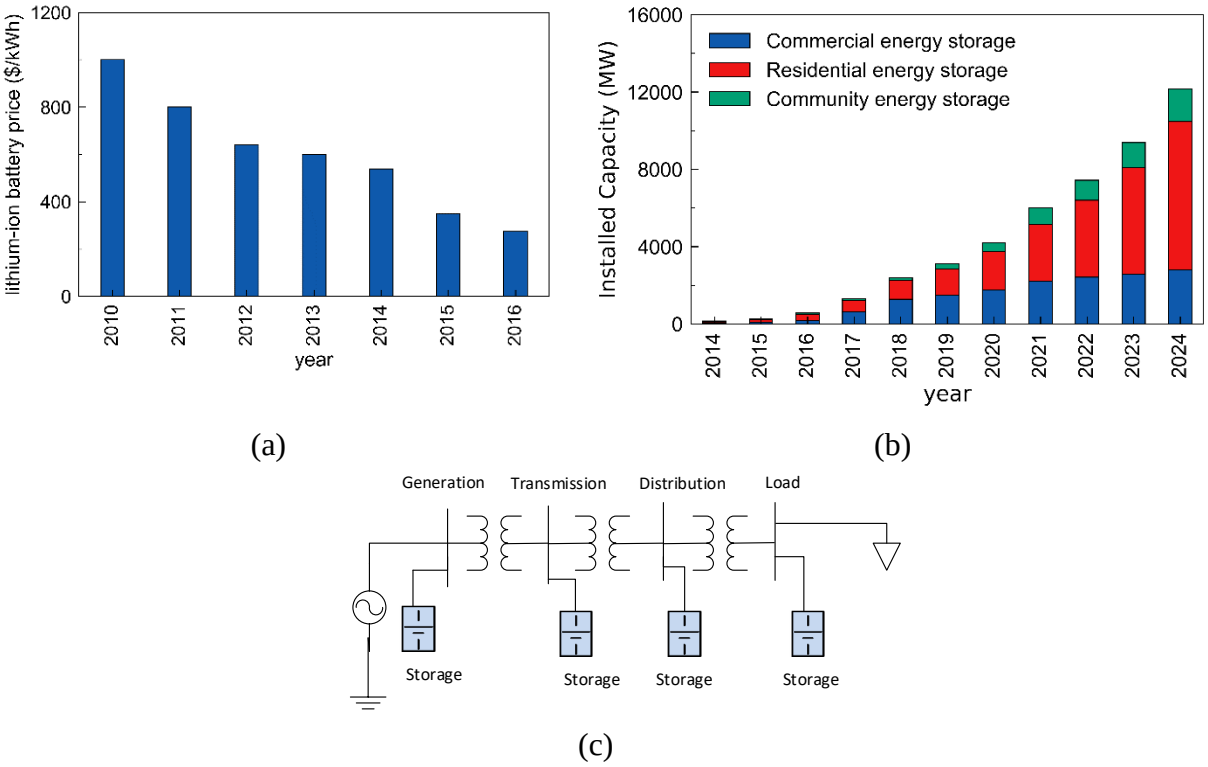

Figure 1.3. (a) Decrease of storage production cost [18], (b) storage deployment in different levels of power system, and (c) Predicted Energy storage growth in U.S.A in different levels (*source: Navigant Research*).

(i) Generation Level

- To integrate renewable energy based power plant into the system, storage plays a significant role. Since most renewable energy resources are non-dispatchable, energy storage can help to maintain grid transient stability by providing the required amount of power and absorbing excess generated power [19].
- Base-load generation plants in a system are required to provide fixed outputs. If they fail to provide these fixed outputs, then standby generators need to fire up to maintain the

balance of the grid. However, storage systems based on battery offer a higher ramp-rate which can improve the frequency regulation during transients and black-start [20], [21].

- Hourly charge/discharge schedule of the battery can resolve unit commitment problem for short-term [22], [23].
- To stabilize the electricity market price, energy storage can help utility companies by maintaining optimal operation point and reduce the usage of fossil fuel-based power plants [24].
- Energy storage reduces the need for peak generation for the sudden ramp of "duck-curve". It can help to avoid the unnecessary cost burdens to the utility companies [25] and improve ancillary services by reducing penalties to the generation companies [26].

(ii) Transmission and Distribution Level

- Instead of upgrading the overall power transmission and distribution system to accommodate more distributed energy resources, energy storage deployment can benefit utilities or independent system operators to reduce electricity delivery-related cost [27].
- Voltage violation due to the integration of renewable energy in power grids can be regulated with the help of energy storage [28].
- Inclusion of an energy storage system can be a solution for providing inertial response and primary frequency regulation for large-scale integration of renewable energy sources in power system [29].
- Congestion in transmission systems occurs when the demand for transmission capacity exceeds the transmission network capability. Congested transmission lines may lead to a violation of network security limits. To avoid transmission system congestion, energy storage might be a helpful solution based on [30].

(iii) Community and Household Level

- At the load level, storage can be used to provide backup if the grid connection is lost.
- Energy storage can reduce the costs of electricity bill for the customer by using the stored energy during peak hours and absorbing the energy during off-peak hours [31].
- Energy storage allows a market-driven electricity dispatch, fostering prosumers to secure their benefits and creates a cost-sharing scheme in the power system [32], [33].
- Community storage can be used in the microgrid for load smoothing and peak shaving [34], [35], [36].

1.3. Existing Solutions for Optimal Control and Sizing of Storage

For optimal control and storage sizing, a comprehensive literature review of the current research on energy storage gives us motivation and guidelines for research on energy storage integration into the power system. The existing optimal control and sizing methods can be divided into three major methods, which are discussed in the following subsections.

1.3.1. Analytical Methods

The analytical methods were based on historical load and solar demand curves or on statistical data analysis [35], [37], [38]. It was used generally for the determination of the optimal size of the energy storage in order to balance between load and renewable energy generation [39], [40]. This method did not consider any constraint. In [41], the authors considered that charging power for energy storage is the difference between PV output and load. Energy storage discharge is commanded to cover the consumption when the PV production is not available for the islanded grid. In a subsequent step, to store the difference between PV output and load, optimal energy storage capacity was calculated. In [42], the size of energy storage for backup supply was

determined based on the outage duration statistics and targeted reliability level. For the chosen level of peak shaving, energy storage size was obtained from real load data in [43].

1.3.2. Quantitative Methods

Quantitative methods emphasize objective measurement through mathematical formulation of a problem and using computational techniques. The quantitative methods applied in the existing literature are discussed below.

(i) Linear Programming (LP)

In [44], sequential Monte Carlo simulation was used to create reliable data and then LP was considered for distributed generation and energy storage dispatch to determine feasible power flow. To improve unit commitment problem for an isolated system with additional pumped storage and system dynamics constraints, the authors in [45] used LP methods. Mixed integer LP (MILP) was used to solve PV panel and storage sizing problem in [46]. Simulation time was divided into two off-peak and peak periods in [47]. During the off-peak period, storage was stated as load and it releases available energy during peak hour. For a distribution system including PV generation, storage size was optimized based on LP to keep voltage constraints within predefined limits in [48]. The main disadvantage of this method is the need for problem linearization, which may cause the loss of some problem characteristics. Additionally, this method requires the use of a specific mathematical solver.

(ii) Convex Optimization

System cost minimization based on convex optimization approaches have been reported in the literature for smart grid residential users equipped with local solar PV power generation and energy storages [49], [50]. The authors did not consider the uncertainty in PV generation. Mixed integer second-order cone programming (SOCP) formulation was used to solve multi-objective

optimization in [50], where energy storage investment cost and weighted operational costs were minimized. The results suggested that for a distribution system with highly distributed energy resources, network operation could be controlled with the placement of a few optimally sized energy storages. The disadvantage of this method is that it is only applicable to nonlinear objective functions.

(iii) Dynamic Programming (DP):

Dynamic programming was applied to maximize fuel-cost savings and benefits due to energy pricing differences between peak and off-peak periods. In [51], [52] and [53], this method was considered for optimal storage capacity sizing and charge-discharge pattern control. The advantage of DP is that it is applicable to all of the optimization problems (LP and Convex problems) and ensures global optimality. The main drawback of DP is the need to discretize the system states into steps.

(iv) Stochastic Programming (SP)

A SP method that minimizes energy storage investment and network operational cost, has been reported in [54]. The algorithm solves DC lossless optimal power flow (OPF) to determine energy storage size, location, and optimal dispatch. For stochastic cases, the discretization of the state space and the different stochastic scenario representations contribute to the 'curse of dimensionality' [55], [56] and to the intractability of real-sized models.

(v) Approximate Dynamic Programming (ADP)

ADP is a broad umbrella of modeling and algorithmic strategies to solve problems which are large, complex and stochastic. It is most often presented as a method for overcoming the classic 'curse of dimensionality' in Stochastic Dynamic Programming (SDP) problem. To minimize the

cost of electricity purchase, ADP is utilized in [57] and [58]. The main disadvantages of these methods are the high data storage requirement and computation time to calculate the optimal path.

1.3.3. Heuristic Methods

Heuristic methods are considered for nonlinear objective functions or constraints. They are applied to the optimization problems where quantifying the solution could be difficult. These methods require long computation time because they need to run the program for numerous iterations until the optimal solution is achieved. Different types of heuristic methods were used in literature for optimal sizing of storage, which are discussed below.

Genetic Algorithm (GA): GA and sequential quadratic programming (SQP) were used in [59] to find the optimal size and location of distributed generators, energy storages, and capacitors in a distribution system considering reactive energy market. GA was used for optimal size and location of units and OPF was solved with SQP to determine optimal dispatch.

Particle swarm optimization (PSO): PSO based simulation was applied to determine optimal capacity of wind generators and battery in a smart household in [60]. Fuzzy based PSO was used in [61] to minimize energy storage cost, power loss, and electricity procurement cost in a distribution system.

1.4. PV Generation and Energy Storage at Residential Level

Above discussed methods were employed for different levels of the power system. One of the primary concerns of this research is to consider energy management of storage at residential level. From the literature review, it is found out that different controlling methods of energy storage for different objectives in residential level were considered [62], [63]. The control of PV-panel and storage were discussed in [56] where the probabilistic method was applied based on the historical data of load to minimize the back feeding of energy. For this work, a rule-based control

strategy is applied and stochastic nature of solar or demand is not considered. In [50], a near-optimal storage control algorithm was developed by solving a convex optimization problem at the beginning of each day to control the PV-storage hybrid unit. Reinforcement learning technique was used then to determine the amount of residue energy in the energy storage module at the end of each day in a billing period. This method requires a huge memory and computation resource to go through the algorithm. To prevent overvoltage issue, active power curtailment of roof-top grid-connected PV was considered in [17] where no storage deployment was considered. None of these works considered to control the energy storage for load variance or to reduce the electricity purchase cost daily for optimal sizing problem of PV-panel and storage considering the impact of changeable parameters like the cost of storage and *ToU* rate.

1.5. Plug-in Electric Vehicle (PEV): Introduction to a New Source of Storage

Similar to the PV, the impact of PEV loads on the existing power grids have drawn a lot of attention recently due to its low carbon emission criteria [64]. The statistics based on Navigant research, which is depicted in Figure 1.4, shows that the popularity of PEV in the USA is increasing day by day. Based on [65], uncoordinated PEV charging in residential level will significantly increase the peak load that will affect the electricity distribution structure. The aggregated PEV charging load curve in residential level for level 1 and level 2 charging [66], is expected to be like Figure 1.5. Thus, the increase in this new storage in the power system can be taken advantage of to have a positive impact on the power system.

PEVs have bidirectional power converters which allow them not only to act as load but also as generators. Therefore, the vehicle-to-grid (V2G) power flow option can be used to help improve the efficiency and reliability of the grid [67], [68]. It aids to reduce the overall cost of energy usage and carbon emissions [69]. However, to achieve these goals, the charging/discharging strategy of

the PEVs needs to be optimally controlled. The uncoordinated charging on distribution networks may cause unnecessary power losses, voltage deviation, and load variance. Coordinated charging strategies can help to mitigate these negative impacts [70], [71]. In [72], estimation of the distributed algorithm (EDA) is applied to maintain voltage constraint in the grid and lower the cost of charging of large scale of PEV in the parking deck. Other works also have considered the energy management of PEVs to control fuel consumption [73] and cost-effective charging strategy in charging station [74] which is based on PSO and DP.

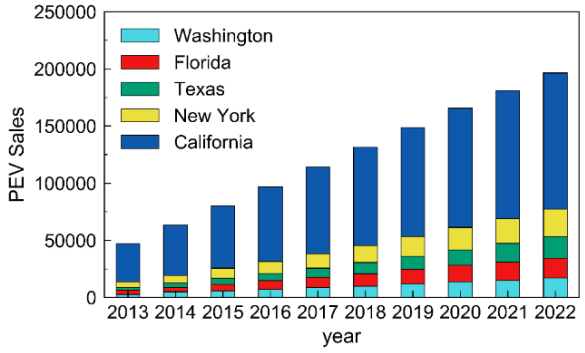

Figure 1.4. Annual global EV sales in U.S.A. *(Source: Navigant Research).*

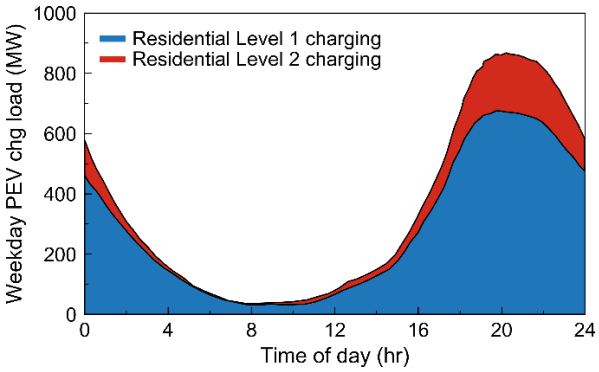

Figure 1.5. Expected aggregated electricity load for PEV in a typical weekday in California by the year 2025 [66].

PEVs are also used to solve some issues that occur due to the penetration of renewable energy resources. To mitigate the voltage rise in a distribution network with a high penetration level of PV resources due to the reverse power flow and to compensate the voltage drop resulting from the peak load, a combined method using the battery energy management of PEVs and the active power curtailment of PV arrays is proposed in [75]. An optimization model for determining the optimal mix of solar-based distributed generation and storage units, and optimal charging prices for PEVs without violating power system constraints is presented in [76]. These works did not consider the uncertainty of PV generation and load profiles that occur due to changes in weather and owners'

usage [77]. In [78], the non-Gaussian uncertainty of wind power and PEV uncertainty are considered and a hierarchical stochastic control scheme for the coordination of PEV charging and wind power in a microgrid is presented to achieve the power balance between supply and demand in the microgrid. Majority of these existing research and solutions are based on distributed networks. Most of them require large communication system for coordination and huge computational resources. However, if a coordination in a smart household system is maintained through a simple and decentralized local control, then many of these issues can be resolved.

1.5.1. PEV at Residential Level

In [79], the control of PEV and home energy scheduling was considered jointly to minimize the electricity cost considering users comfort preferences. In this work, the problem is simplified to solve through LP method. The uncertainty in load demand is handled with model predictive control (MPC) over time horizon. In [80], optimal charging strategy for a household with two PEVs was developed to reduce load variance in a household. In [81], the optimization-based scheme was defined to manage household load outages in the presence of PEV. In [82], charging the storage through DP is applied to reduce the electricity purchase cost. In this work, vehicle to grid electricity flow was developed considering the impact of the lifetime of PEV storage. None of these works showed the charging/discharging schedule of PEV considering load demand uncertainties.

1.5.2. Coordinated Control of PV-Storage Hybrid Unit and PEV-Storage

Based on [83], PV-based storage and PEV deployed household are expected to increase within the next decade. Both types of storage devices can be utilized using a coordinated control algorithm at the residential level. The coordinated control of the two storage devices can be used to provide benefits to the customer giving them independence. From customers' perspective, when

these two storages are used in a household, they can be coordinated optimally to enhance the proper utilization of the system resources. But to properly control the storage devices based on *ToU* rates, the PV generation and the household electricity demand are required to be known beforehand. In [84], PEV control to utilize solar generation in residential level was proposed to reduce electricity purchase cost. But PEV might not be present in the day-time during solar generation. Thus, energy storage is required to utilize solar generation. In [85], coordinated control of PEV and PV-panel energy storage was considered to reduce electricity purchase cost, load shift, and peak shaving. These works did not consider the uncertainties of PV generation and load profile which is discussed in [77]. These uncertainties occur due to changes in weather and owners' usage patterns. In [86], uncertainty of PEV mobility was included to utilize generated solar energy to reduce electricity purchase. In [87], variability of renewable generation and load demand were considered to minimize the operation cost for large-scale energy scheduling problem. This research was conducted to control PEV fleet. But it requires an extensive and effective communication system to implement. There are also privacy and preference concerns of owners. In [88], it was shown that both the load demand and solar generation change due to the variation of weather and they are correlated with each other. Thus, it is necessary to consider the stochasticity of PV generation and electricity demand and the correlation between them in order to have a better formulation of the problem. The coordination between the PV based storage and PEV storage is also necessary if both of them are present in household to improve the solar generation usage and reduce the electricity purchase cost. These two storages are preferred to be controlled from residential level where there is no issue like privacy and preference violation or effective communication system.

1.6. Energy Sharing in a Community

Energy sharing at the community level has also gained attention recently. The significance of community storage in microgrid for load smoothing and peak shaving based on model predictive control for *ToU* rate and hourly basis with the help of community storage was discussed in [34]. A two-level hierarchical optimization method for microgrid community to minimize operational costs in a smart grid environment was proposed in [89] based on deterministic load and renewable generation. A modified auction based joint energy storage ownership scheme was suggested for a number of residential units to determine the fraction of their energy storage capacity that they want to share with the community in order to assist them in storing electricity considering the auction price [90] for short period of time. A dynamic non-cooperative repeated game with Pareto efficient pure strategies was adopted in [91] considering a decentralized approach to determine optimal energy trading amounts for the next day among the users who allowed to utilize their surplus energy from their owned PV generation with the grid and the community energy storage device. To overcome the shortcoming of an unbalanced allocation of one-phase photovoltaic (PV) units, a dynamic mitigation approach using community energy storage was proposed in [92]. A charge/discharge control strategy was developed that will continuously balance and dynamically adjust the power exchange with the grid in real time, and mitigate the neutral current and neutral voltage rise. In [93], an online algorithm based on the Lyapunov optimization was proposed for energy sharing among residents in a cooperative community by exploiting the dynamics of electricity price, and then the charging and discharging behaviors of energy storages are determined. A revenue division algorithm based on the Nash bargaining theory was also performed to fairly share the revenue among residents. In [94], capacity allocation from a central storage was considered for some time interval based on the aggregator-defined price. These studies did not

consider the energy storage sizing of the community storage which was obtained in [95]. In [96], a central community energy storage sizing method was proposed to help the distribution system operators to maintain distribution network's reliability and flexibility. In [97], the remaining power curve associated with the local generation and the uncertainties related to PV output and load consumption was considered to get rid of overvoltage problem. But these works did not include the uncertainty on PV generation and load demand and the comparison between the individual and community-owned storage. To optimally size the storage device taking into account the uncertainty introduced by wind power forecast errors, a two-stage stochastic programming was employed in [98], [99]. The uncertainty on renewable generation was considered in these works, but demand uncertainty was not considered. All of these methods considered centralized community storage for which we need to accommodate someplace. There is also a question about the ownership of the storage. The consideration of sharing storages of the houses in a community can resolve this issue. The impact on the sizing for shared storage case on the residential level is also an important factor to consider.

1.7. Demand Response: A Potential Option for Distribution Service Restoration

Demand response (DR) program in residential systems is considered as another potential option for grid modernization now-a-days. In DR, sensors can perceive peak load and utilize automatic switches to reduce the possibility of overload and power failure as shown in Figure 1.6. Advanced metering infrastructure expands the range of time-rate and direct load control (DLC) based DR program. Smart home energy management (HEM) can also make it easier for consumers to alter their behavior and reduce peak period consumption by controlling the smart appliances such as PV-storage hybrid unit, PEVs, air conditioners, washer-dryers etc. Generally, DR is utilized to

save costs for electricity service providers through reductions in peak demand and the ability to defer construction of new power plants and power delivery systems.

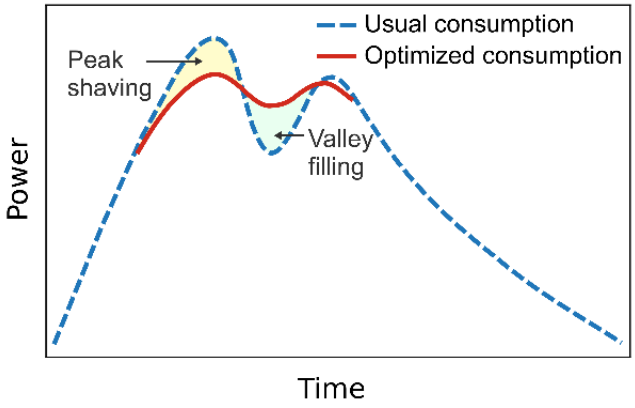

Figure 1.6. Peak shaving and valley filling through DR.

DR can serve various objectives which were reported in [100]. An intelligent DR based residential load management system was proposed in [101] for consumers to attain a reduction in electricity bill and maintain the total load under maximum demand limit by scheduling controllable appliances. A price-based DR of aggregated thermostatically controlled load for load frequency control was suggested in [102]. In [103] and [104], DR and battery storage coordination for load smoothing service and reduction of electricity purchase based on time of use rate were considered, respectively. Similarly, social welfare maximization problem was considered in [105] by dynamic coordination between economic dispatch and DR considering the battery energy storage systems and renewable energy resources. Dynamic energy balancing cost model to handle unit commitment and DR were presented in [106]. DLC and load shedding were proposed to minimize the power outage in sudden grid load changes to reduce the peak-to-average load ratio [107]. These works did not consider the integration of distribution grid topology with DR which were proposed in [108] and [109]. In [110], a framework was proposed to use DR to provide capacity release in distribution

system for reliability and risk implications. But none of these works considered to include DR with PV- storage hybrid unit and PEV control to improve the grid resiliency during natural disasters.

Grid resiliency is an essential feature for future smart distribution systems [111]. Many methods have been proposed to improve the resilience metrics by reconfiguration of the power system, and improvement of preparation for distribution service restoration (DSR). In the literature, most of the studies considered to maximize load pickup, minimize outage duration, and minimize number of operations for switches. Some literature suggested to utilize synchrophasors [112], network reconfiguration [113], [110], inclusion of distributed energy storages [114], control of synchronous machine modes [115], load curtailment [116] and using emergency mobile generators [117] during restoration to serve these purposes. Microgrids formation by leveraging distributed generators (DG) during restoration process are also considered in several works [118], [119], [120]. In [121], a multi-time step model that can generate switching sequences for switches is introduced. However, these existing works in the literature did not consider the contribution of demand response (DR) to facilitate the restoration procedure.

1.8. Real-time Energy Management in Hybrid Residential System

To develop an effective and realistic way of PV-storage hybrid unit management, load and solar generation need to be forecasted as precisely as possible. Effective scheduling of storage will be possible with precise forecast [122]. Over or underestimation of load and solar generation can cause wrong optimization strategy [123]. In recent year, load and solar generation forecast area is focused on utilization of neural networks. Several machine learning algorithms such as Support Vector Machine (SVM) [124], Decision Trees [125], Artificial Neural Network (ANN) was used by the researchers for electricity demand forecasting. Neural network based tools suffer from various issues like slow learning rate, over-fitting, deciding optimal hyper-parameters value etc.

To get rid of these problems deep learning based hybrid model to forecast electricity demand were proposed in [126] and [127]. In [127], the load profiles were clustered through K-means algorithm based on seasons. It did not consider the impact of holidays and weekdays that changes the load pattern. It is very important for us to consider these features for effective energy management. On the other hand, different appliance patterns were considered as features in [126] which requires high memory and a lot of time for calculation.

For real-time storage management design, some works considered the uncertainties of the solar generation and formulated the problem with as a Markov Decision Process (MDP) and solved it by DP [49]. Chance-constrained stochastic optimization was proposed to improve economic gain for a PV-based power plant in [128]. But most of the works have not considered load and solar generation uncertainties together which are considered in [129]. Though in [129], the correlation between the uncertain parameters was not considered which is important according to [130]. For real-time storage control, Lyapunov optimization technique was employed in [131], [132]. These works relied on asymptotic analysis (i.e., infinite time horizon), whereas our problem is based on the finite setting algorithm for a day. In [133], an online algorithm was proposed considering the finite horizon, but it did not consider the expected future costs. Expected future costs are important to reduce electricity consumption cost at finite receding horizon to obtain the optimal strategy, which was mentioned in [128]. In [134] and [135], real-time energy management problem for a system with two cooperative microgrids and a single microgrid system were considered to minimize total energy cost. In these works, the forecasted profiles were considered as fixed value during optimization which is not realistic. In [87], a two-stage stochastic model was considered which was solved through Benders' decomposition method. But to deploy this method in real-time

control strategy directly, challenges like available solar energy remain unused or unnecessary discharge of energy storage can be faced.

1.9. Research Motivation and Proposed Solutions

Based on the above-discussed limitations, the following research objectives are focused in this dissertation:

From the owner's point of view, minimizing the cost of the overall system is the most important objective. Most of the works emphasized only on the sizing of the storage. But the optimal size of the storage-panel combination based on the household demand can optimize the overall system. For designing the storage-panel combination, DP based control strategy for a smart house that includes solar energy generation with storage is proposed in this dissertation. DP is used to achieve maximum savings in terms of electricity purchased from the grid by controlling the storage with different combinations of PV panel sizes and storage capacities. This control strategy is applied to load profiles of different seasons considering a different time of use (*ToU)* rate structures. The DP based results are then used to calculate net present value (NPV) and determine the optimal PV panel size and storage capacity combination while considering the investment cost for corresponding panel and storage [136]. NPV with respect to the lifetime of PV panel and storage is utilized in this research to calculate the optimal size of a PV-storage hybrid system [137].

From electricity service provider's point of view, load regulation is an important parameter to get rid of the 'duck-belly curve'. Rather than considering the complex centralized control from utility companies which requires obtaining the information of load demand from the overall system for each time period, PV panel-storage and PEV can be coordinated to balance the household load locally. As DP faces 'curse of dimensionality' problem, dynamic programming successive

algorithm (DPSA) for load regulation of a smart household including PV panel with storage and PEV is applied for this multi-dimensional problem [138].

In the real world, PV generation and load demand cannot be exactly same as the forecasted value due to the variation in weather and users' preferences. Thus, a control strategy is established for a smart house that includes PV – storage hybrid unit to minimize the electricity purchase cost from the grid while considering the uncertainty in solar PV production [139]. In this control strategy, stochastic dual dynamic programming (SDDP) algorithm applied is applied in the context of stochastic PV generation. Since SDDP does not require a discretization of the state and decision spaces, it solves the challenge of 'curse of dimensionality' in SDP. SDDP constructs a piecewise linear approximation of the future cost function using Benders' cuts that do not require the algorithm to discretize the state and decision spaces. As a result, it requires less computation time and memory [140]. Similar to the PV uncertainty, SDDP algorithm is applied to create a control strategy for charging/discharging profile of the PEV storage considering electricity demand uncertainty for minimizing the household daily electricity purchase costs [141]. In [142], it is shown that both the load demand and solar generation change due to the variation of weather and they are correlated with each other. Thus, it is necessary to consider the stochasticity of PV generation and electricity demand and the correlation between them in order to have a better representation of the problem. Also, coordination between the PV based storage and PEV storage is analyzed in this dissertation rather than controlling them individually in a smart home [143].

Energy storage devices may not always be the economical solution for individual households due to their current cost. However, shared utilization of energy storage may present a robust alternative that can potentially add substantial benefits to the community as a whole. Shared energy management (SEM) not only brings economic benefits to the users but also helps to

improve peak shavings and PV usage compared to a system with individual PV/storage devices. Thus, on the next stage of this work, the benefits of SEM considering the uncertainties both on load demand and PV generation are analyzed. NPVs are also evaluated for energy storage capacity sizing for each house in a community [144].

Through DR program, smart appliances like PV – storage hybrid unit, PEV, air conditioners, washer-dryers can be controlled. In this dissertation, DR is considered to restore loads on the unbalanced distribution feeders using multi-time step dynamic optimization model and utilization of microgrid concept with the presence of DGs after a major disaster. Since generation resources can be limited after a major disaster, DR can play an important role to increase the number of customers served, and/or an increase in the total amount of load restored. An integrated optimization framework to coordinate individual operation of flexible residential appliances and the DSR process is presented in this dissertation. Operational optimization models for residential DR and distribution grid restoration considering the interdependent and intertemporal coupling between DR and DSR is developed [145]. The effectiveness of the proposed method is also conducted in this research.

To utilize the SDDP based control algorithm for real-time energy management, an integrated framework is proposed in this dissertation. This proposed integrated system considers load and solar forecast in rolling horizon through deep learning to reduce the variability consideration and computational complexity for stochastic optimization process. Receding horizon based stochastic optimization is performed utilizing these forecasts. An optimal decision from performed SDDP is then exploited through a rule-based control algorithm. It helps to obtain the optimization strategy in realistic manner [146]. The real-time rule-based control is less

complex to achieve in practical implementation. This method ensures proper usage of solar energy and reduces back-feeding power to the grid.

1.10. Dissertation Outline

In Chapter 2, control of PV -storage hybrid unit is presented using DP algorithm with the aim of minimizing the overall cost of daily household load demand. Then the net present value (NPV) is calculated and used for optimal PV-panel and storage sizing while taking into account the household load at different seasons and *ToU* rate of electricity price. Load leveling of a residential household by means of coordinated control between solar PV system storage and vehicle battery storage is also discussed in this chapter. DPSA is explained to obtain the optimal charging strategies by minimizing the overall load variance of the daily household load demand.

Chapter 3 is divided into four parts. In the first part, problem formulation for energy management of PV panel and storage device is presented considering the stochastic nature of PV generation. The SDDP algorithm is demonstrated for stochastic optimization. Optimal charge/discharge scheduling of PEV is described to minimize the electricity purchase cost of the owner in the second part of the chapter. A multi-stage stochastic optimization model is developed for scheduling to improve on this decision-making process under demand uncertainty. After that, problem formulation of the coordinated control between the PV-storage hybrid unit and PEV for a hybrid household considering load demand and PV generation uncertainties is stated. Finally, benefits of SEM for a community is analyzed. SDDP algorithm to minimize the combined community electricity purchase cost is applied by representing the problem in a multi-stage stochastic optimization approach. The net present value (NPV) calculation is also presented to obtain the optimal capacity sizing of the storage.

Chapter 4 demonstrates that service restoration can be significantly improved by leveraging the flexibility provided by the inclusion of DR. A framework is illustrated by considering integrated control of household level flexible appliances so that the load demand at the distribution grid can be varied to improve the service restoration process. The overall framework of the proposed system is described as a three-step method considering three optimization problems: 1) To calculate feasible controllable range of aggregated load of each bus, 2) to determine candidate buses to perform DR and target load demand, and 3) to maintain the load level in each house through HEM during the restoration process considering uncertainties in load and solar generation sequentially. The optimization problems are formulated as linear programming, mixed-integer linear programming, and SDDP models, which are presented in this chapter.

In Chapter 5, an integrated architecture is presented where day-ahead load and solar generation forecasting is performed in rolling horizon to predict the day-a-head load demand and solar generation, then to use these forecasted profiles to optimize the electricity purchase cost per day through SDDP in receding horizon and to use the solution with rule-based control to implement a realistic control for household system composed of a PV – storage hybrid unit.

CHAPTER 2

Deterministic Model Based Energy Management Method at Residential Level

2.1. Introduction

Residential consumers are integrating solar generation as a source of clean energy with the goal of reducing their monthly energy cost while maximizing their investment return. As a result, PV energy is emerging as one of the most effective alternative energy options in a smart household. However, an important aspect of solar power generation is that it does not necessarily align with the household load demand. In other words, the generated peak PV power cannot be consumed by the customer effectively during the daytime and the evening peak load demand cannot be solely met by the solar resources since solar generation is reduced during this time. To overcome this, energy storage can be added in a hybrid unit to maximize solar power usage. Adding the battery storage option can potentially reduce the household electricity purchase cost from the grid, and in addition, preserve the value of solar PV installations in an evolving policy and regulatory environment. But storage and PV panel comes at a premium cost. Similarly, *ToU* rates offered by different utility companies are also needed to be analyzed. An optimal control strategy based on *ToU* rate will impact on savings on electricity purchase that helps us to determine whether it is profitable to invest in particular panel-storage size combination or not. In the first part of this chapter, a deterministic model-based method for energy management and finding a suitable combination of the battery storage with the PV generation to gain optimal benefit from the overall system are analyzed.

On the second part of this chapter, a deterministic model based energy management method for load regulation in residential level is discussed. Inclusion of PEV is considered along with the PV -storage hybrid unit in a smart residence. To avoid the problem like ‘duck-belly curve’,

curtailment of PV generation is a solution that at the cost of underutilization of the solar PV panels. Instead of curtailing this solar generation from household, regulation of electricity demand by controlling a storage along with the PV-panel offers an attractive alternative solution. Similarly, when PEV returns to the household, they are plugged into the system to be charged that also worsen the situation of 'duck-belly curve'. Improving the grid infrastructure would be a necessity to supply such loads. Instead of charging PEV during the high demand period, PEVs can be charged during the low demand period to make the load demand as much smooth as possible. Vehicle-to-grid (V2G) power flow option can be used to help improve the reliability of the grid. If a PEV is capable of delivering power to the household, then it may discharge in times of higher demand. As DP faces 'curse of dimensionality' problem, dynamic programming successive algorithm (DPSA) for load regulation of a smart household including PV panel with storage and PEV is presented for this multi-dimensional problem [138].

2.2. PV-Panel and Energy Storage Sizing

A household with power flow direction is shown in Figure 2.1. PV panels, battery storage and other loads are connected to the household with bidirectional power flow. The electric grid is connected to the system which can accommodate unidirectional power flow. Thus, the grid can only deliver power to the household. Forecasted data is required for optimal energy management of the storage; both the PV generation and load forecasting data are dependent on weather. Day-Ahead scheduling is performed to determine the scheduling of the power flow of PV. The forecasted PV and load demand data for a 24-hour period are provided as the input to an optimization algorithm, which computes the optimal state of charge (SOC) strategy of the battery storage considering its constraints.

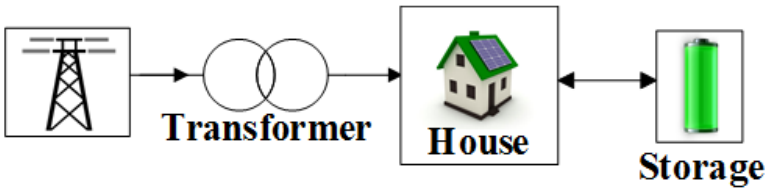

Figure 2.1. Household system.

2.2.1. Deterministic Model Development

To minimize the overall daily electricity purchase cost, the objective function is formulated as:

$$J = \min \sum_{k=1}^{T} [(P_t - (P_{PV,t} + P_{c,t}))\, C_t] \tag{2.1}$$

Given that

$$-P_{c,min} \leq P_{c,t} \leq P_{c,max} \tag{2.2}$$

where J represents the objective cost function to be minimized, C_t is the ToU cost at time t, P_t is considered as the day-ahead household demand, $P_{PV,t}$ is solar power, and $P_{c,t}$ is the operating power of the charger for storage at time t. $P_{c,t}$ is positive while the storage is being charged and negative when it is being discharged within the given limits. For the SOC calculation of the storage, it is required to know whether it is charging or discharging. The sign function sgn is used to represent the charging/discharging scenarios, and the SOC_t of the PV storage is calculated based on the power flow as shown below:

$$sgn_t = \begin{Bmatrix} 1 & (P_{c,t} \geq 0) \\ -1 & (P_{c,t} < 0) \end{Bmatrix} \tag{2.3}$$

$$SOC_t = \begin{Bmatrix} \dfrac{E_{b,initial} + P_{C,t}(\eta_c)_t^{sgn} \Delta t}{Q_b} ; t = 1 \\ SOC_{t-1} + \dfrac{P_{C,t}\,(\eta_c)_t^{sgn} \Delta t}{Q_b} ; t = 2 - T \end{Bmatrix} \tag{2.4}$$

$$SOC_{min} \leq SOC_t \leq SOC_{max} \tag{2.5}$$

Here $E_{b,initial}$ is the initial charge of the battery, η_c is the efficiency of the charger, and Q_b is the total capacity of the battery. Since storage lifetime is considered for calculating NPV, storage degradation costs due to charging and discharging are not included in the objective function.

The problem is based on the following assumptions:

Assumption 1: The grid can only deliver power to the household. There is no back feeding of energy to the grid and no net metering compensation is provided.

Assumption 2: The storage can be charged from PV generation and it discharges only to deliver power to the household.

Among the available options, DP ensures reaching the globally optimal path by considering all of the possible paths whereas the other methods may not be able to find global optimal paths for certain cases. Furthermore, the algorithm is not dependent on the objective function whether it is linear or non-linear. DP is an optimal control tool used for solving a complex problem by breaking it down into sub-problems. The method uses Richard Bellman's principle and ensures global optimality [55]. DP is based on Hamilton-Bellman-Jacobi (HBJ) equation. For the system of Figure 2.2, the HBJ model can be written as:

$$J\left(t+1, SOC^{i}(t+1)\right) = \min_{SOC(t+1,SOC^{i})} \left\{ \begin{matrix} c\left(SOC^{i}(t), SOC^{j}(t+1)\right) \\ +J\left(t, SOC^{j}(t)\right) \end{matrix} \right\} \quad (2.6)$$

In (2.6), $J\left(t+1, SOC^{i}(t+1)\right)$ is the optimal value obtained from the previous stage for $SOC^{i}(t)$. $c\left(SOC^{i}(t), SOC^{j}(t+1)\right)$ is the cost of transitioning from state SOC^{i} at time t to SOC^{j} at time $t+1$. The set $SOC\left(t+1, SOC^{i}(t+1)\right)$ defines the set of all feasible reachable points at time

$t+1$ on SOC^j from the current state *t*. $J\left(t+1, SOC^i(t+1)\right)$ is the optimal value function to go from time step *t* to next time $t+1$ at SOC^j point. Therefore, the optimal point is $SOC^i(t+1)$ among all possible set of $SOC^i(t)$ for which the optimal value. $J\left(t+1, SOC^i(t+1)\right)$ is obtained at point $SOC^j(t+1)$. This control strategy ensures the consideration of all possible transitions to future states to achieve cost minimization.

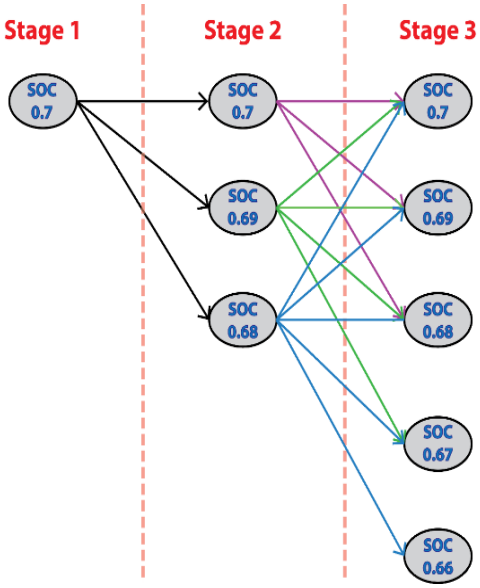

Figure 2.2. Dynamic programming with SOC as a state.

The solution process through DP in the context of research at hand can be visualized with the help of Figure 2.2 where a three-stage problem is considered for simplicity. Stage 1 defines the initial SOC where it is considered to be 0.7. While going from stage 1 to stage 2 with an increase in time, the corresponding costs are calculated for reaching different possible SOC points. A certain limit is needed to be considered for the next SOC level range based on the previous SOC value. To go from stage 2 to stage 3, the cost of each different possible path is calculated. For example, at stage 3 when the SOC is 0.7, the optimal path to reach SOC 0.7 is obtained by calculating and comparing the cost of all possible paths leading to SOC value of 0.7. Similarly, the

costs for all other SOC points are also calculated in stage 3. Then after comparing the cost for all SOC points at stage 3, the point for which minimum value is obtained is determined as the most cost-effective path.

2.2.2. NPV based PV-Panel and Storage Sizing

NPV is a tool used for capital budgeting to analyze the profitability of an investment. Generally, an investment with a positive NPV will be a profitable one and one with a negative NPV will result in a net loss. For the calculation of NPV, the investment cost of PV panel and energy storage, $I(Q_{PV}, Q_b)$, as well as the net annual saving from DP based control strategy, $S(Q_{PV}, Q_b)$, based on the size of PV panel, Q_{PV}, and storage capacity, Q_b,are required to consider. DP based control strategy is applied to the load and PV profiles for four days of four different seasons and the obtained savings are considered as the net annual saving. From the maximum NPV, the optimal size of PV panel and storage capacity for the particular household can be found. The equation for obtaining the required optimal PV panel and energy storage can be expressed as

$$Z\ (Q_{PV}^*, Q_b^*) = \max_{Q_{PV}, Q_b} \{\frac{S(Q_{PV}, Q_b) - I(Q_{PV}, Q_b)}{(1+r)^k}\} \tag{2.7}$$

where *k* is the lifetime of the PV panels in years, and *r* is the discount rate. $Z\ (Q_{PV}^*, Q_b^*)$ is the the maximum NPV which is determined for the optimal size of PV panels, Q_{PV}^*, and storage capacity, Q_b^* .

2.2.3. Impact of DP, Storage Cost, and ToU rate

Simulation analysis is carried out for a typical household with a PV and storage installation to demonstrate the effectiveness of the DP technique on minimizing household cost. The parameters of the system are listed in Table 2.1. Solar irradiance and load profiles for different seasons vary, which is shown in Figure 2.3 and Figure 2.4 based on data obtained from [147] and

[148]. Day-Ahead scheduling is performed to determine the scheduling of the power flow of PV and storage.

The forecasted PV and load demand data for a 24-hour period for 15-minute resolution are provided as the input to the optimization algorithm, which computes the optimal *SOC* path of the battery storage considering its constraints. Because of the variation of the load demands, PV profiles and *ToU* rate structure for different seasons, simulation results of four days of four different seasons are shown in Figure 2.5. These results are shown for a 3 kW solar panel with a 4 kWh storage and *ToU* rate 1 [Appendix A: Table I]. For comparison, simulation results for heuristic control are also provided. In heuristic control, the available solar energy is used to charge the storage whenever there is excess generation than demand. The storage is discharged and grid delivers power during the period when there is more demand than the available solar energy [149]. Referring to Figure 2.5 (a) and (b), the results indicate that the DP based control strategy prefers to store generated PV energy during the partial-peak period which is until hour 13:00 to serve for the peak hour period. During peak period from hour 13:00 to hour 20:00 in summer and fall, the stored energy is utilized to serve the load demand. Due to this reason, the load demand from the grid for DP based control strategy is higher during the partial peak hour and lower during peak hour than the heuristic based control strategy. Similarly, according to the results of Figure 2.5 (c) and (d) for spring and winter, DP based control tries to utilize the available capacity of storage to store the solar energy during the off-peak period until hour 17:00 and use this energy to serve after hour 17:00 to hour 20:00 (peak period) to reduce the electricity bill of the household owner. As a result, the load demand from the grid becomes lower than the heuristic control during hours 17:00 to 20:00 for DP based control due to comparatively higher *ToU* rate.

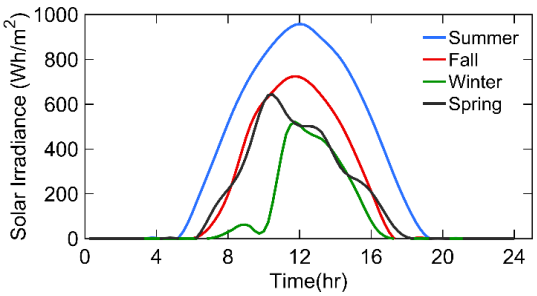

Figure 2.3. Solar profiles for different seasons.

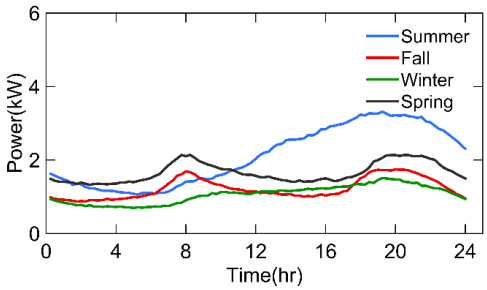

Figure 2.4. Household profiles for different seasons.

Table 2.1. System parameters for residential PV-panel and energy storage.

Parameter	**Value**
PV panel size range	1-4 kW
Panel lifetime	20 years
Battery capacity range, (Q_b)	0-7 kWh
Maximum operating power of the charger (P_{PV})	1 kW
Efficiency, η_b^c	92%
SOC_{min}	20%
SOC_{max}	80%
Battery type	Li-ion
Battery lifetime	10 years
Battery cost range [150]	$350- $150/kWh
PV panel, inverter, installation & maintenance cost [151]	$3.46/W
Discount rate	10%

For the next step of the proposed strategy, the overall cost saving based on PV panel life is calculated to get the NPV for the system since solar panel installment and maintenance cost, and battery lifetime are known from Table 2.1. Storage cost is considered as $350/kWh. Figure 2.6 shows the comparison of NPVs between heuristic and DP based control for different storage sizes with a 3 kW solar panel. It is clear from this figure that storage with optimal control gives higher benefit than heuristic control for all sizes of storage options with fixed panel size.

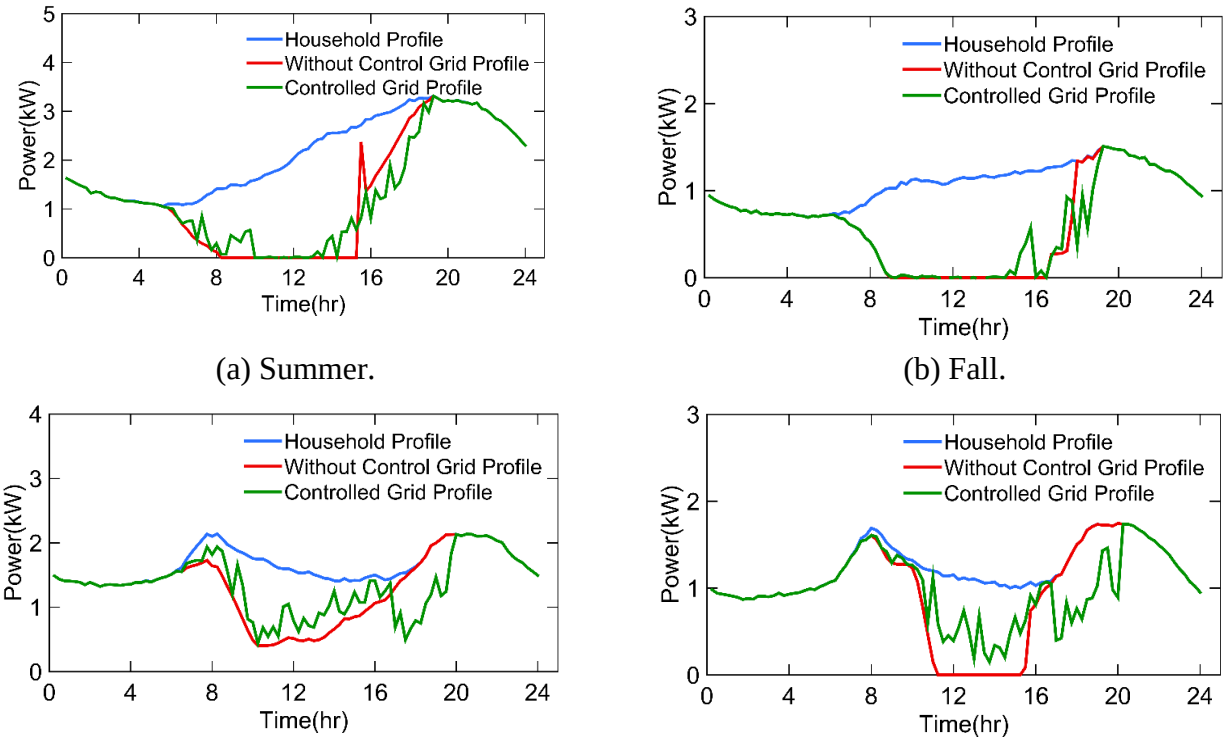

(a) Summer. (b) Fall.

(c) Spring. (d) Winter.

Figure 2.5. Household power management with *ToU* rate.

The analysis on NPV is done by varying the panel and storage sizes. For comparatively higher *ToU* rate 1 and $350/kWh storage unit cost, the optimal sizes of the PV panel and storage capacity for the given household load demand are calculated for the DP based controlled load profiles. The result of Figure 2.7 indicates that it is always beneficial to the customer to use a 3 kW PV panel for the given household load profile irrespective of the storage size. It is also found that with an increase in the size of the PV panel, it is beneficial to add a specific size of storage to the system. However, for the lower size of PV panel, the inclusion of storage reduces NPV. Since an increase in storage size decreases the NPV, it is not beneficial to add storage when its cost remains as high as $350/kWh. Therefore, the cost of storage is also a critical factor. As per unit cost of storage is decreasing according to [150], the effect of storage costs ranging from $350/kWh to $150/kWh are considered for analysis. NPV is calculated considering the DP based

charge/discharge control for different storage capacity. Figure 2.8 shows that NPV increases and becomes higher than $3200 (which is the NPV without considering any energy storage) when the cost of storage decreases to $250/kWh or less. The results also show that the NPV starts decreasing after reaching a peak with an increase in storage capacity. For both $250/kWh and $150/kWh storage costs, 4 kWh is the optimal size for the considered household with *ToU* rate 1 and 3 kW panel.

To analyze the effect of *ToU* on NPV, in addition to the typical higher *ToU* rate 1, a typical *ToU* rate 2 (Appendix A: Table II) is used that provides a comparatively lower rate and has a small deviation between off-peak and peak hour rate. The DP based control strategy is applied to different panel and storage sizes for the given household profiles and a lower storage cost of $150/kWh. The comparison among the NPVs for different panels of *ToU* rate 2 are given in Figure 2.9. It can be seen that NPVs for *ToU* rate 2 cases are always negative which means that it is not always beneficial to use a PV panel, with or without energy storage, if there is less difference between peak and off−peak hours or no incentives are provided to the household owner for PV generation.

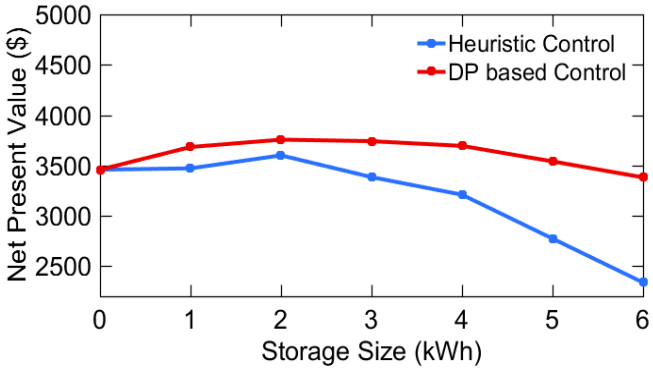

Figure 2.6. Comparison of NPVs between DP and heuristically controlled PV-storage hybrid system for a 3 kW PV panel with $350/kWh storage cost.

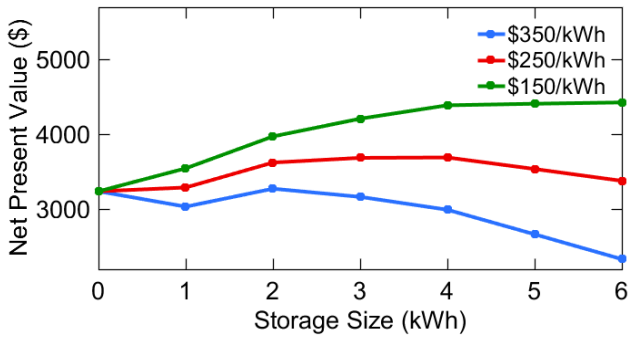

Figure 2.7. Optimal size of storage for different storage per kWh costs.

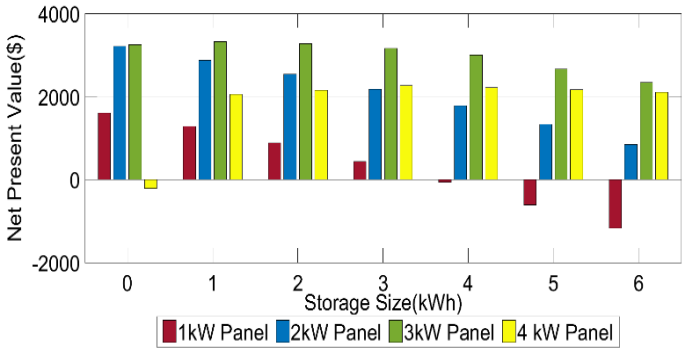

Figure 2.8. Optimal size of the PV-panel and storage system for the given household profile with compensation to the homeowner.

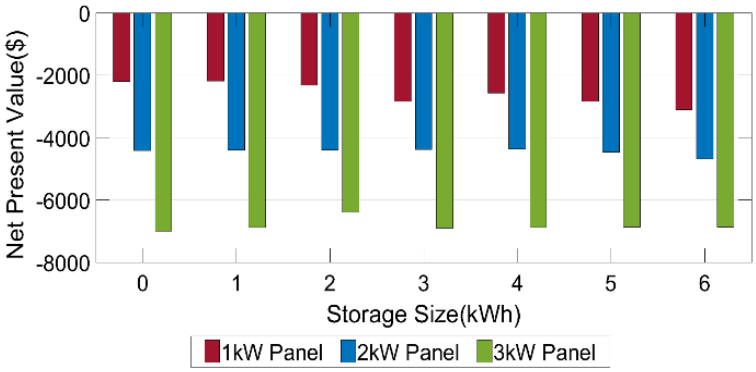

Figure 2.9. Comparison of NPV of different panel and storage size for lower *ToU* rate.

2.3. Load Regulation with PV -Storage Hybrid Unit and PEV

For load regulation, the similar household system is considered as shown in Figure 2.1. Only PEV is included in the system which is shown in Figure 2.10. When PEV is available, it can be connected to the system through a bidirectional charger so that it can either charge or discharge; therefore, the PEV power flow can either be positive or negative. The smart household system consists of sensor networks like the smart meter and the power management unit. The meter measures the electricity usage within the household microgrid and the power measurement unit helps to maintain the power-flow management within the microgrid according to the usage. In the first stage, the collection of forecasting data is required. It should be mentioned that both the PV power and load forecasting data is depended on the weather. A block diagram of the forecasted data based on which the system takes decisions is provided in Figure 2.11. As day-ahead scheduling is performed to determine the scheduling of the power flow of PEV and PV, the forecasting data is taken for 24 hours ahead.

The forecasted PV data, load demand, and availability of the PEV in the grid are provided as the input to the dynamic programming successive approximation (DPSA). DPSA computes the optimal SOC strategy of the battery storage and the PEV storage considering their constraints.

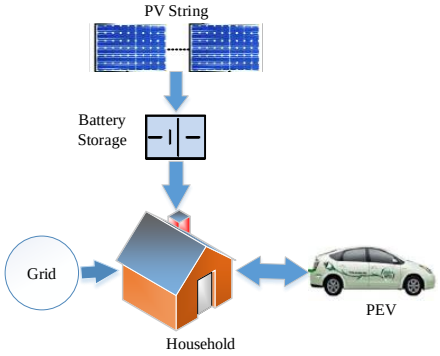

Figure 2.10. Household system with PEV.

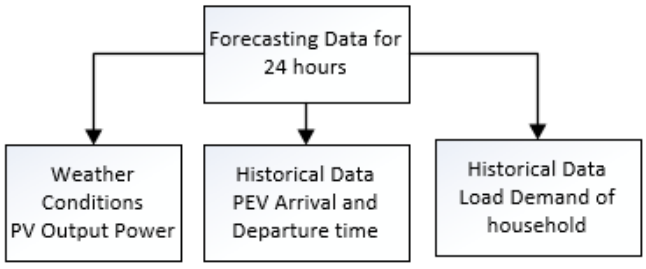

Figure. 2.11. Block diagram of forecasting data.

2.3.1. Deterministic Model Development

Load variance minimization of a household microgrid can help achieve smooth operation of the system. It helps accomplish peak shaving and valley filling. As both the PEV and PV battery storage have the benefit of storing energy and discharging it when required, they can be controlled to reduce the load variance. For this study, a one-day cycle from 0hr to 24hr is considered. A 24hr period is divided into T time periods and the length of each time period is considered as Δt. If P_t is considered as the day-ahead household demand, $P_{PEV,t}$ is the vehicle power, $P_{PV,t}$ is solar power, $P_{b,t}$ is the solar battery storage at time period t and μ is the average household demand in one day. In this case, the objective function can be written as

$$\text{Minimize, } J = \sum_{k=1}^{T} \left[\frac{1}{T} \left(P_t - \mu + P_{PEV,t} - P_{PV,t} + P_{b,t} \right)^2 \right] \tag{2.8}$$

Subject to

$$-P_{PEV,min} \leq P_{PEV,t} \leq P_{PEV,max} \; ; \; \left(t = t_{PEV,start} - t_{PEV,end} \right) \tag{2.9}$$

$$-P_{b,min} \leq P_{b,t} \leq P_{b,max} \quad (t = 1 - T) \tag{2.10}$$

where J represents the objective function to be minimized. $P_{PEV,t}$ and $P_{b,t}$ can be negative while the storages start charging and become positive when they discharge within some limits.

For the calculation of state of charge (SOC) of PEV and PV storage components, it is required to know whether they are charging or discharging. If the battery draws a charge from the grid or solar power, the sign function *sgnt* is considered positive and is considered negative when discharging. In addition, PEV has constraints those are needed to consider. The PEV is connected to the grid for a certain period of time and needs to complete its charging within this time. So, the $SOC_{PHEV,t}$ and the $SOC_{b,t}$ of both the PEV and PV storage can be calculated based on charging and discharging condition of the system.

$$\mathrm{sgn}_t = \begin{cases} 1 & (P_{PEV,t}, P_{b,t} \geq 0) \\ -1 & (P_{PEV,t}, P_{b,t} < 0) \end{cases} \quad (2.11)$$

$$SOC_{b,t} = \begin{cases} \dfrac{W_{b,initial} + P_{b,t}(\eta_b^C)_t^{sgn}\Delta t}{Q_b} \\ SOC_{b,t-1} + \dfrac{P_{b,t}(\eta_b^C)_t^{sgn}\Delta t}{Q_b} \end{cases} \quad (2.12)$$

$$SOC_{PEV,t} = \begin{cases} \dfrac{W_{PEV,initial} + P_{PEV,t}(\eta_{PEV}^C)_t^{sgn}\Delta t}{Q_{PEV}}; & (t = t_{PEV,start}) \\ SOC_{PHEV,t-1} + \dfrac{P_{PEV,t}(\eta_{PEV}^C)_t^{sgn}\Delta t}{Q_{PEV}}; & (t = t_{PEV,start} - t_{PEV,end}) \end{cases} \quad (2.13)$$

$$SOC_{PEV,min} \leq SOC_{PEV,t} \leq SOC_{PEV,max} \quad (2.14)$$

$$SOC_{b,min} \leq SOC_{b,t} \leq SOC_{b,max} \quad (2.15)$$

where $W_{b,initial}$ and $W_{PEV,initial}$ are the initial charge of the batteries, η_b^C and η_{PEV}^C are the efficiency of the charger, Q_b and Q_{PEV} are the total battery capacity of the PV and PEV respectively.

2.3.2. Dynamic Programming Successive Algorithm (DPSA) for Coordinated Control*:*

It is hard to manage multidimensional problem through DP, because of the dimensional complexities. The DPSA decomposes the multidimensional problem in a sequence of one-dimensional problems which are much easier to handle [70]. The optimizations work with one variable at a time while keeping the other variables at a constant value. All the variables are evaluated the same way. This technique converges to an optimum solution for convex problems. Figure 2.12 shows the flowchart of DPSA technique for the optimization problem discussed in this paper. Using this method, when DP is applied to solar storage, the charging profile of PEV storage is kept constant. After the completion of DP on the solar storage, DP is applied to the PEV storage while the solved charging profile for solar is kept unchanged.

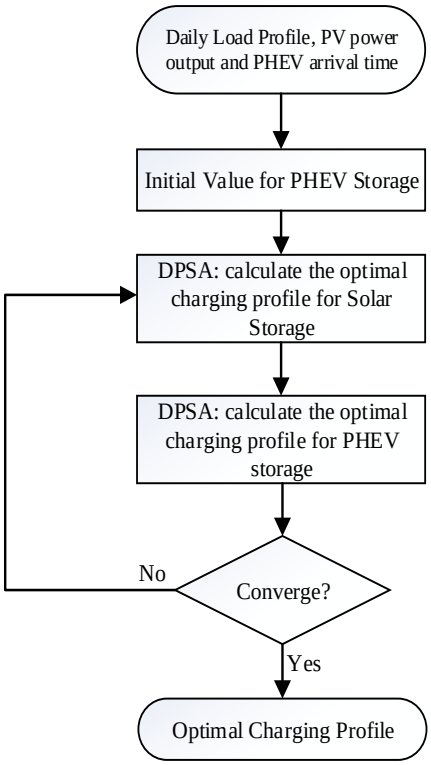

Figure 2.12. Algorithm of Control charging through DPSA.

2.3.3. Improvement on Load Regulation

Simulation analysis is carried out for a typical household with one PEV and PV installation to demonstrate the effectiveness of the DPSA technique on minimizing household load variance. The parameters of the system are listed in Table 2.2. For a working day, it is assumed that the PHEV connects to the grid at time 18:00 and leaves the grid at 8:00 the next day. The solar power for a sunny day is considered for this simulation. Both the household load profile obtained from [147] and solar power generation profile obtained from [148] for a typical household PV system are shown in Figures 2.13 and 2.14, respectively.

The simulation results after the regulation are shown in Figure 2.15 which shows that if both the PV storage and PEV storage charging and discharging profile is controlled, then the load variance improves. It can be seen from Figure 2.16 that for this scenario, when the PEV connects

to the household power system, it is forced to discharge to contribute to the load leveling since the household load demand is high during this time. However, the results indicate that the PEV power flow is managed such that it starts charging when the demand is low to once again contribute to load leveling of the total household profile. Similarly, from Figure 2.17, it can be concluded that solar power generation is managed to charge the batteries when the demand is relatively low, while during peak load this energy is consumed to meet high load demand.

In order to further outline the importance of coordinated control among different energy storage units available in a smart household, four different scenarios are considered and simulated. In scenario one – no PEV and PV storage are present in the system and variance is calculated. In scenario 2, both PEV and PV storage are considered but they are not controlled which results in an increase in variance compared to the previous case. In this case, PEV storage starts charging instantly when the owner comes back at home and the vehicle is plugged in. Since at that time load demand is also higher, the overall demand increases further. On the other hand, PV storage does not charge that much in this scenario, since most of the energy produced from solar at daytime is used to meet the energy demand. In scenario 3, only PEV storage is controlled but PV storage remains uncontrolled. In this case, the variance is also reduced compared to scenario 1. However, the best result is found in terms of minimizing the load variance is obtained when both the PEV and PV storage components are controlled in scenario 4.

In Table 2.3, the load variance of the four discussed scenarios is given. From the results, it is concluded that load variance increases when the system faces uncontrolled PEV and PV energy. It is also clear from the results that controlled PEV and PV energy system with storage has the most influence in minimizing the household load variance.

Table 2.2. Parameters for PV- storage hybrid unit and PEV.

Parameter	Value
PEV arrival time, t_{start}	18:00
PEV leaving time, t_{end}	8:00
Initial SOC of PEV	40%
Initial SOC of PV	20%
SOC_{min}	0.2
SOC_{max}	0.8
Battery Capacity, (Q_{EV})	14kWh
Battery Capacity, (Q_b)	5kWh
Maximum operating power of the charger of PEV, (P_{EV})	1 kW
Maximum operating power of the charger of PV battery, (P_{PV})	2 kW
Efficiency, η_b^C	0.92
Efficiency, η_{PEV}^C	1
Time period, t	15 min

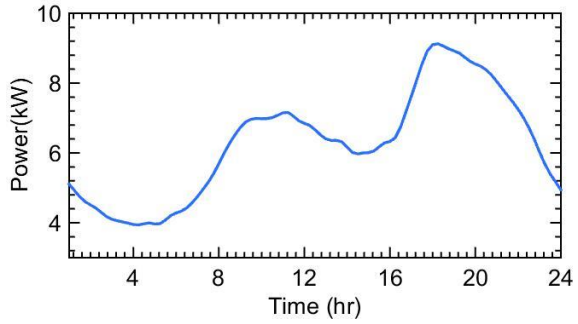

Figure 2.13. Typical household load demand.

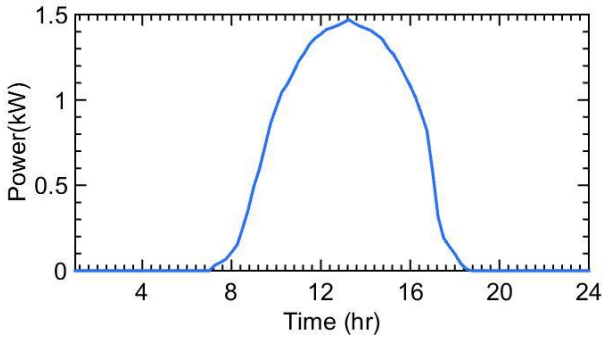

Figure 2.14. Solar power output on a sunny day.

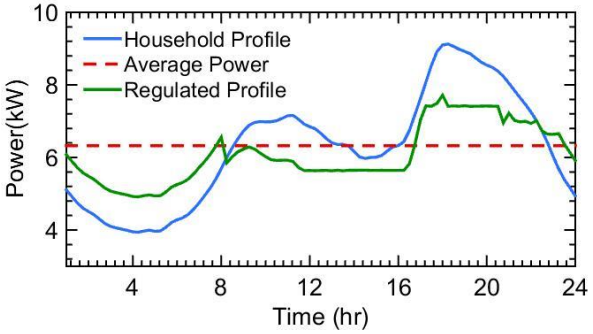

Figure 2.15. Regulated profiles after control.

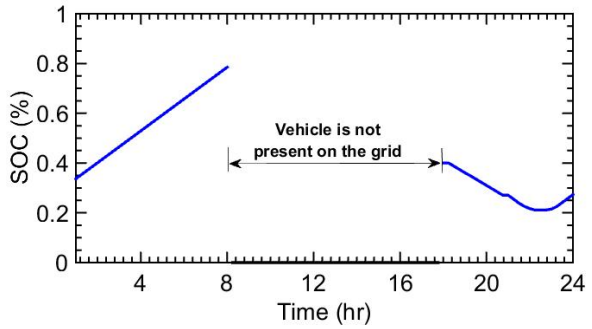

Figure 2.16. PEV charging and discharging profile.

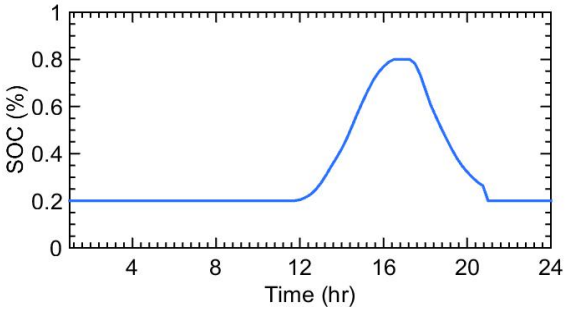

Figure 2.17. PV battery storage charging and discharging profile.

Table 2.3. Comparison results of load variance for different cases.

No PHEV and PV Energy (kW)	PEV and PV Energy (Uncontrolled) (kW)	Controlled PEV and Uncontrolled PV Energy (kW)	Controlled PEV and PV Energy (kW)
2.31	2.75	0.90	0.35

2.4. Conclusion

In this chapter, deterministic model-based energy management for PV panel and storage sizing and load regulation of a residential system are presented. Simulation analysis for PV panel and storage sizing can be summarized as: If DP based control strategy is performed for energy management between storage and PV panel, then the overall NPV increases for the same size of storage. Due to the increase of NPV, DP based control strategy finds higher optimal capacity for storage than the heuristic control method. Though increasing the PV panel size means an increased amount of PV generation, it is not always beneficial. Optimal PV panel size is required to get the most economic benefit. With the change of storage cost, the NPV changes. A lower storage cost results in a higher NPV for the same size of storage and thus, the preferred optimal storage capacity will be higher. If the *ToU* rate structure is very low and no incentives are provided, then using PV panel along with storage is not cost effective even if DP based control strategy is performed and

the storage cost reduces to $150/kWh. The simulation results obtained from DPSA for load regulation show that by controlling each energy storage component in the system, it is possible to minimize household load variance that can help grid to alleviate the problem of the “duck-belly curve”.

CHAPTER 3

Uncertainty Consideration in Energy Management at Residential and Community Levels

3.1. Introduction

The intermittency of PV power depends on the real-time weather conditions (such as cloud passing). Due to this uncertainty, it is necessary to represent PV generation with different stochastic scenarios in order to better represent the problem at hand and derive a more robust energy management method. A control strategy framework for a smart house that includes PV - storage hybrid unit while considering the uncertainty in solar PV production is developed in the first part of this chapter. The control strategy is based on the SDDP algorithm applied in the context of stochastic PV generation.

In a real scenario, household load demand also experiences uncertainty due to the preference of the consumers. This uncertainty is considered to develop a control strategy to minimize the cost for charging/discharging a PEV. This strategy relies on some basic information such as charge duration, residual charge of the PEV while connected to the grid, electricity ToU rate and target charging level. The SDDP algorithm is applied to create a control strategy for charging/discharging the PEV under electricity demand uncertainty which is discussed in the second part of this chapter.

When two storages are used in a household, they can be coordinated optimally to enhance the proper utilization of the system resources. A coordinated control strategy between PV - storage hybrid unit and PEV is developed on the third part of this chapter while considering the uncertainties in solar production and household electricity demand for a house. Since both the load demand and solar generation change due to the variation of weather and they are correlated with

each other, it is necessary to consider the stochasticity of PV generation and electricity demand and the correlation between them in order to have a better formulation of the problem. Thus, the scenario are generated considering the correlation between load and solar production with Cholesky factorization procedure. The problem is formulated for the coordinated system and the SDDP algorithm is applied to optimize the system in the context of stochastic PV generation and household electricity demand. The comparisons between uncoordinated and coordinated control schemes are also shown through case studies.

Energy storage devices may not always be considered as the most economical solution for individual households due to their current costs. Shared utilization of energy storage may be viewed as a robust and attractive alternative to a community as a whole. On the last part of this chapter, a method is developed that achieves reductions in the overall electricity cost for a household, including electricity purchases from the grid and energy storage investments. The SDDP method is applied to solve the multi-stage stochastic models of the SEM. NPVs are also considered to obtain the optimal storage capacity.

3.2. PV Uncertainty Consideration for Hybrid System

A similar household system consisting of a PV-storage hybrid unit described in Figure 2.1 is considered. The forecasted household load profile (single point forecast) gives the demand value that is used as the deterministic information in the decision-making model. For solar PV generation, a stochastic representation based on forecasted data for cloud covering and sudden weather changes is employed. To minimize the overall cost in a day, simulation of the proposed modeling framework is performed to determine the scheduling and usage of system components. The forecasted load demand information and the stochastic solar PV scenarios generated data for

a 24-hour period are given as input to the mathematical model of the system and the SDDP algorithm, which computes an optimal SOC strategy.

3.2.1. Model Formulation

Cost minimization of a household with optimal operation of the PV-storage hybrid unit can significantly benefit a customer. In this study, a one-day cycle from 0hr to 24hr with a 15-minute resolution is considered. The total 24hr is divided into T time periods based on a resolution Δt. Let C_t be the *ToU* based electricity tariffs, $P_{load,t}$ is the day-ahead forecasted household load demand, $P_{PV,t}^{\omega_t}$ is the generated solar power, and $P_{grid,t}$is the power demanded from the grid at time t; the objective function J and constraints can then be written as –

$$\min J = \sum_{t=1}^{T} [C_t \cdot P_{grid,t}] \tag{3.1}$$

with the following structural constraints and operational limits.

A. Power balance constraint

$$P_{grid,t} - P_{b_{ch},t} + P_{b_{disch},t} - P_{slack,t} = P_{load,t} - P_{PV,t}^{\omega_t} \tag{3.2}$$

B. Charge balance constraint

$$SOC_{b,t} = SOC_{b,t-1} + \frac{P_{b_{ch,t}} \eta_{b,ch,t}}{Q_b \, \Delta t} - \frac{P_{b_{disch,t}}}{Q_b \ \eta_{b,disch,t} \Delta t}, \forall t \in T \tag{3.3}$$

C. Charge and discharge operational limits based on PV and load, respectively

$$P_{b_{ch,t}} \leq P_{PV,t}^{\omega_t}, \forall t \in T \tag{3.4}$$

$$P_{b_{disch,t}} \leq P_{load,t}, \forall t \in T \tag{3.5}$$

D. Nonnegativity requirement for purchases from the grid

$$P_{grid,t} \geq 0, \forall t \in T \tag{3.6}$$

E. Upper and lower bounds of the decision variables

$$SoC_{b,min} \leq SoC_{b,t} \leq SoC_{b,max}, \forall t \in T \quad (3.7)$$

$$P_{b_{ch}}^{min} \leq P_{b_{ch,t}} \leq P_{b_{ch}}^{max}, \forall t \in T \quad (3.8)$$

$$P_{b_{disch}}^{min} \leq P_{b_{disch,t}} \leq P_{b_{disch}}^{max}, \forall t \in T \quad (3.9)$$

In the system under consideration, the PV unit does not provide power to the grid. Therefore, if there is more PV generation than the electricity demand at a specific time and the storage unit is fully charged, then $P_{slack,t}$ will take care of the excess generation as deferred PV energy. $P_{b_{ch,t}}$ and $P_{b_{disch,t}}$ are the instantaneous charging and discharging power of the storage device. $SOC_{b,t}$ is the state of charge of the energy storage at time t. The lower and upper bounds of decision variables are provided in Table 3.1. The parameters Q_b is the total capacity of the storage unit and $\eta_{b,ch,t}$ and $\eta_{b,disch,t}$ are the efficiency of the charger for charge and discharge.

If the household demand needs to be satisfied by both PV generation and battery discharged power, then according to (3.2) and (3.3) it is less efficient to charge the battery with PV power. In that case, PV generation will be used directly to satisfy the demand with the option to use energy that is already stored in the battery as well as purchase power from the grid. On the other hand, if PV generation is higher than the demand, the surplus will be stored in the battery (if there is storage capacity available) and there will be no discharge. Thus, charging and discharging the storage device simultaneously is not possible. The different scenario representations for solar PV based on the forecasted solar generation $P_{PV,t}$ is obtained using (3.10) [152].

$$P_{PV,t}^{\omega_t} = P_{PV,t} \pm \rho_t^{\omega_t} P_{PV,t};\ \omega_t \epsilon \forall \Omega_t, \forall t \in T \quad (3.10)$$

where ω_t is a scenario within Ω_t that is the set of all scenarios that represent the PV power generation, and $\rho_t^{\omega_t}$ is a normally distributed random parameter.

3.2.2. Multi-Stage Optimization for Uncertainty Consideration

A general T-stage stochastic linear program for the problem at hand can be formulated as follows:

$$\min_{x_1} \; c_1 x_1 + \mathbb{E}_{b_2|b_1} h_2(x_1, b_2) \tag{3.11}$$

Subject to:

$$A_1 x_1 \; = \; B_1 x_0 + b_1 : \pi_1 \tag{3.12}$$

$$x_1 \geq 0 \tag{3.13}$$

where for $t = 2, \ldots, T$,

$$h_t(x_{t-1}, b_t) = \min_{x_t} \; c_t x_t \; + \; \mathbb{E}_{b_{t+1}|b_t} h_{t+1}(x_t, b_{t+1}) \tag{3.14}$$

Subject to:

$$A_t x_t \; = \; B_t x_{t-1} + b_t : \pi_t \tag{3.15}$$

$$x_t \geq 0 \tag{3.16}$$

The decision variables of a particular stage t are considered as a vector x_t, which includes electricity purchases from the grid, charge and discharge power of the battery and SoC of the battery for the problem. The parameter b_t represents stochastic PV supply at stage t. Equations (3.11) and (3.16) represent the objective functions to minimize the total cost that includes first (present) and t^{th} (expected future) stage costs, respectively. Equations (3.12) and (3.15) are the model's structural constraints which include power balance and charge balance equations. Dual variables (denoted by π_t) derived from the structural constraints (or from the dual optimization model) are used later to construct a piece-wise linear approximation of the future cost function following Benders' decomposition scheme. Equations (3.13) and (3.16) are simple bounds on the decision variables. In the objective function defined in (3.11), $\mathbb{E}_{b_2|b_1} h_2(x_1, b_2)$ represents the expected cost function of stage 2 based on decisions x_1 taken in stage 1. The realization of the

random parameter b_2 affects the system condition at stage 2. Similarly, for equation (3.14), $\mathbb{E}_{b_{t+1}|b_t} h_{t+1}(x_t, b_{t+1})$ calculates the expected cost function of stage $t+1$ given the decisions x_t in stage t. The realization of the random parameter is b_{t+1}.

To solve our version of the general model, a version of SDDP is implemented which is originated from the work of Pereira and Pinto [140], [153]. The SDDP is, to date, the state-of-the-art method for solving multi-stage stochastic linear programs. The SDDP algorithm avoids the well-known curse of dimensionality of DP by constructing an approximation of the future cost function with piecewise linear functions represented through Benders' cuts that are added iteratively. This process stops when a stopping criterion is reached.

A visualization of how SDDP works to solve this problem is depicted in Figure 3.2 which shows the process for a simple three-stage problem; however, it is important to mention that the tree sizes of interest are quite large. For example, in our system, a tree with 10 scenarios per stage with 96 stages is considered. Once a sampled scenario tree like Figure 3.1 (a) is available for the SDDP, the process is started by sampling the forward paths in this tree as highlighted in Figure 3.1 (b). These paths are considered for the problem to proceed for the forward pass. During the forward pass, a sequence of models like (3.14) - (3.16) is solved at each time stage using the simplex method. During the solution process, Benders' cuts, which are accumulated from previous iterations for the certain stage, are used as additional constraints to create a better approximation of the future costs and improve the decision-making process. Then the sample mean of the costs associated with all the sampled forward paths provides an estimate of the expected future cost. At the final stage of the forward pass, the total expected cost is estimated which is considered as the upper bound of the problem. The lower bound for the sampled problem is calculated from solving the first stage problem. After a finite number of iterations, the upper and lower bounds tend to

converge and the algorithm can be stopped. A stopping criterion based on the desired level of precision in the convergence process is used. If upper and lower bound costs do not reach the desired convergence level, then another SDDP iteration is needed. At each iteration, new forward paths are sampled independently.

For reaching the desired convergence level, the algorithm proceeds to the backward pass shown in Figure 3.1(c). In the backward pass, the algorithm computes new Benders cuts for certain stage to better approximate the expected future cost function. As there is no future cost after the final stage T, cuts are not used in that stage. In Figure 3.1(c), the highlighted nodes are selected in this iteration's backward pass. Figure 3.1(d) depicts the sets of cuts corresponding to all the nodes on each stage for each iteration. If the future cost obtained from forward pass is θ_t for a sampled path ω_t, and from the solved linear problem for stage $(t+1)$ the dual variables are represented by $\pi_{t+1}^{\omega_{t+1}}$ and optimal cost by $h_{t+1}^{\omega_{t+1}}$, then the Benders' cut for the stage t is calculated using (3.17)-(3.19).

$$\theta_t - G_t x_t \geq g_t \tag{3.17}$$

$$G_t = \sum_{\omega_{t+1} \in \Delta(\omega_t)} \pi_{t+1}^{\omega_{t+1}} B_{t+1} \tag{3.18}$$

$$g_t = \sum_{\omega_{t+1} \in \Delta(\omega_t)} h_{t+1}^{\omega_{t+1}} - G_t [x_t^{\omega_t}]^k \tag{3.19}$$

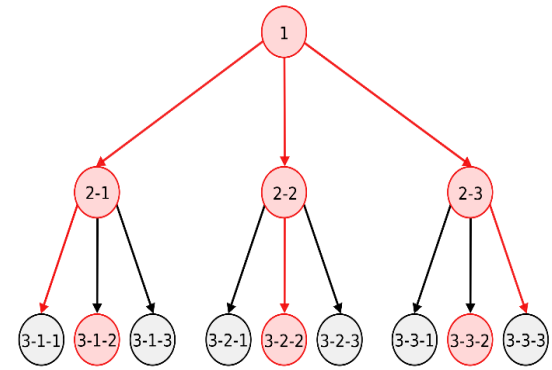

(a) Scenario tree.

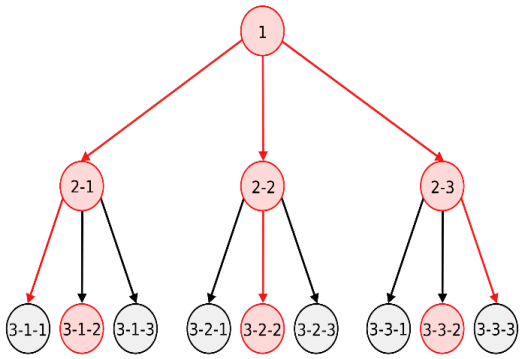

(b) Forward paths selection.

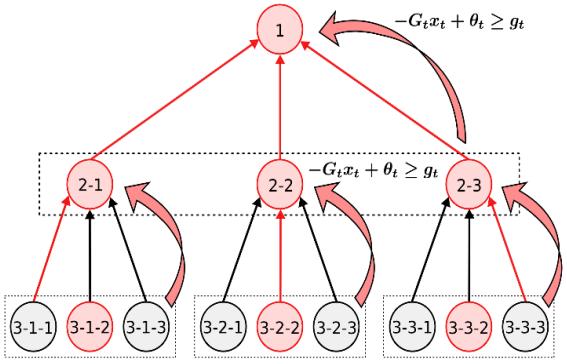

(c) Backward recursion.

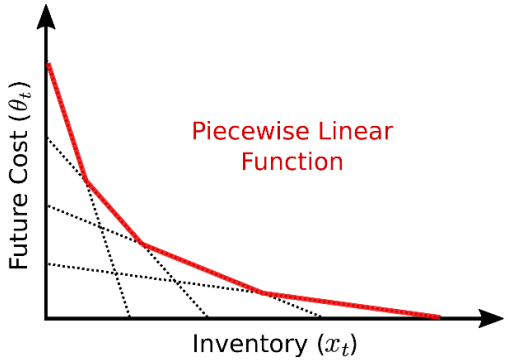

(d) Future cost function represented by Benders' cut.

Figure 3.1. Optimization solution process via SDDP.

All the sampled forward paths solved in the forward pass do not have to be solved in the backward pass. The SDDP can select a subset of sampled forward paths in order to compute the Benders' cuts. As the backward pass calculation takes more time than the forward pass calculation, the number of selected paths can be reduced to enhance the speed of convergence. After the completion of the backward pass for all the stages, a different set of forward paths are sampled from the scenario tree to imply the accumulated cuts, which are obtained from the backward pass of each iteration for each stage of the system.

3.2.3. Impact of PV Generation Uncertainty Consideration

The parameters used to represent the system characteristics for simulation analysis are listed in Table 3.1. Forecasted solar power profile for a summer day and a typical household summer load profile are obtained from [147] and [148] and shown in Figure 3.2. The summer ToU rate for residential customer varies over the day based on off-peak, partial peak and peak hours which is represented in Figure 3.3. The solar energy production is considered to be a stochastic parameter since solar PV generation can often be considered as a random resource depending on climate and weather characteristics. Thus, the normally distributed random noise parameter $\rho_t^{\omega t}$ in Equation (3.10) is sampled from the set $\mathcal{N}(0,1)$[kW] to generate different solar PV energy profiles.

Table 3.1. Parameters for hybrid system.

Parameter	Value
PV panel installed power	3 kW
Battery capacity, (Q_b)	4 kWh
Efficiency, η_b^c	0.92
Initial SOC	20%
SOC_{min}	20%
SOC_{max}	80%
$P_{b_{ch}}^{min}$	0 kW
$P_{b_{ch}}^{max}$	3 kW
$P_{b_{disch}}^{min}$	0 kW
$P_{b_{disch}}^{max}$	3 kW
Battery type	Li-ion
Time period, t	15 min

In a heuristic control strategy, the storage device gets charged when there is an excess of solar generation and discharged with an increase in demand than the generated solar energy. The storage device will not be charged when there is no PV generation since it is not connected to the grid. The heuristic control strategy does not address the maximization of benefits to the homeowner. Our objective is to develop an improved storage energy control strategy to minimize

the overall cost of the customer for a particular day based on SDDP. SDDP solves the multi-stage stochastic program designed for the problem and provides an optimal policy to charge and discharge of the storage.

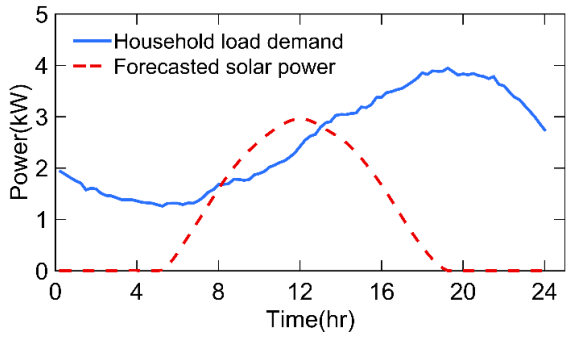

Figure 3.2. Household and solar generation profiles.

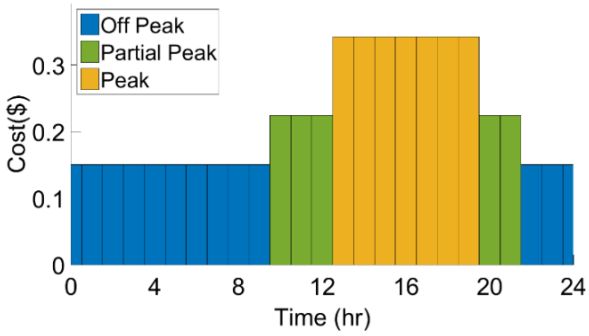

Figure 3.3. *ToU* rate.

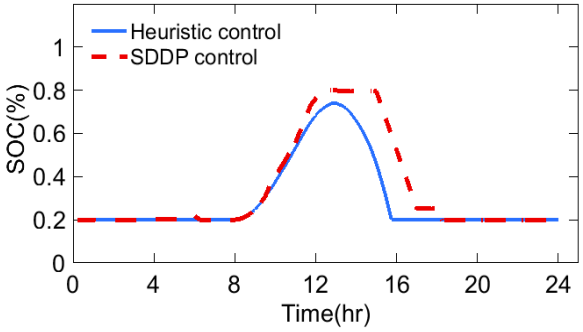

Figure 3.4. SOC profiles for heuristic and SDDP based control of a scenario.

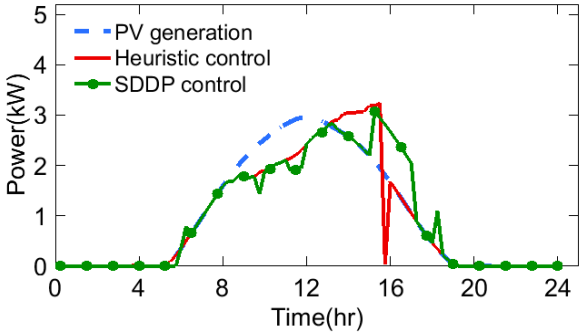

Figure 3.5. PV usage profiles for heuristic and SDDP based control policies of a scenario.

The SOC profiles of the energy storage and PV energy usages by the load for a day with a solar generation scenario similar to the forecasted one for both strategies, SDDP based control, and heuristic control, are provided in Figure 3.4 and Figure 3.5, respectively. For the SDDP based control strategy, it can be seen that when the ToU rate is lower and there is enough solar energy production only then the storage system starts charging. But all the available PV generation during the off-peak hours are not used to charge the storage though the *ToU* rate is the lowest rate during that time. The storage needs to have enough capacity to store excess PV generation, which occurs during partial peak period to avoid the waste of solar energy. Thus, SOC keeps increasing during

off-peak and a little in the partial peak period. Due to the use of PV energy to charge the storage device, its usage for directly supplying the load sometimes becomes lower for SDDP based control when compared to the heuristic control strategy during off-peak and partial peak periods. In the SDDP based control, during peak hours the available generated PV and energy stored in the battery are used mostly to satisfy the household demand and reduce the overall costs for the customer. The SOC level decreases and PV energy usage (the combination of the available PV energy and the stored PV energy) by the load during peak period becomes higher than the heuristic control strategy for the same time interval. Therefore, *ToU* rate and PV generation will influence the SOC level of the storage device and PV usage by the load for SDDP based control strategy. The overall electricity purchases from the grid for both control strategies for this solar generation profile are given in Figure 3.6 and Figure 3.7.

Heuristic control strategy and deterministic dual dynamic programming control (DDDP) are compared with SDDP based control in a policy evaluation procedure. The goal of such procedure is to assess how the different control policies perform using out-of-sample test cases representing the problem uncertainty; for further details, the reader should refer to [154]. For DDDP, only a deterministic solar generation scenario is used to create an instance of the model (3.1) - (3.8), instead of the stochastic scenario tree (Figure 3.1(a)) which is adopted when using the SDDP algorithm.

In order to perform policy evaluation analysis, 100 solar profiles are generated using normal distributed random values sampled from an N(0,1) [kW] for $\rho_t^{\omega_t}$ at each time stage and used as data in equation (3.10). These randomly generated PV profiles are used to find out the average usages of PV energy, peak hour savings and electricity purchase costs for different control policies. Figure 3.8 shows that the average operational costs of 100 different solar profiles for a

summer day is lower for SDDP than other control policies. Table 3.2 gives the idea of improvement of average PV usage by load, average peak hour savings and reduction of average electricity purchase cost using the SDDP control policy. If the system is controlled by DDDP, the average cost saving is 3.6% per day compared to the average cost of heuristic control. The control strategy with SDDP algorithm reduces the total cost by 9.2% per day compared to 5.7% per day with the DDDP algorithm. Therefore, using the SDDP control strategy for the PV-storage hybrid unit, an average of $25.8 per month can be saved. The peak hour saving is not only beneficial to the homeowner but also helps utility companies to reduce large load variations during peak periods.

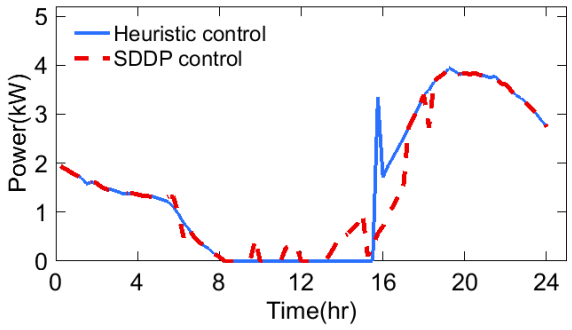

Figure 3.6. Electricity demands from the grid for heuristic and SDDP based control policy for a scenario.

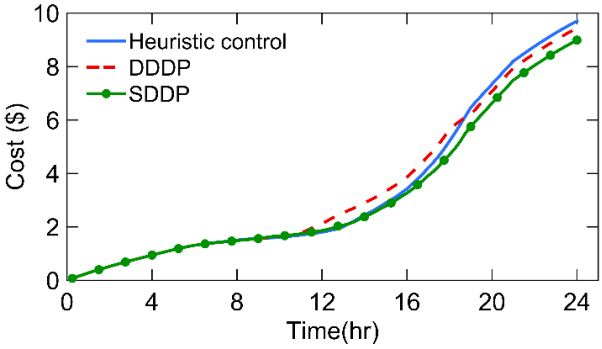

Figure 3.7. Policy evaluation of overall cost for heuristic control, DDDP and SDDP.

Table 3.2. Comparison of different control strategies.

Control Strategy	PV Usage per day (%)	Peak hour Saving per day (%)	Electricity purchase cost per day ($)
Heuristic Control	87.4	29.6	9.8
DDDP	88.1	48.1	9.4
SDDP	97.3	48.7	8.9

3.3. Demand Uncertainty Consideration for PEV

A method of minimizing costs associated with electricity purchases from the grid for a household with optimal operation of the integrated PEV system can provide significant benefits to a customer. Figure 3.8 shows that the power flow between the household and PEV is bidirectional.

PEV not only can get charged from the household but can also provide charge to the household with the aim of reducing the cost of the overall energy purchased from the grid.

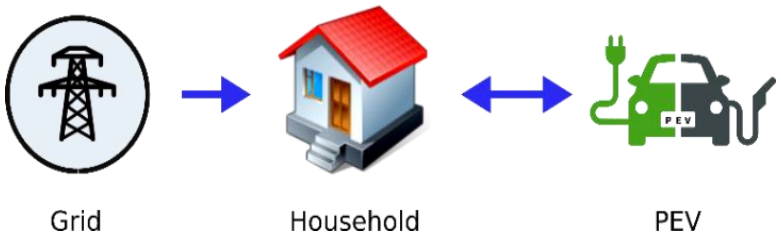

Figure 3.8. PEV charging system.

3.3.1. Model Formulation

In this study, a one-day cycle from 0hr to 24hr with 15-minute resolution is considered for the system. The total 24hr period is divided into T time periods based on time intervals Δt. We consider C_t as the electricity ToU price; $P_{load,t}^{\omega_t}$ is the day-ahead demand forecast for the household; t_{start} is the PEV charge/discharge time in the system; t_{leave} is the time when the PEV leaves (disconnects from) the system. PEV can only deliver power to the household, not to the grid. A penalty factor k is applied to the objective function to ensure that the PEV storage can reach its target SOC level (SOC_{target})before leaving the system. $SOC_{t,leaving}$ is considered as the charge level when PEV leaves or is disconnected. It is important to note that it is not possible for the PEV battery to charge above its target level at the end of the charging process due to the effect of the penalty factor k in increasing the cost. The objective function J and model constraints can be written as:

$$J = \min\left[\sum_{t=1}^{T}\left(P_{grid,t}\, C_t\right) + \left(SOC_{target} - SOC_{t,leaving}\right)k\right] \tag{3.20}$$

Subject to.

A. Power balance constraint:

$$P_{grid,t} - P_{bat_{ch},t} + P_{bat_{disch},t} = P_{load,t}^{\omega_t} \quad (3.21)$$

B. Charge balance constraint:

$$SOC_t = SOC_{t-1} + \frac{P_{bat_{ch,t}} \cdot \eta_{b,ch,t}}{Q_b \cdot \Delta t} - \frac{P_{bat_{disch,t}}}{Q_b \cdot \Delta t \cdot \eta_{b,disch,t}} \quad (3.22)$$

C. SOC upper and lower bounds:

$$SOC_{min} \leq SOC_t \leq SOC_{max} \quad (3.23)$$

$$P_{bat_{disch},t} \leq P_{load,t} \quad (3.24)$$

$$P_{grid,t} \geq 0 \quad (3.25)$$

$$P_{bat_{ch},t}, P_{bat_{disch},t}, SOC_t = 0; [t \leq t_{start}\,; t \geq t_{leave}] \quad (3.26)$$

where $P_{bat_{ch,t}}$ and $P_{bat_{disch,t}}$ are the instantaneous PEV storage device charging and discharging power. There are boundaries for the charging and discharging power that is provided in Table 3.3. $\eta_{b,ch,t}$ and $\eta_{b,disch,t}$ are the charging and discharging efficiencies of the storage device and Q_b is its total storage capacity. The different scenario representations for electricity demand based on the demand forecasts represented by $P_{load,t}$ are obtained using (3.27).

$$P_{load,t}^{\omega_t} = P_{load,t} \pm \rho_t * P_{load,t};\ \omega_t \epsilon \forall \Omega_t \quad (3.27)$$

where ρ_t is drawn from a normal probability distribution and ω_t is the considered scenario from the set of different scenarios Ω_t.

Table 3.3. System parameters for PEV.

Parameter	Value
Battery capacity range, (Q_b)	85 kWh
Maximum operating power of the charger (P_{PV})	10 kW
Efficiency, η_b^c	92%
SOC_{min}	20%
SOC_{max}	80%
Battery type	Li-ion
Time period, t	15 min

3.3.2. Impact of Demand Uncertainty Consideration

The parameters used to represent the system for simulation analysis are listed in Table 3.3. Typical forecasted household summer and winter load profiles are obtained from [147] which are shown in Figure 3.9 and Figure 3.13, respectively. The summer and winter time-of-use (*ToU*) rate for residential customers is given in Figure 3.10 and Figure 3.14, respectively which are provided in [155]. Since load demand profiles are considered as a stochastic parameter, a normally distributed random noise is applied to generate different scenarios based on the forecasted household demand profiles. For simulation, PEV is plugged into the system at 6:00 PM with 30% of SOC and it is assumed that it will leave at 7:00 AM with a desired SOC of 60% on the next day. Generally, when no control is applied to the system, PEV starts charging instantly when it is plugged into the grid. The model's objective is to control the charging/discharging to minimize the overall cost to the customer for a particular day. SDDP solves the multi-stage stochastic program designed for this problem and provides a control policy which is used to calculate cost savings per day for two different seasons.

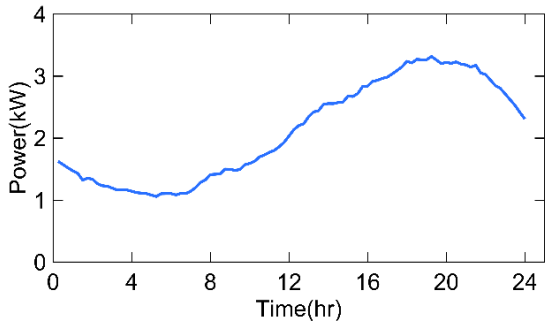

Figure 3.9. Forecasted summer household profile.

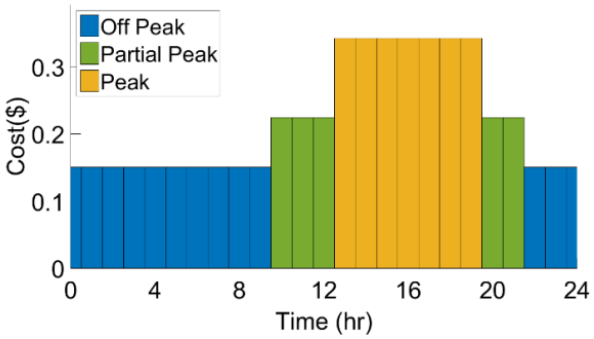

Figure 3.10. Summer *ToU* rate.

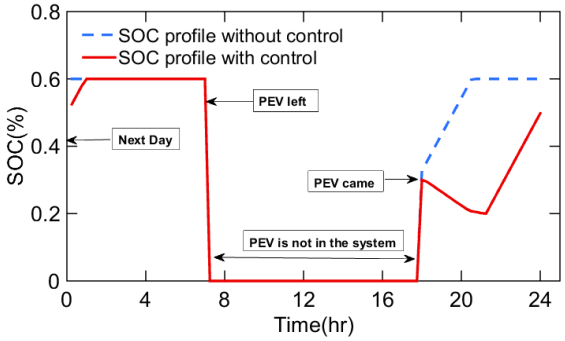

Figure 3.11. Comparison of SOC profiles of PEV storage when no control is applied and when control is applied to summer profile.

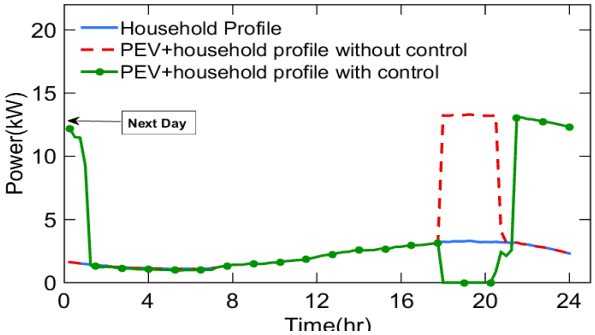

Figure 3.12. Comparison of household profiles including PEV charging/discharging when no control is considered and when control is applied to summer profile.

For the same level of initial charge and time period, SDDP is applied for PEV charging/discharging strategy for two days of different seasons as ToU rate and load profile change with the season. Figure 3.11 and Figure 3.15 represent the SOC level for cases with and without control during summer and winter periods, respectively. SOC is considered as zero when PEV is not present in the system. The controlled and uncontrolled electricity demand from the power grid is provided in Figure 3.12 and Figure 3.16. It can be seen that for both seasons in the controlled case when the *ToU* rate is higher, the available energy stored in the battery is mostly used to satisfy the household demand and reduce the overall electricity purchase cost for the customer. Thus both SOC and electricity purchases from grid reduce. But when the *ToU* rate becomes low, the storage system starts charging to avoid the penalty cost which is introduced in the objective function. As

a result, SOC increases and electricity demand becomes higher during that period. For the summer season, cost remains comparatively higher until 21:00 hr. Therefore PEV does not start charging until that period. Rather it discharges until it's lower SOC threshold level to reduce the overall cost which is shown in Figure 3.11. According to Figure 3.12, demand increases as PEV starts charging after 21:00 hr. During winter peak hour which occurs between 17:00 hr – 20:00 hr, PEV discharges according to the load demand to minimize cost. During this period, SOC decreases and load demand with control goes down as it can be seen from Figure 3.11 and Figure 3.12. Since the load demand for winter was not as high as summer season, PEV did not reach the lower threshold level of SOC. Furthermore, it can be seen from Figure 3.15 and Figure 3.16, for winter off-peak period, PEV started charging just after 20:00 hr and thus the load demand started to increase significantly.

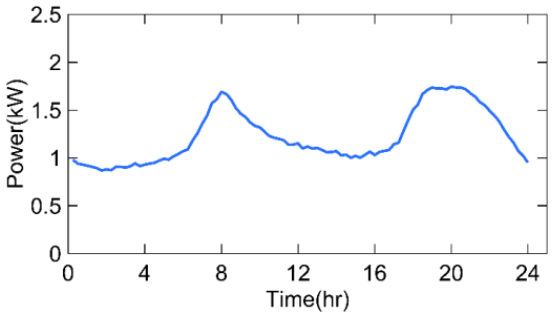

Figure 3.13. Forecasted winter household profiles.

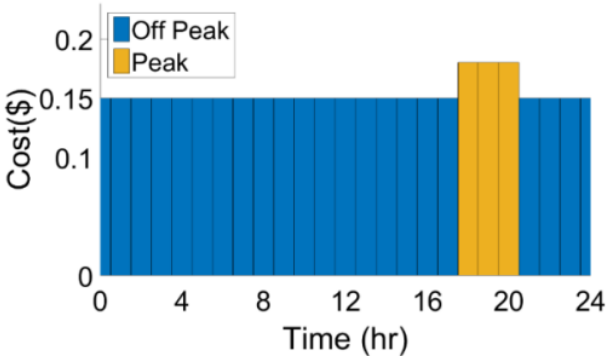

Figure 3.14. Winter *ToU* rate.

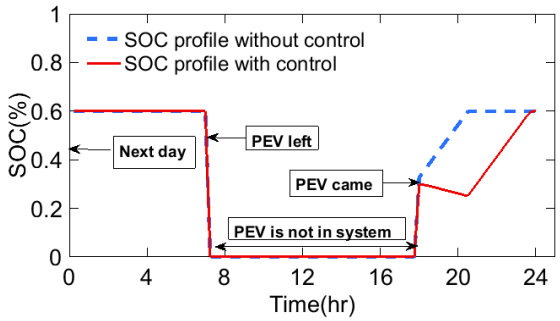

Figure 3.15. Comparison of SOC profiles of PEV storage when no control is considered and when control is applied to winter profile.

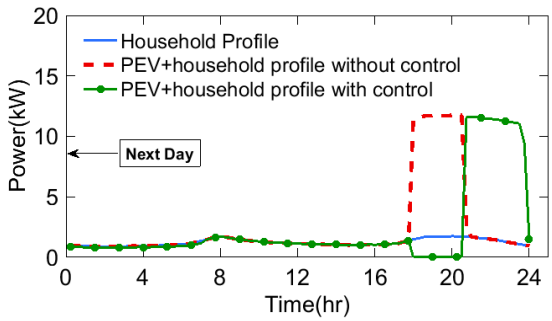

Figure 3.16. Comparison of household profiles including PEV charging/discharging when no control is considered and when control is applied to winter profile.

Table 3.4. Comparison for different cases.

Case	Summer	Winter
	Electricity purchase cost per day ($)	Electricity purchase cost per day ($)
Without Control	19.7	9.2
DDDP	14.3	8.5
SDDP	14.1	8.2

Table 3.4 shows the cost savings per day comparison for the different cases. To get the impact of considering the stochastic and deterministic case, the deterministic forecasted profile is applied to the dual dynamic programming algorithm instead of the stochastic scenario tree of Figure 3.1 (a). This control algorithm is called deterministic dual dynamic programming (DDDP). For policy evaluation, Benders' cuts determined from both the SDDP and DDDP algorithm are applied to 100 randomly independent scenarios to test the performance of the different control policies in out-of-sample cases. Then the average costs of the scenario are computed for each control strategy. According to the results presented in Table 3.4, for the instances used for this analysis, the control strategy obtained using the SDDP algorithm provides better results compared with other strategies.

3.4. PEV with PV-Storage Hybrid Unit

A household system consisting of a PV-storage hybrid unit and PEV is shown in Figure 3.17. The PV panel delivers energy to the household and also to the energy storage through a DC bus and AC-DC converter. Energy storage is connected to the same DC bus through a bidirectional DC-DC converter. PEV is connected to the household with another DC bus through a bidirectional converter. From DC bus to household, DC-AC inverters are connected. In this configuration, the PV- storage hybrid unit and the PEV can only deliver power to the household. The PV panel and the energy storage devices do not deliver power to the grid; hence, there is no reverse power flow

to the grid. The household load and PEV can receive power from the grid, the PV panel, and the energy storage. PV panel, storage and PEV can communicate to a controller through modbus communication. The controller sends the charge/discharge command to control the energy storage.

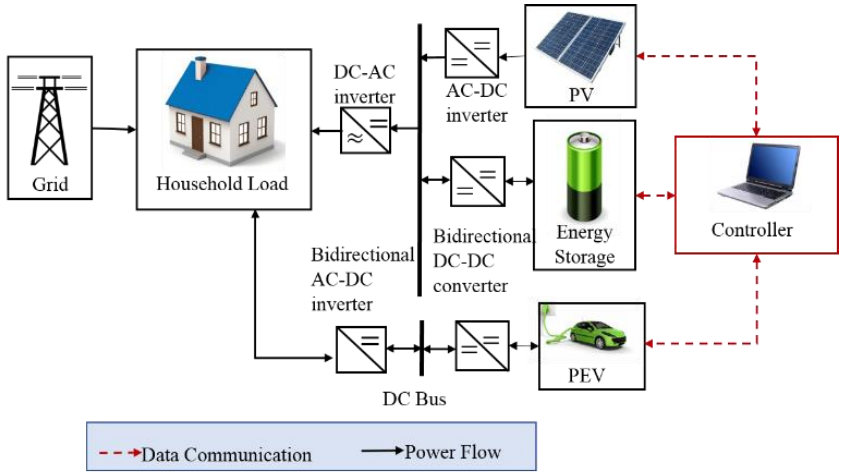

Figure 3.17. PV-Storage hybrid unit in a household system.

3.4.1. Model Formulation for Coordinated Control

Cost minimization of a household with optimal operation of energy storage devices integrated with PV and PEV in a system can significantly benefit a customer. In this study, a one-day cycle from 0hr to 24hr with a 15-minute resolution is considered. The total 24hr is divided into T time periods based on a resolution Δt. Let C_t be the *ToU* electricity tariffs, $P_{L,t}^{\omega_{L,t}}$ and $P_{PV,t}^{\omega_t}$ are the generated load and solar profiles from the sets of all generated load and solar profiles $\Omega_{L,t}$ and $\Omega_{PV,t}$, correspondingly. $P_{g,t}$is the power demanded from grid at time *t;* a penalty factor *k* is applied to the objective function to ensure that the PEV storage can reach the target *SOC* level SoC_{tar} before leaving the system. $SOC_{t,leave}$ is considered as the charge level when PEV will leave the household. It is important to notice that it is not possible for the PEV battery to charge above its target level at the end of the charging process due to the effect of the penalty factor *k* as it will significantly

increase the total cost. C_d is another penalty factor which is assigned to avoid discharging of the PEV, $P_{d,t}^{PEV}$ during off-peak hour. If this penalty term is not introduced in the objective function, then the PEV will discharge up to the threshold level to minimize the cost function. If the PEV discharges during off-peak hours to its threshold level, it will have to charge again to reach its target level for the next day. As charging during off-peak hours is economical, it will prefer to regain charge during the off-peak hours. So, charging and discharging during off-peak hours will not be economical, and will cause energy loss. To avoided discharging during off-peak hour, this penalty cost is introduced which is chosen between the value of partial peak and off peak *ToU* rates. The objective function *J* and model constraints are written as:

$$\min J = \sum_{t=1}^{T} [(P_{g,t}\, C_t) + |SOC_{tar} - SOC_{t,leave}|k + C_d P_{d,t}^{PEV}] \tag{3.28}$$

A. Power balance constraint:

$$P_{g,t} - P_{c,t}^{PV} + P_{d,t}^{PV} - P_{c,t}^{PEV} + P_{d,t}^{PEV} - P_{def,t} = P_{L,t}^{\omega_{L,t}} - P_{PV,t}^{\omega_{PV,t}} \tag{3.29}$$

B. Charge balance constraint:

$$SOC_t^{PEV} = SOC_{t-1}^{PEV} + \frac{P_{c,t}^{PEV}\eta_{PEV}}{Q_{PEV}\,\Delta t} - \frac{P_{d,t}^{PEV}}{Q_{PEV}\,\eta_{PEV}\Delta t}, \forall t \in T \tag{3.30}$$

$$SOC_t^{PV} = SOC_{t-1}^{PV} + \frac{P_{c,t}^{PV}\eta_{PV}}{Q_{PV}\,\Delta t} - \frac{P_{d,t}^{PV}}{Q_{PV}\;\eta_{PV}\Delta t}, \forall t \in T \tag{3.31}$$

C. Charge and discharge operational limits based on PV and load respectively

$$P_{c,t}^{PV} \le P_{PV,t}^{\omega_{PV,t}}, \forall t \in T \tag{3.32}$$

$$P_{d,t}^{PV} - P_{c,t}^{PEV} \le P_{L,t}^{\omega_{L,t}}, \forall t \in T \tag{3.33}$$

$$P_{d,t}^{PV} + P_{d,t}^{PEV} \le P_{L,t}^{\omega_{L,t}}, \forall t \in T \tag{3.34}$$

$$C_t^{off\_peak} \le C_d \le C_t^{partial,peak} \tag{3.35}$$

$$k > 0 \tag{3.36}$$

D. Non-negativity requirement for purchases from the grid

$$P_{g,t} \geq 0 \,, \forall t \in T \tag{3.37}$$

E. Upper and lower bounds for the model decision variables

$$SOC_{min}^{PEV} \leq SOC_t^{PEV} \leq SOC_{max}^{PEV} \,, \forall t \in T \tag{3.38}$$

$$SOC_{min}^{PV} \leq SOC_t^{PV} \leq SOC_{max}^{PV} \,, \forall t \in T \tag{3.39}$$

$$P_c^{PEV\_min} \leq P_{c,t}^{PEV} \leq P_c^{PEV\_max} \,, \forall t \in T \tag{3.40}$$

$$P_d^{PEV\_min} \leq P_{d,t}^{PEV} \leq P_d^{PEV\_max} \,, \forall t \in T \tag{3.41}$$

$$P_c^{PV\_min} \leq P_{c,t}^{PV} \leq P_c^{PV\_max} \,, \forall t \in T \tag{3.42}$$

$$P_d^{PV\_min} \leq P_{d,t}^{PV} \leq P_d^{PV\_max} \,, \forall t \in T \tag{3.43}$$

where $\omega_{L,t} \epsilon \forall \Omega_{L,t} \,, \forall t \in T$ and $\omega_{PV,t} \epsilon \forall \Omega_{PV,t} \,, \forall t \in T$

In the system under consideration, $P_{def,t}$ is defined to be the deferred energy amount, $P_{c,t}^{PV}$ and $P_{d,t}^{PV}$ are the instantaneous charging and discharging power of the energy storage, $P_{c,t}^{PEV}$ and $P_{d,t}^{PEV}$ are the instantaneous charging and discharging power of the PEV. SOC_t^{PV} and SOC_t^{PEV} are the state-of-charge of the energy storage and PEV at time *t*. The lower and upper bounds of decision variables are provided in Table 3.5. The parameters Q_{PV} and Q_{PEV} are the total capacity, η_{PV} and η_{PEV} are the storage charger efficiency and the PEV charger efficiency, respectively.

This problem is based on two basic assumptions. First, the grid can only deliver power to the household; there is no net metering compensation provided. Second, the storage devices can only be charged by using solar PV generation and they discharge only to deliver power to the household. A multi-stage stochastic model is represented and then the SDDP algorithm is employed to solve it.

3.4.2. Scenario Generation

One important step to model and solve the energy management problem under uncertainty (or stochastic energy management) in a multi-stage context is to develop a scenario tree to represent possible events associated with the existent random parameters. Solar PV generation and electricity

demand are sampled from probability distributions, defined using information based on existent data, in order to construct a sampled scenario tree with different scenarios. A straightforward way to model random variables that represent solar PV generation and electricity demand in a scenario tree is to assume that vectors are interstage independent. Interstage independence from one period to the next means that the realization of the random variable at a future stage has no relationship with the realization of random variables from previous stages. As solar generation and electricity demand vary due to weather, temperature, cloud cover and other patterns it is reasonable to assume that this information can be treated as independent over time to forecast solar radiation. For example, one could imagine a forecasting model (e.g. a Multi-layer perceptron neural network model) for electricity demand based on temperature forecasts, i.e., once trained, this model would receive future temperature forecasts and come up with demand forecasts without relying on the previous information.

In order to generate more realistic scenarios for demand and solar PV generation, it is important to represent the correlation between these two random variables. To accomplish that, past data are used to estimate the existing correlation between solar PV generation and electricity consumption. Once the correlation is computed, one way to represent this information and generate combined scenarios for solar PV generation and electricity demand is to perform independent draws from normal distributions $\mathcal{N}[\mu, \sigma^2]$ (where μ is the average and σ^2 is the variance of the probability distribution) and then pass the correlation between the parameters using the Cholesky decomposition approach [156]. Suppose the number of stages is T and number of uncertain parameters is n. Let X be a matrix ($T \times n$) with independent identically distributed draws from a normal distribution $\mathcal{N}[0,1]$, and let R be the correlation matrix between electricity demand and solar PV generation. The Cholesky decomposition of R is a lower triangular matrix L such that:

$$R = LL' \tag{3.44}$$

$$Y = LX \tag{3.45}$$

where Y will then be a matrix with correlated draws. Thus, Y will correspond to draws from $\mathcal{N}[0, \Sigma]$. The original draws are from a $\mathcal{N}[0,1]$, and the covariance matrix $\Sigma = R$. If we want correlated draws for electricity demand and solar PV generation, for households $i = 1, 2, \ldots, N$ at some stage *t* given by $\mathcal{N}_{j,i}[\mu_i, \sigma_i^2]$, we can multiply the draws from column *i* of the *Y* matrix by σ_i and add the mean μ_i associated with electricity demand (when generating values for demand) and solar PV generation (when generating values for solar PV) that were estimated using past data. For example, an element of the matrix Y, say $y_{j,i}$ corresponding to the *j*-th draw, can be defined as (3.46):

$$\hat{y}_{j,i} = \mu_i + y_{j,i} \cdot \sigma_i \tag{3.46}$$

Thus (3.46) will be a draw from $\mathcal{N}[\mu_i, \sigma_i^2]$. By following this procedure it is possible to generate scenarios for our random parameters taking into account the correlation structure among them. During night, the scenario realizations of solar PV generation are considered to be zero and the correlation between electricity demand and solar PV generation is not considered. In other words, during the night period, the generated solar PV generation values are zero and random for the electricity demand, which are generated considering only its own probability distribution.

3.4.3. Impact of Coordinated Control with PV and Demand Uncertainties

In this section, the computational results are illustrated to show the impact of coordinated control. The system parameters used for simulation analysis are listed in Table 3.5. Forecasted solar power profile for a summer day and a typical household summer load profile are obtained from [148] and [157], and shown in Figure 3.18. The correlation coefficient between them for this case study is -0.15. The *ToU* rate for residential customer varies during the day based on off-peak, partial peak and peak hours from PGE [155]. PEV is considered to be plugged into the system at

18:00 hr with 40% of *SOC* and it is assumed that it will leave at 07:00 hr on next day with the desired *SOC* of 80% on the next day. The model's objective is to control the charging/discharging of the storage devices to minimize the overall cost to the customer on a particular day. SDDP solves the multi-stage stochastic program designed for this problem and provides control policies to the PV-based storage and PEV storage to increase cost savings per day. The degradation cost of the storage is not considered and have not changed the availability of PEV in the grid. The optimization problem is solved in MATLAB on an Intel Core i5-4600U with a 1-GH CPU, 4 GB of RAM, and 64-bit operating system PC. The accurate degradation modeling of storage and variation in the availability of PEV will be studied further in future work.

Table 3.5. System parameters for coordinated control.

Parameter	**Value**	**Parameter**	**Value**
PV panel installed power capacity	3 kW	SOC_{min}^{PEV} , SOC_{min}^{PV}	20%
PV based battery capacity, (Q_{PV})	4 kWh	SOC_{target}^{PEV}	80%
PEV battery capacity, (Q_{PEV})	85 kWh	SOC_{max}^{PEV} , SOC_{max}^{PV}	80%
η_{PEV}, η_{PV}	92%	$P_C^{PV\_max}$, $P_D^{PV\_max}$	3 kW
Initial SOC_t^{PV}	20%	$P_c^{PEV\_min}$, $P_C^{PV\_min}$ $P_D^{PEV\_min}$, $P_D^{PV\_min}$	0 kW
Initial SOC_t^{PEV}	40%	$P_c^{PEV\_max}$, $P_D^{PEV\_max}$	20 kW

For comparison, heuristic control of PV is considered. In heuristic control strategy, PV based storage is charged when there is an excess of solar generation than demand and discharged when the load is higher than the solar generation. PEV starts charging up to its target level whenever it is present at the grid in heuristic control. Impact of standalone control of PV- storage hybrid unit control and PEV storage control is also shown in result analysis.

A) Effect on Electricity Purchase Savings

The *SOC* profiles of PV based storage and PEV storage for these two control strategies are shown in Figure 3.19 and Figure 3.20. From Figure 3.19, it can be seen that PV based storage

prefers to charge during off-peak and partial-peak hours and discharge during peak hours for coordinated control. It also started charging when PEV leaves from house in the morning. Before that, PV generation is utilized to charge the PEV which is shown in Figure 3.20. As PV generation is utilized to charge the PEV, there remains more capacity for PV based storage to store solar energy. As a result, it shows that PV - storage hybrid unit has reached its threshold level for heuristic control during higher generation. But as PV based storage has higher capacity, it can utilize solar generation more than the heuristic control.

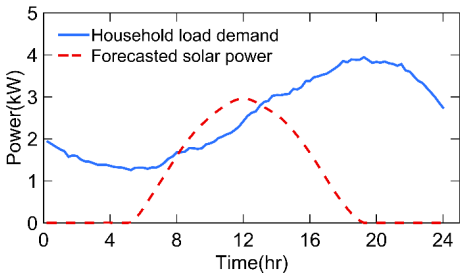

Figure. 3.18. Household and solar generation profiles.

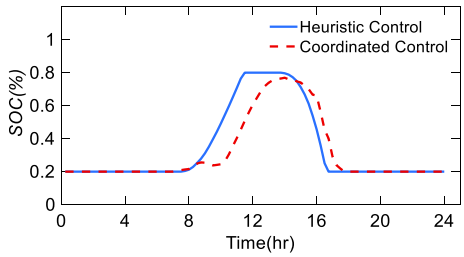

Figure 3.19. *SOC* profiles of PV-based storage.

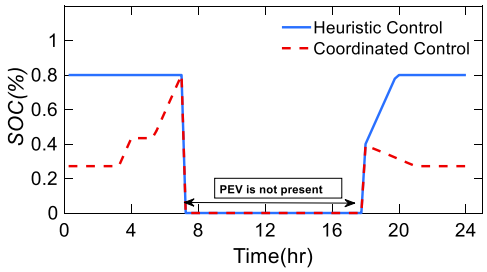

Figure 3.20. *SOC* profiles of PEV storage.

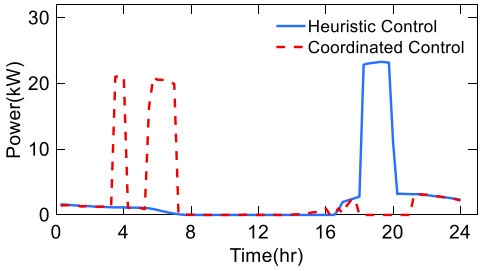

Figure 3.21. Household load profile after control.

From Figure 3.20, it is shown that PEV based storage starts to discharge during peak hours to meet the household demand if coordinated control is applied. Due to this reason, load profile in Figure 3.21 is lower for coordinated control during peak hours. But *SOC* of PEV increases for the heuristic control, as it starts charging whenever it is present in the house. So, load profile in Figure 10 increases for heuristic control during peak hours. As for our case study, it is assumed that PEV will leave next day at 07:00 hr, PEV started charging during the off-peak period for coordinated

case to avoid the defined penalty in the objective function. If a customer wants to get rid of excess charging cost of PEV, he can define the target level of *SOC*. Thus, the load profiles in Figure 3.21 increases during the off-peak hours to charge the PEV for the coordinated case.

Simulations are performed for different seasons due to the variation of load demand, solar generation and *ToU* rate. The impact of standalone SDDP based control for PV storage with heuristic control of PEV and standalone SDDP based control for PEV storage with heuristic control of PV based storage to minimize cost are also considered. The comparison of the electricity purchase costs from the grid for different control strategies is shown in Figure 3.22. It is found that the proposed coordinated control strategy outperforms among all other control strategies. The results show that coordinated control saves about around 37% of cost during summer and 12.7% of cost during winter days than the heuristic control. If the average of these savings is considered, it can be said that in the proposed control strategy can save almost 26% of the cost compared to the heuristic control annually.

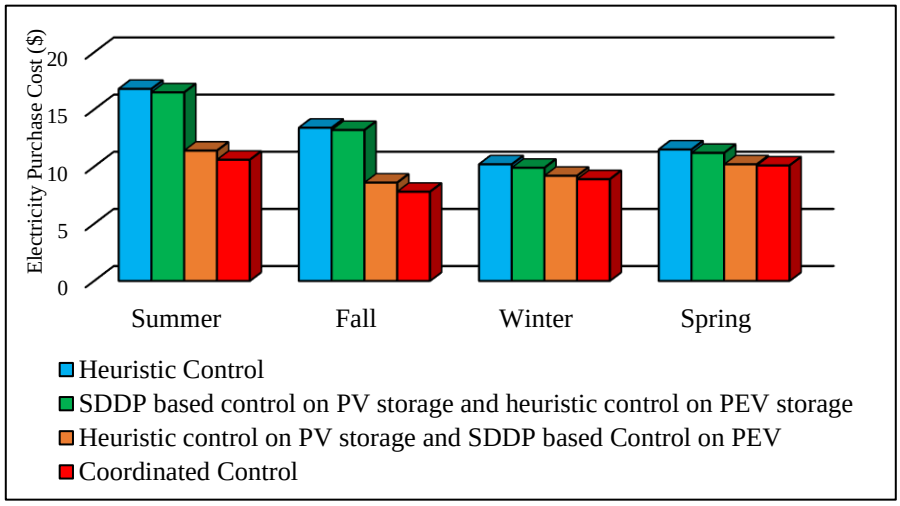

Figure 3.22. Comparison of daily electricity purchase cost for different methods on different seasons.

B) Effect on Peak-hour Savings

Peak hour energy savings help the utility companies to avoid various grid problems such as load variation and congestion or higher local marginal pricing cost. For different methods, peak hour energy savings for different seasons are also calculated which is depicted in Table 3.6. As the heuristic method prefers to discharge PV based storage while load is higher than PV generation and does not consider cost savings, peak hour savings are comparatively lower during summer and fall for this method. There is no peak hour saving for winter and spring as energy storage discharges before peak hour period in this method. For our proposed method, the objective function is to reduce overall electricity purchase cost per day. It tries to reduce peak-hour electricity purchase from the grid by utilizing solar generation and stored energy from energy storage and PEV as much as possible. Thus, peak hour savings are always higher for the coordinated control method.

Table 3.6. Comparison of peak hour energy savings for different methods on different seasons.

Control Strategies	Summer	Fall	Winter	Spring
Heuristic control	30%	21%	0.01%	0.30%
SDDP based control on PV storage and heuristic control on PEV storage	31%	22%	5.7%	5.7%
Heuristic control on PV storage and SDDP based control on PEV	96%	99%	97.5%	97.4%
SDDP based coordinated control	93%	99.7%	99.9%	98%

C) Effect on PV generation usage:

The more solar PV generation will be utilized to mitigate demand, the less energy will be required to be purchased from grid, which is the objective function of our proposed method. As a result, it can be seen that PV generation usage is 100% on our proposed method in Table 3.7. The level of 100% utilization of solar generation gives the maximum return on the investment and the

largest cost savings for the user. When PV based storage is controlled through the SDDP based method, it also ensures 100% utilization of solar generation for all seasons. However, with heuristic control of energy storage, solar generation is deferred during summer and fall due to unavailable capacity of energy storage shown in Figure 3.19. PV generation usage becomes comparatively lower for this control strategy on energy storage presented in Table 3.7. During winter and spring season, solar generation is lower than the demand. Thus, all methods can utilize solar generation.

Table 3.7. Solar generation usage when PEV is present from 18:00 hr for different seasons.

Control Strategies	Summer	Fall	Winter	Spring
Heuristic control	67.7%	59%	100%	100%
SDDP based control on PV storage and heuristic control on PEV storage	100%	100%	100%	100%
Heuristic control on PV storage and SDDP based control on PEV	68%	59%	100%	100%
SDDP based coordinated control	100%	100%	100%	100%

D) Impact of Calculation Time

Due to scenario generation, correlation consideration, and iteration process to reach the stopping criteria, the SDDP algorithm requires comparatively higher time than the heuristic control strategy. As the number of scenarios considered during forward and backward pass increases, the simulation time increases. Compared to the heuristic control strategy, the SDDP method requires more computation time. For 50 forward and 20 backward pass consideration, computation time requirement for different methods are shown in Table 3.8. The data in the table illustrates that due to the increase of the model size and the uncertainty representation in the SDDP control approach, the computation time increases. Higher computational time is the limitation of applying SDDP,

which can be improved with more computational resources and by choosing different strategies for the algorithm of SDDP convergence criteria. It is important to note that the energy management control periods are designed in the scale of minutes and the SDDP based approaches can meet the requirements in reasonable amounts of time.

Table 3.8. Computation time when PEV is present at 18:00 hr on a summer day.

Control Strategies	Computation time
Heuristic Control	4s
Heuristic control on PV storage and SDDP based Control on PEV	63s
SDDP based control on PV storage and heuristic control on PEV storage	142s
Coordinated Control	207s

3.5. Uncertainty Consideration on Energy Management at Community Level

An individual owned solar PV- storage hybrid unit and a community system composed of *N* houses are shown in Figure 3.23 (a) and (b) respectively. The hybrid PV-panel and battery system is considered to be connected on a DC bus. The individual energy management (IEM) strategy is designed considering the system depicted in Figure 3.23 (a) and it is used for energy management in each separate house that is part of the community system. To ensure a higher ratio of solar utilization, it is assumed that the storage devices are not allowed to store energy by charging from the grid.

The shared energy management (SEM) strategy is designed considering together all the households that are part of the community along with their respective solar PV panels and storage devices as the system depicted in Figure 3.23 (b). In this scheme, energy produced by solar PV panels from all houses can flow between the storage devices and the households through a common dc bus [158]. The inverters of the storage devices are considered to have bidirectional capabilities; however, this is used only to satisfy the needs within the community. It is assumed that the storage

devices will only store energy generated from the solar PV panels and discharge to meet the different household demands, but as in the IEM strategy it is not allowed to store electricity from grid purchases and there is no back-feed power to the utility grid.

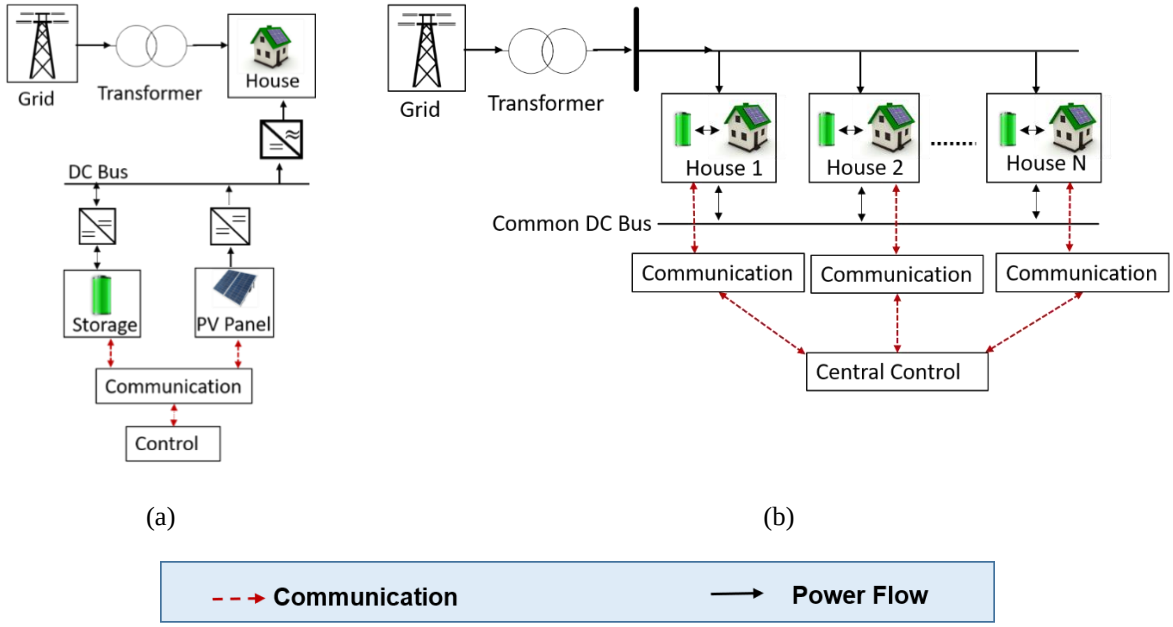

Figure 3.23. (a) Hybrid community system and (b) central control system for storage.

The shared community system can be managed by a communication system composed of smart meters and a charge control unit as described in [159]. The central controller communicates with each house to control the usage of the overall solar PV production between households and charge/discharge patterns of the storage devices through an energy management scheme, which is shown in Figure 3.24. Data from electricity demand forecasts as well as solar PV generation are required to use in an optimization model designed to create the control policies and use them to obtain the optimal energy management including handling storage devices' charging/discharging and power flow among the houses in a given day. For solar PV generation and electricity demand information, a stochastic representation based on data from point forecasts is employed in the scenario generation procedure. It is assumed that each house will receive an equal amount of

credits that will be compensated by the other houses that will use their generated solar PV considering the utility *ToU* rate as a monetary metric. In this assumption, it is considered that the smart meter can measure the electricity usage from the grid and also can track the generated solar PV provided to the community from each household.

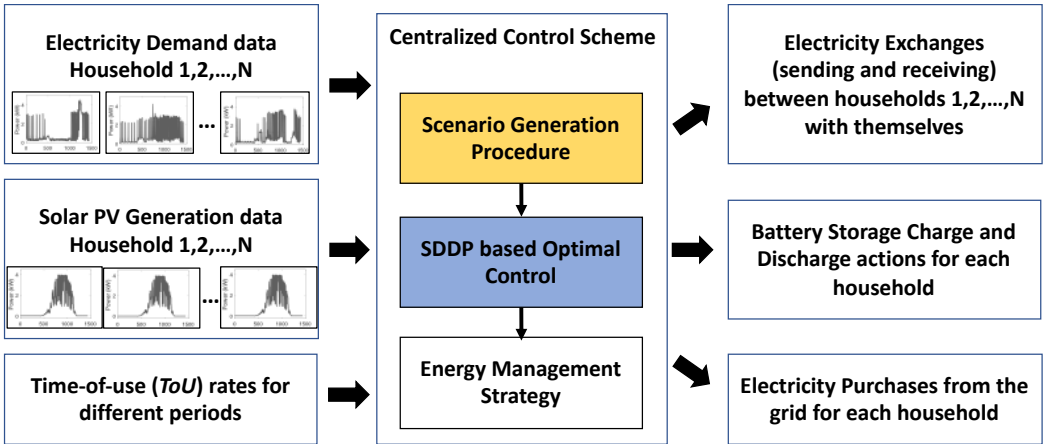

Figure 3.24. Proposed framework for central control based on a shared community system with PV and storage.

3.5.1. Model Formulation

The forecasted household electricity demand and corresponding PV generation profiles for N houses are used as inputs for the community system model. For minimizing electricity purchase costs from the grid, one-day cycle from 0hr to 24hr with a 1-minute resolution is considered. The model formulation, under specific scenario realizations defined by ω, has the objective function J represented in (3.47) and constraints stated in (3.48) - (3.54).

$$\min J = \sum_{t=1}^{T}[C_t \cdot \sum_{i=1}^{N} P_{g,t}^{i}\ ] \tag{3.47}$$

where $P_{g,t}^{i}$ Electricity purchases from the i^{th} house at stage t

Subject to:

i. Power balance equation for the individual house i:

$$P_{g,t}^{i} = P_{dem,t}^{\omega_L^i} - P_{PV,t}^{\omega_{PV}^i} + P_{C,t}^{i} - P_{D,t}^{i} + \sum_{j=1,j\neq i}^{N} P_{i-j,t}^{j} - \sum_{j=1,j\neq i}^{N} P_{j-i,t}^{j} + P_{def,t}^{i}, \forall t \in T, \forall i \in I \tag{3.48}$$

ii. Charge balance constraint for the individual house *i*:

$$SOC_t^i = SOC_{t-1}^i + \frac{P_{C,t}^i \eta}{Q_i \, \Delta t} - \frac{P_{D,t}^i}{Q_i \eta \Delta t} \forall t \in T, \forall i \in I \quad (3.49)$$

$$\sum_{i=1}^{n} P_{C,t}^i \leq P_{PV,t}^{\omega} \, , \forall t \in T \quad (3.50)$$

$$\sum_{i=1}^{n} P_{g,t}^i \geq 0 \, , \forall t \in T \quad (3.51)$$

iii. Upper and lower bounds for decision variables for individual house *i* are:

$$SOC_{min}^i \leq SOC_t^i \leq \ SOC_{max}^i \, , \forall t \in T, \forall i \in I \quad (3.52)$$

$$P_{C,max}^i \leq P_{C,t}^i \leq \ P_{C,min}^i, \forall t \in T, \forall i \in I \quad (3.53)$$

$$P_{D,max}^i \leq P_{D,t}^i \leq \ P_{D,min}^i \, , \forall t \in T, \forall i \in I \quad (3.54)$$

For the above model, $P_{dem,t}^{\omega_L^i}$ and $P_{PV,t}^{\omega_{PV}^i}$ are changed based on each individual household and scenario realization. This problem is solved through multi-stage dual dynamic programming approach.

3.5.2. Energy Storage Capacity Sizing

For the annual energy savings calculation, a variation of *ToU* rate during summer and winter are considered. Load shape of houses and PV profile also change with seasons and has an impact on NPV. For simplification, annual load profiles of a particular house can be divided into four seasonal load profiles: spring, summer, fall, and winter. Four average load profiles are calculated by considering all the load profiles during these seasons. The SDDP algorithm is then applied individually to the load profiles for each season considering corresponding *ToU* rate to minimize electricity purchases from the grid. The cumulative sum of energy savings for the seasons provides the net annual savings.

To calculate NPVs, a discount rate, r (Table 3.7) is used to bring the future cash flows to the current date. Based on the discount rate, NPVs are calculated by considering the replacement of batteries based on their life cycle. Expenditure of battery for the projected time period is calculated with the corresponding equation:

$$C_b = \frac{Q.\Psi.\gamma}{(1+r)^k} \tag{3.55}$$

where C_b is the battery investment cost during solar PV panel life time, γ is storage device cost, Ψ is number of replacements for storage devices, and k is the solar panel life time

As the project span is based on the PV panel life, *ToU* rate will vary during this period. The variation of *ToU* rate for previous 10 years is provided in [155]. This deviation is averaged and implied on the calculation of net energy savings. NPV will be the difference between the saving and expenditure for the entire project. The equation for NPV is

$$\text{NPV} = \sum_{k=1}^{K} \frac{F_s\,(\Delta ToU)^k}{(1+r)^k} - C_b \tag{3.56}$$

Here, F_s is the net annual savings calculated from energy management strategy,and ΔToU is the change of ToU rate for PV panel over years. The flowchart for the NPV based calculation and the determination of optimal energy storage capacity based on the IEM and SEM control strategies for each house and the community is provided in Figure 3.25.

The results of the energy storage sizing discussed above are utilized for each individual house of the shared scenario. This procedure will help to avoid an exhaustive search process by varying the energy storage size of each individual house in the community one by one and find the optimal NPV for the whole community. Thus, the optimal storage size q_i^* for each house is calculated following the flow chart from Figure 3.25. These results help us to get the idea that if a house has lower electricity demand and higher solar PV generation, then its individual storage

capacity requirement is higher than the other houses of the community, which will be reflected between the ratio of the q_i^* and the total individually controlled optimal storage capacity of all houses. Thus, for each of the variation of total community storage, Q_c the storage size of each house, Q_i follows Equation (3.57).

$$Q_i = Q_c \frac{q_i^*}{\sum_{i=1}^{N} q_i^*} \tag{3.57}$$

After getting the storage size for each house, Q_i the SDDP is runs based on the SEM method to find out the net energy savings. The NPV is computed in a similar manner to the IEM control strategy case. The highest NPV value ensures the optimal storage size Q_c^* for the whole community, where Q_c^* is divided among the houses of the community by following Equation (3.57). From the power balance defined in (3.48), it is possible to calculate how much power is exchanged between houses. If a house is sending power to another house, it is assumed that it will get an equal amount of credit computed using the energy amount and the *ToU* rate from the utility company. This energy credit for the first house is a debt. The house that receives energy has to payoff to maintain fairness in the community in terms of exchanges.

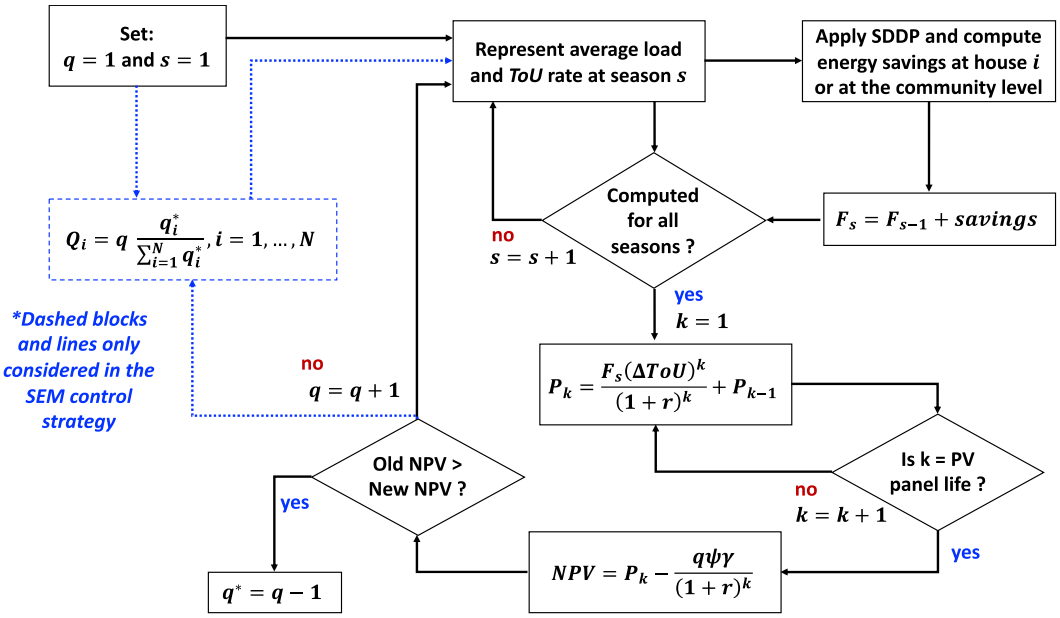

Figure 3.25. Flowchart for optimal storage size calculation for the IEM and the SEM control strategies. The flowchart is applied to each house individually in the IEM control strategy case to obtain q^* and then $q_i^* = q^*$ is set. In the SEM control strategy case q_i^* was previously defined from the results of the IEM analysis and q^* is obtained for the community, and so $Q_c^* = q^*$ is set. Note the dashed lines and blocks are only considered in the SEM control strategy case.

3.5.3. Impact of Shared Energy Management

In order to investigate the importance of the SEM strategy for a community system, it is considered the analysis of the two systems depicted in Figure 3.23. The goal is to evaluate the benefits for the community as a whole and each individual house that is part of that community when the energy management is performed at the system level. Although the analysis is performed considering four seasons of the year and their associated typical days representing different electricity demand and solar PV profiles, it is concentrated here in showing the results only for a typical summer day. The *ToU* rates considered to represent the price that the customer has to pay for electricity purchases from the grid on a summer day is obtained from [155]. The household electricity demand profiles of five houses along with their corresponding solar PV generation

profiles from the same spatial area are obtained from [157] and shown in Figure 3.26. It is to mention that, *ToU* rates (Appendix A) also change for different seasons, and this is considered when applying the SDDP algorithm to solve the model. It is noted that the *ToU* rate considered here does not include demand charges at the residential level, therefore, this *ToU* structure is simply composed of energy charges. However, if a different *ToU* structure was to be considered with the addition of demand charges, the control strategies presented here would again attempt to reduce the overall costs by reducing the peak energy utilization from the grid. Moreover, following the proposed control strategies would potentially help to reduce the community demand contracts with utilities, due to a smaller peak demand, which would potentially incur smaller demand charges and larger benefits to the community.

Table 3.9. System parameters for hybrid houses in a community.

Parameter	**Value**
PV panel lifetime	20 years
Battery lifetime	7 years
Battery capacity	0-7 kWh (Houses); 5-10 kWh (Community)
Battery cost [23]	$350/kWh
Efficiency, η	0.92
Initial *SOC*	20%
SOC_{min}	20%
SOC_{max}	80%
$P_{D,min}, P_{C,min}$	0 kW
$P_{C,max}, P_{D,max}$	5 kW

A) Impact of Electricity Purchase Saving

There is an impact of SDDP algorithm for the shared control scheme to minimize the electricity purchase cost for a summer day. In Figure 3.26, the aggregated solar generation for a day is provided. From Figure 3.27, it can be observed that when the *ToU* rate is lower and solar energy is available, then as the storages of all houses utilized the solar generation to be charged. Thus the load profile of the shared control scheme did not change though there was solar generation

during that time. They discharged during peak hour periods and maintained enough capacity to store solar energy when demand is lower than the PV generation to reduce the electricity purchase costs. As a result, the aggregated electricity demand during peak hours is comparatively lower. Similarly, SDDP is applied to the selected households individually with their corresponding solar profiles. The simulation results show the benefits of applying the SDDP algorithm to establish the IEM and SEM control strategies, with the goal to minimize electricity purchases from the grid on a typical summer day. A scenario tree with 100 scenarios per stage with 1441 stages is constructed using $\mathcal{N}[0,1]$ to create inter-stage independent scenarios at each stage. The SDDP is applied to the scenario tree in order to obtain the policy (collection of Benders cuts at each stage) for both, the IEM and the SEM strategies. For comparison, a heuristic control policy is also considered. For the heuristic control strategy, solar PV based storage is charged when there is an excess of solar generation (more than the demand) and the device is discharged when the household demand is higher than the solar generation.

From Figures 3.27 and 3.28, it can be observed that when the *ToU* rate is lower and solar energy is available, the household storages undergo charging. Thus, the load profile of the IEM and SEM does not change although there is solar generation during that time. The storage devices discharge during partial-peak and peak-hour periods and maintain enough capacity to store solar energy production when demand is lower than the electricity produced in order to reduce the purchase costs from the grid. As a result, the aggregated electricity demand during peak-hours is comparatively lower for IEM and SEM control strategies. But as it can be observed by following the SEM control strategy the system can store more solar generation (surplus) than in the IEM strategy case, therefore, the SEM strategy helps to alleviate demand during peak time more than

the IEM strategy. With closer observation during peak hours in Figure 3.27 and 3.28, one can notice peak demand reduction from adopting the SEM control strategy.

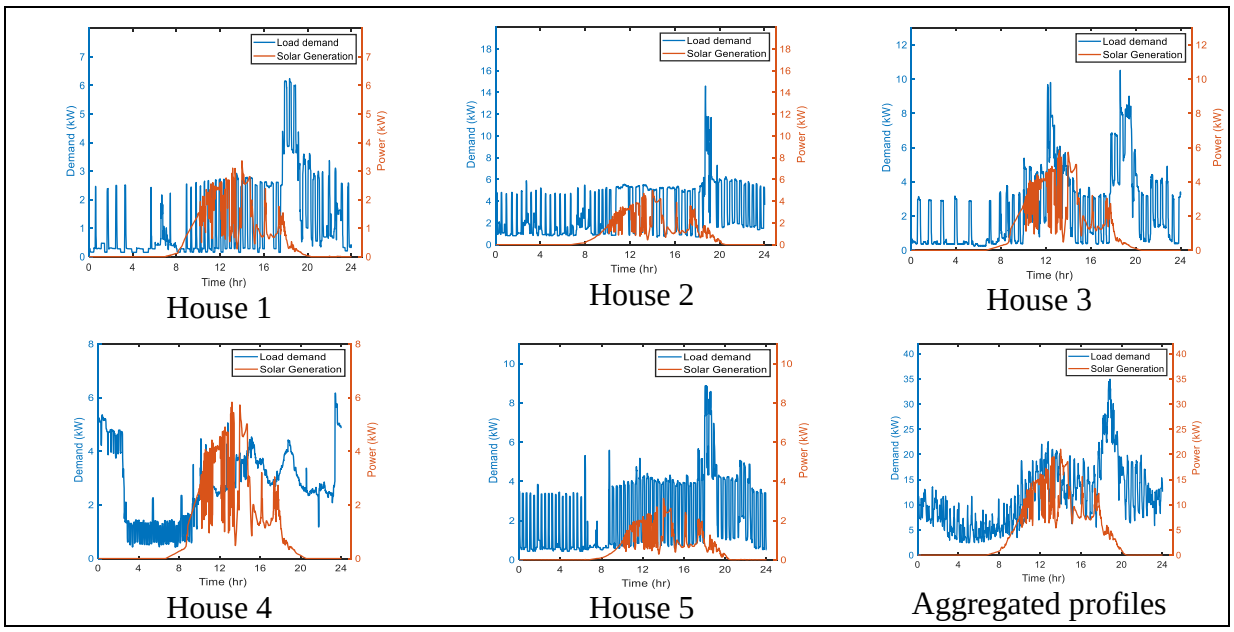

Figure 3.26. Electricity demand and solar generation of five houses on a summer day and their aggregated demand and solar generation profiles.

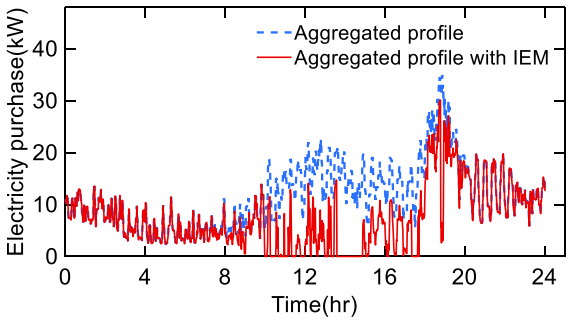

Figure 3.27. Electricity purchases from the grid with and without the IEM control strategy.

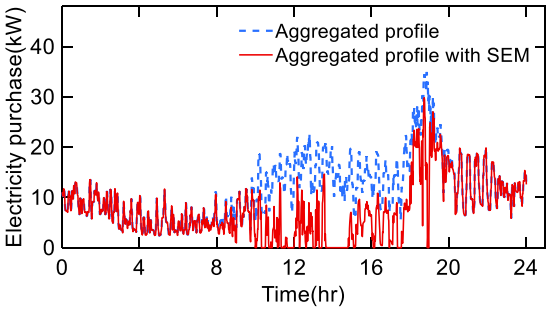

Figure 3.28. Electricity purchases from the grid with and without the SEM control strategy.

Table 3.10. Electricity purchase costs of each house ($/day) for a summer day when no storage is used and different control strategies are used.

	Heuristic	IEM	SEM
House 1	4.7	3.8	3.6
House 2	12.2	11.5	11.3
House 3	8.3	7	6.7
House 4	6.5	6.2	5.8
House 5	9.7	9.5	9.4
Total	41.4	38	36.8

Table 3.11. Comparison of different control strategies for a summer day using the aggregated profile of the community.

	Heuristic	IEM	SEM
Electricity purchase ($/day)	41.4	38	36.8
Peak energy savings (%)	43.74	45.5	60.4
PV usage (%)	74.9	93.3	97.8

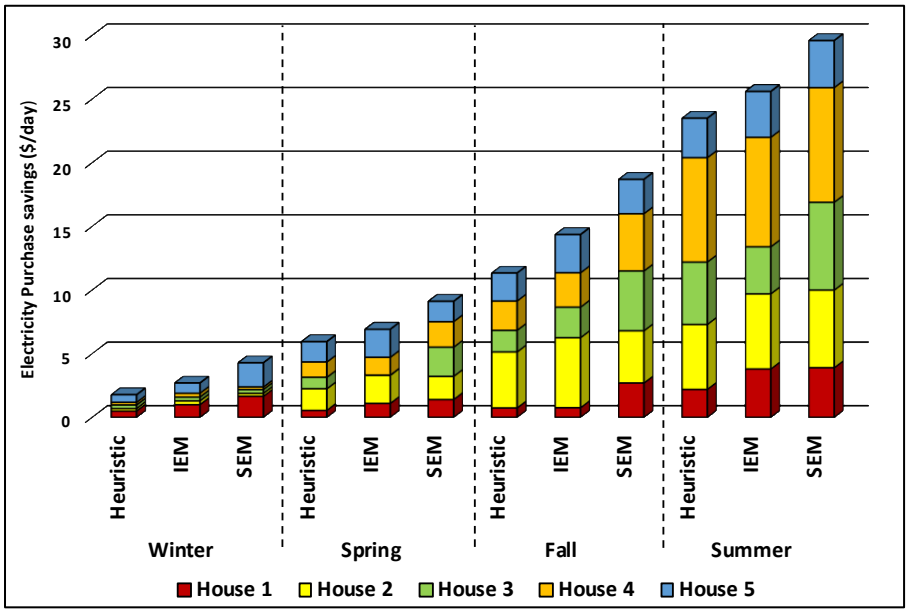

Figure 3.29. Comparison of daily electricity purchase savings (from electricity purchase without solar) for different seasons and different control strategies.

The SDDP is applied to the households with their corresponding solar and demand profiles for standalone IEM control. To compare the impact of different control strategies, a policy evaluation analysis is performed by generating 1,000 independent and random forward paths to represent future possible scenario realizations for the uncertainty parameters considering the summer season (when the demand and solar generation are at their peak). The policies obtained by running the SDDP in the original scenario tree are then separately applied to each individual forward path and the model (3.47) - (3.54) is simulated to minimize the cost at each stage of each forward path scenario. Then the average value of 1,000 profiles (each representing the sum of the costs of all the stages associated with one forward path scenario) for each house is considered as the point estimator for the total cost in our analysis. During our simulations, the optimal storage capacity is used for each house (more details are discussed in the next subsection). The comparison results of energy purchases from the grid for each house, overall peak shaving, and solar PV generation usage are presented in Table 3.10 and Table 3.11. Our results show that the suggested shared storage usage along with the SEM control strategy outperforms the individual ownership storage with heuristic or IEM control strategies in terms of minimization of net electricity purchase costs for the homeowners. A similar analysis is conducted for demand and solar PV profiles of three other seasons considering the *ToU* rate for the corresponding seasons. The electricity purchase savings from grid for different methods are shown in Figure 3.29. It ensures the total electricity consumption reduces in the SEM control strategy for all seasons compared to other methods.

B) Impact on Energy Storage Capacity Sizing

The optimal capacity of storage sizes for the IEM and SEM control strategies for five houses are calculated based on the method discussed in Section 3.5.2. The results of NPV

calculation for five houses based on the IEM strategy are shown in Figure 3.30. Figure 3.31 presents the NPV calculation results based on the SEM strategy applied to the aggregated profile. The optimal storage sizes are selected based on the maximum NPV values for both control strategies. For the SEM control strategy, following equation (3.57), the storage size for each house is calculated. The comparison of storage sizes for five houses based on the IEM and the SEM control strategies with the proposed sizing method is shown in Figure 3.32. To increase the surplus solar PV generation usage, a comparatively higher storage capacity is required for individually owned and controlled storage devices. On the other hand, the household with surplus solar PV generation receives equal credits valued by *ToU* rate to supply the excess energy to the other houses that participate in the community SEM control strategy. Therefore, the houses with higher solar PV generation will prefer to save the energy produced for meeting their peak demand first and then send the excess to the other houses in order to meet other community needs instead of storing in their batteries. This allows for the individual storage devices capacities to be reduced for each house when it is compared to the IEM control strategy case. Though the capacity of storage reduces for SEM control strategy, the overall solar PV energy usage increases. Thus, the storage sharing will provide benefits for individual houses with a reduction in their electricity purchase and investment costs.

The comparative results between the IEM and the SEM control strategies are presented in Figure 3.33. The cost and the storage capacity size reductions improve the NPV in the SEM control strategy compared to the IEM control strategy. Due to the comparatively higher electricity purchase costs shown in Table 3.10, it is expected that the heuristic control strategy will show lower NPV than the IEM and the SEM control strategies for the same size of storage. Thus the comparison of storage size for heuristic control strategy is not shown.

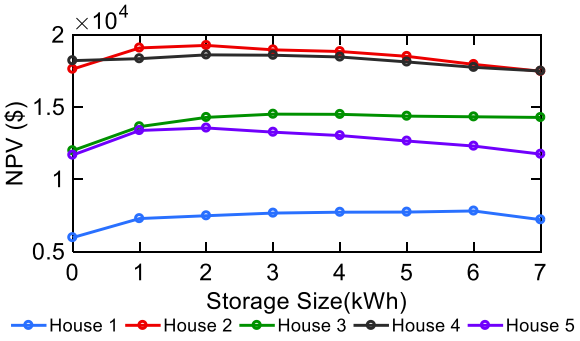

Figure 3.30. NPVs of houses for different storage sizes for IEM control.

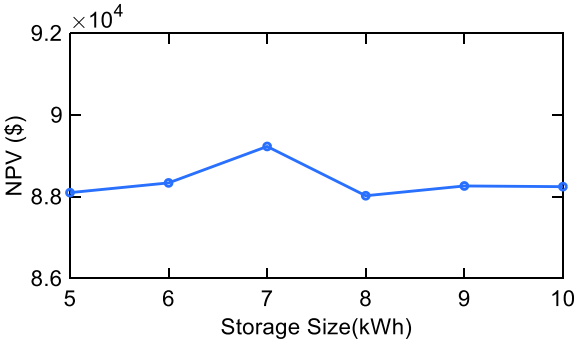

Figure 3.31. NPVs of different storage sizes for SEM control.

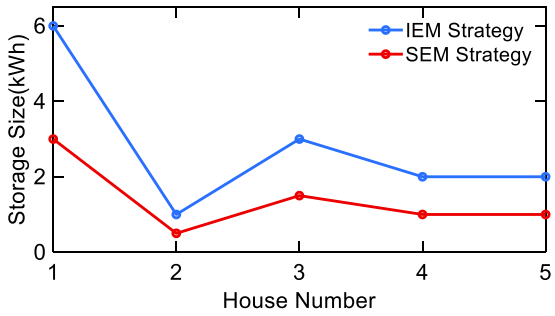

Figure 3.32. Comparison of optimal storage sizes for different houses for IEM and SEM control strategies.

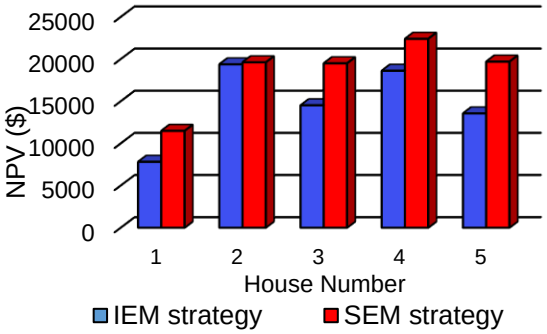

Figure 3.33. Comparison of NPVs for different houses for IEM and SEM control strategies.

3.6. Conclusion

In this chapter, four models are formulated to address the energy management of energy storages considering PV generation and electricity demand uncertainties at the residential and community levels. By modeling these problems as a multi-stage stochastic programming, a realistic representation is created where multiple uncertain scenarios are used with the goal to achieve reliable results in the control process than in the deterministic control representation. The results obtained from applying the SDDP for an optimal state of charge and control trajectories show that by controlling the charging schedule of the PV based storage and PEV storage device, it is possible to minimize the household cost of purchasing power from the grid. At community

level, it shows that optimal scheduling through SEM method helps to improve the economic benefit for the owners of PV- storage hybrid unit.

CHAPTER 4

Distribution Service Restoration Utilizing Demand Response

Indices

t	Index for time.
l	Index for Nodes.
γ	Index for controllable loads.
i	House.
a, b, c	Phases.
$\omega_{L,t}$	Generated scenario for load.
$\omega_{PV,t}$	Generated scenario for solar generation.

Sets

$\mathcal{L}$	Set of all buses in the distribution system.
B	Set of households in a bus.
φ	Set of phases.
$\Omega_{PV,t}$	Set of generated scenario for load.
$\Omega_{L,t}$	Set of generated scenario for solar generation.

Parameters

θ_t^{out}	Outside temperature at time *t*.
$\underline{\theta_t^{in}}, \overline{\theta_t^{in}}$	Minimum and maximum preferable temperature inside house.
α, β	Thermal parameters of the environment and the appliances in household.
$\underline{P_{ac}}, \overline{P_{ac}}$	Maximum and minimum AC power.
Δt	Time interval.
$\underline{E}, \bar{E}$	Maximum and minimum washer-dryer energy demand.
Q_b, Q_{PEV}	Capacity of energy storage and PEV storage.
η	Efficiency of the charger.
$P_{PV,t}$	Solar generation at time period *t*.
$P_{load,t}$	Load demand at time period *t*.
$\underline{SOC_t^B}, \underline{SOC_t^{PEV}}$	Minimum state of charge of energy storage and PEV.
$\overline{SOC_t^B}, \overline{SOC_t^{PEV}}$	Maximum state of charge of energy storage and PEV.
$\underline{P_{b,t}^{ch}}, \underline{P_{PEV,t}^{ch}}$	Minimum charging power of energy storage and PEV.
$\overline{P_{b,t}^{ch}}, \overline{P_{PEV,t}^{ch}}$	Maximum charging power of energy storage and PEV.

$\underline{P_{b,t}^{disch}}, \underline{P_{PEV,t}^{disch}}$	Minimum discharging power of energy storage and PEV storage.
$\overline{P_{b,t}^{disch}}, \overline{P_{PEV,t}^{disch}}$	Maximum discharging power of energy storage and PEV storage.
$\overline{P_{l,t}^{\varphi}}, \underline{P_{l,t}^{\varphi}}$	Maximum and minimum demand at each bus at time period *t.*
T	Total restoration time period.
w_l	Weight factor of each load.
$P_{b,t}, P_{f,t}$	Base and flexible load at time period *t.*
tf_t	Temperature factor.

Variables

θ_t^{in}	Inside temperature at time period *t.*
$P_{ac,t}$	AC load at time period *t.*
$P_{w,t}, P_{d,t}$	Washer- dryer load demand at time period *t.*
E_w, E_d	Washer-dryer energy at time period *t.*
SOC_t^B, SOC_t^{PEV}	State of charge of energy storage and PEV at time period *t.*
$P_{b,t}^{ch}, P_{PEV,t}^{ch}$	Charging power of energy storage and PEV at time period *t.*
$P_{b,t}^{disch}, P_{PEV,t}^{disch}$	Discharging power of energy storage and PEV at time period *t.*
$P_{def,t}$	Deferred solar energy at time period *t.*
$P_{g,t}$	Load demand from grid at time period *t.*
μ_t	Ratio of flexible and critical load.
Γ_i^t	Local target load.
$P_{l,t}^{\varphi}$	Load demand in a bus at time period *t.*
$x_{l,t}$	Determines whether bus is energized or not $\{0,1\}$.
y_l	Determines whether bus is controllable or not $\{0,1\}$.

4.1. Introduction

Electric power utilities are paying more attention to grid resiliency and technologies that can reduce the duration of post-disaster outages. This chapter is concerned with utilizing demand response (DR) to restore loads on unbalanced distribution feeders using a multi time-step dynamic optimization model and a microgrid concept with the presence of distributed generators (DGs) after a major disaster. Because generation resources can be limited after a major disaster, DR can play an important role in increasing the number of customers served, and/or increasing the total amount of load restored. In this chapter, a framework to integrate demand response (DR) with the distributed service restoration (DSR) framework based on a multi-time-step dynamic optimization model is explained.

4.2. Motivation and System Overview

The motivation of utilizing DR on a DSR process is shown in Figure 4.1 for a three-bus sample distribution system. Two DGs of 15kW and 10kW were supplying two loads, L1 and L2, which are assumed to be directly connected to the buses. This system can represent a microgrid that is temporarily formed during restoration by sequentially closing the switches and starting the DGs. From Figure 4.1 (a), it can be seen that DG1 and L2 are already energized, and DG2 must be started by external cranking power. If L1 and L2 are fixed-demand loads, L2 cannot be restored by closing the switch between bus 2 and bus 3, since DG1 will be overloaded and the protection may trip DG1 before starting DG2. However, if DR can be utilized to reduce 5kW load in L1 temporarily, overloading of DG1 can be avoided while restoring L2, as shown in Figure 4.1 (b). After starting DG2 and having sufficient capacity to support L1 and L2, L1 demand can bounce back to normal demand. In this sense, DR can facilitate releasing capacity constraints and can help ride-through some moments when generation (solar, wind, etc.) is temporarily insufficient. DR

can also temporarily improve voltage profile until some components with voltage regulation capabilities are energized, such as voltage regulator, capacitor banks, and dispatchable DGs.

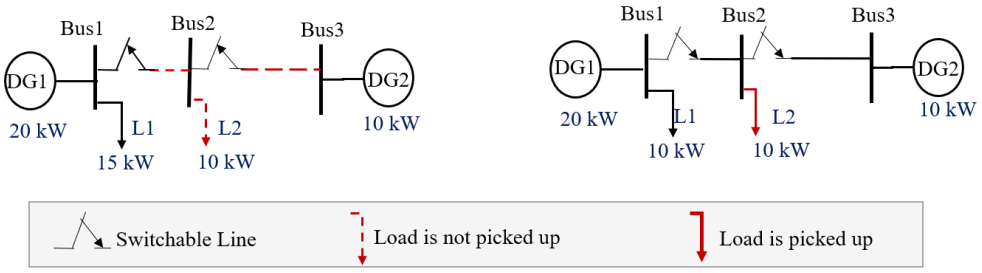

Figure 4.1. Load restoration process of a sample distribution system for (a) fixed load and (b) reduced load.

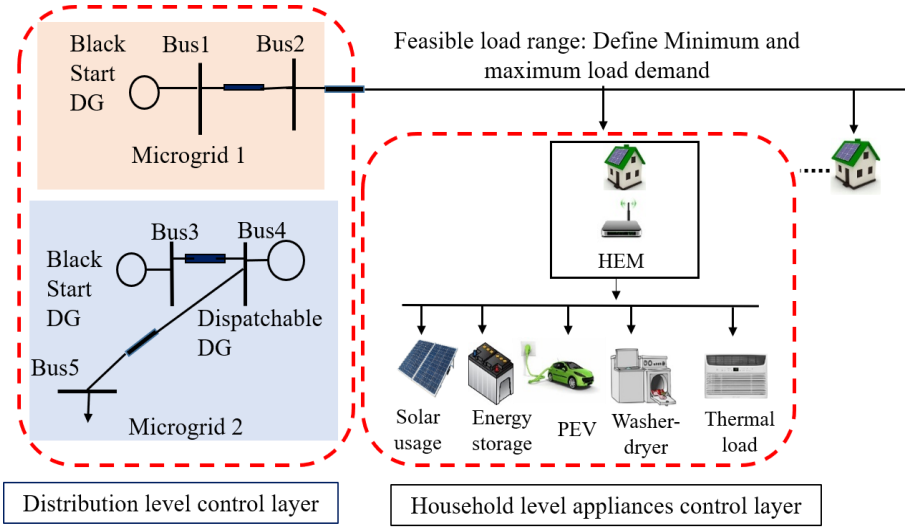

Figure 4.2. Two level direct load control-based architecture from household appliances to the distribution system during restoration process while microgrids are formed in the distribution level.

To leverage the flexibility provided by DR on a particular bus, the feasible range of load variation should be known for each time period. The feasible range can be calculated considering different types of smart appliances in households, which are located in the region served by that particular bus. The two-level control architecture from household appliances to a distribution bus is shown in Figure 4.2. If the homeowners are willing to participate in DR program, they can

communicate with the utility regarding the minimum demand considering reduction of some flexible loads like air conditioners, heaters, washer-dryer, PV- storage hybrid unit, plug-in electric vehicles (PEV) etc. To quantify minimum load considering comfort level of the homeowners, an optimization method is proposed to be performed in the household. The forecasted load demand can be considered as the maximum load demand of the household. As load forecast is not the primary concern of this work, it is assumed that the forecasted load is known beforehand. The aggregated maximum and minimum load range for all the houses located on a particular bus can define its feasible range of load demand. This is step 1 in our proposed framework which is shown in Figure 4.3.

On the second step of the proposed framework, whether a bus is energized or not, controllable or not and how much load demand will be restored in a particular bus of the distribution level to improve DSR, are required to be determined. To obtain answers to these questions, the entire DSR process can be performed through an optimization process. This optimization process can consider the load variation limit along with the constraints such as voltage limit, transformer and line capacity, DG connectivity, DG current unbalance, DG ramp rate, DG output power, load connectivity, sequencing topology similar to [121] to make a decision. If only a subset of nodes is selected to provide DR, the proposed optimization model should find out the optimal selection of the nodes and their corresponding target load profile over the time horizon. This step will define the target load for each bus in the system which is shown in step 2 of Figure 4.3.

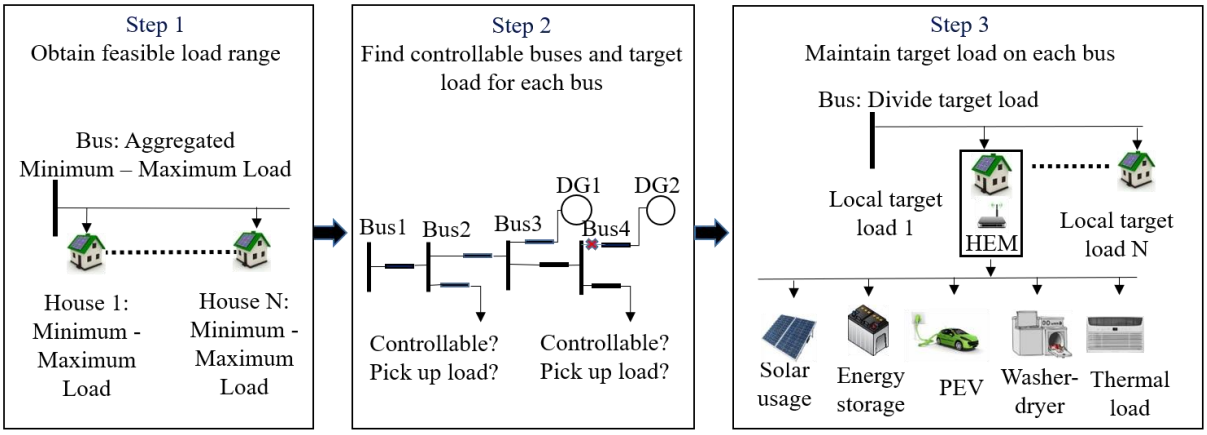

Figure 4.3. Proposed system overview.

After obtaining the target load value from DSR for each bus of the corresponding distribution system, maintaining that load in buses is another issue. This issue can be resolved by scheduling different types of smart appliances at the household level, which is third step in our proposed framework. The target load obtained from step 2 for a particular bus can be divided among all the existing houses considering their flexible and fixed loads. The divided values can be considered as local target load for each house. Local target load can be maintained through home energy management (HEM) system by controlling all the flexible appliances. In HEM, an optimization algorithm can be performed to change the original demand of the flexible loads considering uncertainty while their operational constraints and customers' comfort are maintained. As the control is performed considering the uncertainties at the household level to maintain the target level, the load demand can be considered as deterministic at the distribution level. Target load division among houses, and local target maintenance by controlling the smart house appliances in the house are depicted in step 3 of Figure 4.3.

4.3. Problem Formulation

In this section, three optimization models corresponding to the three steps introduced in Section

4.1 are described.

4.3.1. Optimization Problem 1: Household Level Minimum and Maximum Load

To evaluate the minimum loads for each distribution level node, optimization needs to be performed at the household level considering the duration of the restoration process. Day-ahead forecasted load, solar generation, and atmospheric temperature profiles for each household are considered. For direct load control (DLC), appliances are classified into critical, interruptible and deferrable loads [109]. Household thermal loads, solar generation, PEV, and energy storage are considered as an interruptible load or source. Washer and dryers are considered as deferrable loads. Other loads are considered as critical loads for the household.

For thermostatically controlled loads, such as ACs and heaters, household owners prefer to have indoor temperature at a bearable range. The temperature control equations are set as [109]:

$$\theta_t^{in} = \theta_{t-1}^{in} + \alpha\left(\theta_t^{out} - \theta_{t-1}^{in}\right) + \beta P_{ac,t} \tag{4.1}$$

$$\underline{\theta_t^{in}} \leq \theta_t^{in} \leq \overline{\theta_t^{in}} \tag{4.2}$$

$$\underline{P_{ac}} \leq P_{ac,t} \leq \overline{P_{ac}} \tag{4.3}$$

Equation (4.1) evaluates the temperature change. Equation (4.2) and (4.3) define the comfortable temperature range for a house and AC load power range.

Deferrable loads like washer and dryer depend on energy consumption. The total consumption can be represented as:

$$E_w = P_{w,t}.\Delta t \tag{4.4}$$

$$\underline{E_w} \leq E_w \leq \overline{E_w} \tag{4.5}$$

$$E_d = P_{d,t}.\Delta t \tag{4.6}$$

$$\underline{E_d} \leq E_d \leq \overline{E_d} \tag{4.7}$$

where Equation (4.4) and (4.6) state the energy consumption of washer and dryer. Equation (4.5) and (4.7) define maximum and minimum range of energy consumption of washer and dryer.

If solar generation and energy storage are available in a house, energy storage control is considered using the following equations:

$$SOC_t^B = SOC_{t-1}^B + \frac{P_{b,t}^{ch}.\Delta t.\eta}{Q_b} - \frac{P_{b,t}^{disch}.\Delta t}{Q_b.\eta} \tag{4.8}$$

$$P_{b,t}^{ch} \leq P_{PV,t} \tag{4.9}$$

$$\underline{SOC_t^B} \leq SOC_t^B \leq \overline{SOC_t^B} \tag{4.10}$$

$$\overline{P_{b,t}^{ch}} \leq P_{b,t}^{ch} \leq \underline{P_{b,t}^{ch}} \tag{4.11}$$

$$\underline{P_{b,t}^{disch}} \leq P_{b,t}^{disch} \leq \overline{P_{b,t}^{disch}} \tag{4.12}$$

SOC of energy storage will change based on the charging and discharging power which is stated in Equation (4.8). Energy storage will be charged from the available PV generation based on Equation (4.9). Maximum and minimum level of SOC of energy storage, charging and discharging rate of the charger are defined in Equation (4.10) - (4.12).

Similarly, if PEV is available in a house, the storage charging pattern can be controlled considering the upper and lower bound of the storage and charger rating which is shown below:

$$SOC_t^{PEV} = SOC_{t-1}^{PEV} + \frac{P_{PEV,t}^{ch}.\Delta t.\eta}{Q_{PEV}} - \frac{P_{PEV,t}^{disch} * \Delta t}{Q_{PEV}.\eta} \tag{4.13}$$

$$\underline{SOC_t^{PEV}} \leq SOC_t^B \leq \overline{SOC_t^{PEV}} \tag{4.14}$$

$$\underline{P_{PEV,t}^{ch}} \leq P_{PEV,t}^{ch} \leq \overline{P_{PEV,t}^{ch}} \tag{4.15}$$

$$\underline{P_{PEV,t}^{disch}} \leq P_{PEV,t}^{disch} \leq \overline{P_{PEV,t}^{disch}} \tag{4.16}$$

To include DR, an optimization problem is formulated to minimize the overall load. The mathematical model for the optimization problem for household *i* is described below:

$$H_i = min\left\{\sum_{t=0}^{T} P_{grid,t}^{i}\right\} \tag{4.17}$$

Subject to:

Constraints (4.1) – (4.16) and

$$P_{critical,t} + P_{f,t} - P_{PV,t} - P_{b,t}^{disch} - P_{PEV,t}^{disch} - P_{def,t} = P_{grid,t}^{i} \tag{4.18}$$

$$P_{grid,t}^{i} \leq 0 \tag{4.19}$$

where the flexible loads can be defined as:

$$P_{f,t} = P_{ac,t} + P_{w,t} + P_{d,t} + P_{b,t}^{ch} + P_{PEV,t}^{ch} \tag{4.20}$$

Equation (4.18) is the power balance constraint. As back feeding power to the grid may cause overvoltage and safety issues to the grid, it is avoided by maintaining the constraint defined in equation (4.19). After solving the above problem, the minimum requirement of load is calculated from the grid during the restoration process for each household. The maximum load demand is considered by subtracting the forecasted solar generation from the forecasted load demand of the house. To avoid back feeding power to the grid, negative loads are considered as zero and excess solar generation is considered as deferred energy. Thus, the minimum and maximum loads in bus *l* are:

$$\underline{P_{l,t}^{\varphi}} = \sum_{i \in B} P_{grid,t}^{i} \tag{4.21}$$

$$\overline{P_{l,t}^{\varphi}} = \sum_{i \in B} (P_{load,t}^{i} - P_{PV,t}^{i}) \tag{4.22}$$

4.3.2. Optimization Problem 2: Distribution Level Loads for Each Bus

For the distribution level optimization problem during the restoration period, the procedure described in [121] is followed. The proposed sequential service restoration (SSR) method in [121]

coordinated all the controllable components (e.g. DGs, switchable lines, etc.) in a distribution system to restore as much load as possible across multiple steps ensuring that all the distribution level constraints were satisfied. But coordinated control between load and SSR were not considered. Thus, the optimization model of [121] is extended to pick up as much energy as possible during the restoration period by including the time-varying flexible load constraints. The objective functions and new load variation constraints are defined below.

$$Z = max\left\{\sum_{l\in\mathcal{L}}\sum_{t\in T}\sum_{\varphi\epsilon\{a,b,c\}} w_l.P_{l,t}^{\varphi}.\Delta t\right\} \tag{4.23}$$

Subject to:

$$\underline{P_{l,t}^{\varphi}} \le P_{l,t}^{\varphi} \le \overline{P_{l,t}^{\varphi}} \tag{4.24}$$

$$\overline{P_{l,t}^{\varphi}} - M.y_l \le \underline{P_{l,t}^{\varphi}} \le \overline{P_{l,t}^{\varphi}} + M.y_l \tag{4.25}$$

$$\begin{aligned} x_{l,t}\underline{P_{l,t}^{\varphi}} + \left(x_{l,t} - x_{l,t-1}\right).tf_t.\underline{P_{l,t}^{\varphi}} - M.(1-y_l) \le \underline{P_{l,t}^{\varphi}} \\ \le x_{l,t}.\underline{P_{l,t}^{\varphi}} + \left(x_{l,t} - x_{l,t-1}\right)tf_t.\underline{P_{l,t}^{\varphi}} + M.(1-y_l) \end{aligned} \tag{4.26}$$

$$tf_t = \frac{(1-\alpha)}{\beta} \tag{4.27}$$

$$\overline{P_{l,t}^{\varphi}} = x_{l,t}\overline{P_{l,t}^{\varphi}} + \left(x_{l,t} - x_{l,t-1}\right).tf_t.\overline{P_{l,t}^{\varphi}} \tag{4.28}$$

$$\sum_{l\epsilon L} y_l \le \mathrm{C} \tag{4.29}$$

Other constraints, i.e., system model constraints, system operations constraints, DG operation constraints, connectivity constraints, topological and sequencing constraints; are considered from [121].

Equation (4.24) considers the time-varying flexible load range on each bus of the distribution system, as calculated in Section 3.1. The big-M method is used in equations (4.25)–

(4.26) to ensure that the inequality constraints are applied for controllable buses. Here M is a large number that should be selected carefully. If the load is not controllable, then y_l will become zero. The minimum and maximum loads will be equal to the defined maximum load based on equation (4.25); $x_{l,t}$ ensures if a bus is energized or not in equation (4.26); and y_l becomes 1 if a bus is controllable. For controllable buses, the minimum load requirement will change because the indoor temperature of houses will be equal to the outside temperature before energizing the bus. To include this temperature impact on minimum and maximum load demand just after energizing the bus, tf_t is considered in equation (4.27), which is calculated based on equation (4.1). Thus, equation (4.26) shows that if a bus is controllable and it is energized, then the minimum load demand will increase based on the temperature impact during energization. Maximum load demand of a bus will remain zero until it is not energized. Equation (4.28) ensures this constraint including the temperature impact on maximum load while bus is energized. Because maximum load demand is calculated based on the forecasted load demand, this parameter does not consider temperature impact. A controllable number of buses can be maintained through equation (4.29).

4.3.3. Optimization Problem 3: Home Energy management

The target $P_{l,t}^{\varphi}$ which is calculated from subsection 4.3.2 optimization problem, is divided among the houses of each node following the strategy described in [107]. Based on [107], the load is divided among houses considering the aggregated flexible and fixed loads of each house. The following equation are considered for dividing the target $P_{l,t}^{\varphi}$ among the houses of each bus.

$$\mu_t = \frac{P_{l,t}^{\varphi} - \sum_{i \in B} P_{b,t}^{i}}{\sum_{i \in B} P_{f,t}^{i}} \tag{4.30}$$

$$\Gamma_t^i = P_{baset}^i + \mu_t . P_{f,t}^i \tag{4.31}$$

Here, Γ_t^i is considered as the local target load for each house.

If $\mu_t \leq 0$, it be set as $\mu_t = 0$. In this case, all flexible appliance will be not be turned on in house to maintain the target load. Only the available amount of supply will be provided to the houses to meet its demand.

If $\mu_t \geq 0$, it can be set as $\mu_t = 1$ In this case, all flexible appliance will be turned on to match with the target load in house.

In household level, the optimization problem is formulated as to maximize the load to grid, $P_{g,t}$ by maintaining the target level electricity demand Γ_t^i from the grid.

$$H = max\left\{\sum_{t=0}^{T}\left[P_{g,t}^{i}\right]\right\} \tag{4.32}$$

Subject to:

Constraints (4.1) – (4.16) and

$$P_{g,t}^{i} - P_{def,t} = P_{base,t}^{\omega_{L,t}} + P_{f,t} - P_{PV,t}^{\omega_{PV,t}} - P_{b,t}^{disch} - P_{PEV,t}^{disch}; \tag{4.33}$$

$$P_{b,t}^{ch} \leq P_{PV,t}^{\omega_{PV,t}} \tag{4.34}$$

$$P_{b,t}^{disch} + P_{PEV,t}^{disch} \leq P_{load,t}^{\omega_{L,t}} + P_{f,t} \tag{4.35}$$

$$P_{g,t}^{i} \leq \Gamma_t^i; \tag{4.36}$$

As load demand and solar generation at household level are uncertain, the target load demand can be maintained considering the scenario generation procedure of these two parameters described in chapter 3. The power balance equality constraint considering the generated scenario is shown in Equation (4.33). Equation (4.34) ensures the charging of storage only from solar generation to reduce electricity purchase from grid. Equation (4.35) ensures avoiding back feeding power to the grid to avoid overvoltage issue. Equation (4.36) maintains the power demand to grid up to the target level.

To solve the above maximization problem considering uncertainties, SDDP is applied following the method described in chapter 3.

4.4. Case Study and Analysis

4.4.1. Simulation Set-up

For simulation, IEEE 123 node test feeder is considered [160]. Four faults and seven DGs are introduced in this test feeder to validate the proposed restoration process. Figure 4.4 shows the one-line diagram of IEEE 123 node distribution feeder with faults. The three optimization problems are defined as LP, MILP and SDDP are solved in Gurobi optimization solvers by Python on an Intel Core i7-4600U with a 2-GH CPU, 8 GB of RAM, and 64-bit operating system PC. The restoration time is considered as 8 hours and 1-hour time interval is considered. The parameters of seven DGs are shown in Table 4.1. Status "1" indicates that a black start DG and "1/0" indicates a non-black start DG.

Household load profiles and historical temperature were downloaded from Pecan Street [157] and historical climate data of U.S.A [160], respectively. From [157], the detail load profiles for each electrical appliances and solar generation profiles were imported. For a household, the AC load, washer-dryer, PV based storage, and PEVs are controlled optimally to restore the overall load of the grid for 8 hours restoration period. Residential appliance parameters considered for simulation are provided in Table 4.2. To maintain the spot load level of each bus defined in [160], the number of houses assigned in each bus in a way that the highest value in the maximum aggregated load profile did not go beyond that level. Suppose 40kW spot load at bus no. 16 was assigned. Ten houses were assigned in this bus so that highest value of the maximum aggregated load profile did not go beyond 40kW. For comparison with the proposed method, when DR is not applied for restoration defined as without DR method later.

Table 4.1. Parameters of DGs added to IEEE 123 test feeder.

Parameters	DG1	DG2	DG3	DG4	DG5	DG6	DG7
Bus position	13	18	25	47	60	77	105
Maximum power (MW)	0.9	1.05	1.2	1.5	1.2	0.8	0.7
Minimum power (MW)	0	0	0	0	0	0	0
Maximum reactive power (MVar)	0.7	0.8	0.5	0.5	0.4	0.3	1.2
Minimum reactive power (MVar)	-0.5	-0.5	-0.5	-0.5	-0.6	-0.3	-0.9
Status	1	1	1/0	1/0	1	1/0	1

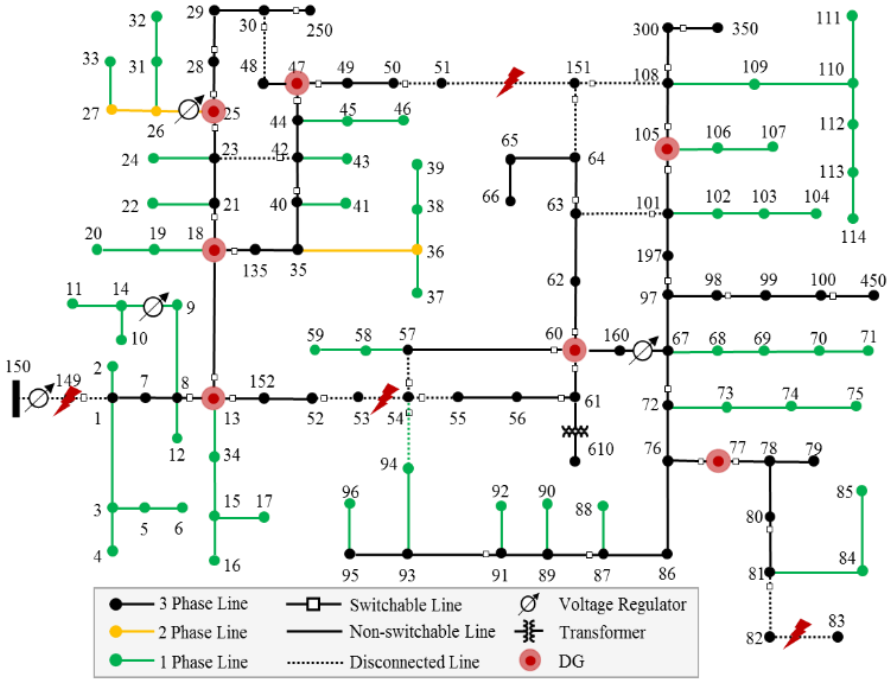

Figure 4.4. IEEE 123 node distribution feeder with faults.

Table 4.2. Residential appliances parameters.

Parameters	Value	Parameters	Value
$\underline{\theta_t^{in}}, \overline{\theta_t^{in}}$	72˚ F, 78˚ F	$\underline{P_{b,t}^{disch}}, \overline{P_{b,t}^{disch}}$	0 kW, 2 kW
α	0.9	$\underline{P_{PEV,t}^{ch}}, \overline{P_{PEV,t}^{ch}}$	0 kW, 2 kW
β	-5	$\underline{P_{PEV,t}^{disch}}, \overline{P_{PEV,t}^{disch}}$	0 kW, 20 kW
$\underline{P_{ac}}, \overline{P_{ac}}$	0 kW, 5 kW	Q_b, Q_{PEV}	4 kWh, 85 kWh
$\underline{E_w}, \overline{E_w}$	0 kW, 2kW.	$\underline{SOC_t^B}, \overline{SOC_t^B}$	20%, 80%
$\underline{E_d}, \overline{E_d}$	0 kW, 2kW.	$\underline{SOC_t^{PEV}}, \overline{SOC_t^{PEV}}$	20%, 80%
$\underline{P_{b,t}^{ch}}, \overline{P_{b,t}^{ch}}$	0 kW, 2 kW	η	92%

4.4.2. Effect of DR in System Resilience Improvement

1) *Without DR*: If the load demands are not controlled with DR, it can be seen in Figure 4.5 that some buses are not energized. It occurs due to the voltage violation with limited DG capacity compared to the requirement of loads. Voltage violation is considered as the constraint during the restoration of the optimization problem defined in Equation (4.20) in [121].

2) *With DR, energy storage and PEV control in the system:* In our proposed approach, we consider the loads are changeable within certain ranges and this change will be implemented through DR. Based on our proposed method, number of preferable controllable buses can be defined. From simulation result, it is found that for 20 controllable buses, all the buses in the distribution are energized. It is as visible in Figure 4.6. Locations of the 20 preferred controllable buses are selected using our proposed optimization method. Other buses are picked up as unchangeable loads. Figure 4.7 shows that, overall, 20% more energy restoration is possible with 20 controllable buses, compared to the without DR restoration method. Optimal load profiles for

all the buses were obtained from the solution of optimization model (4.23)-(4.28) which is maintained through the application of HEM which is described later.

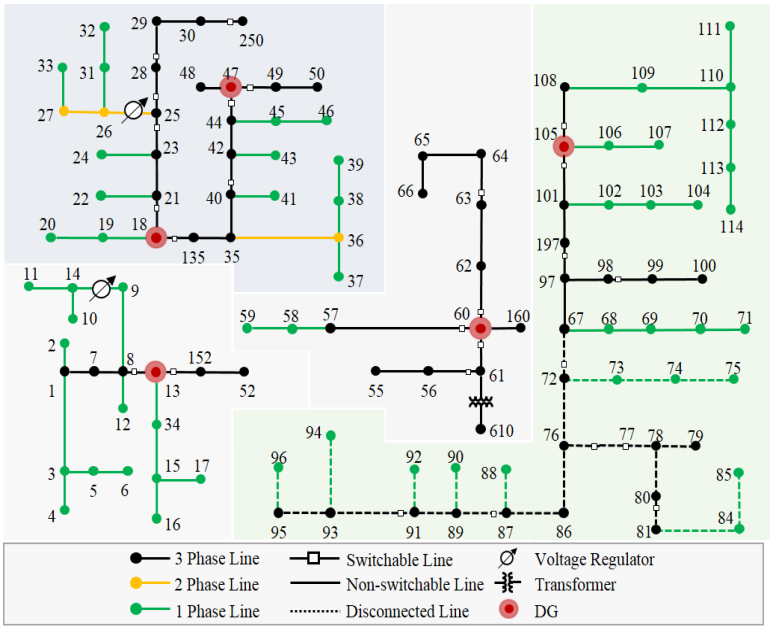

Figure 4.5. Some buses are not energized if loads are not controllable.

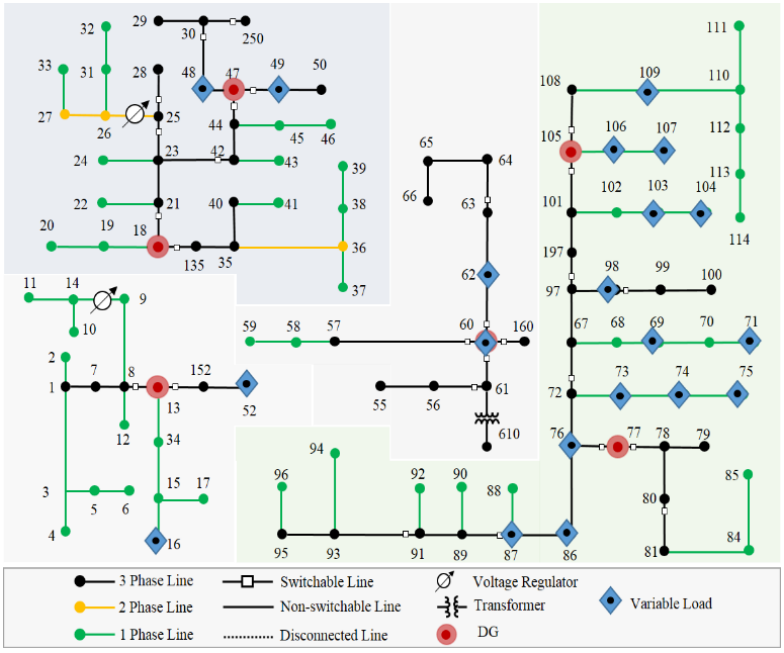

Figure 4.6. All buses are energized by controlling loads of 20 buses within the restoration time.

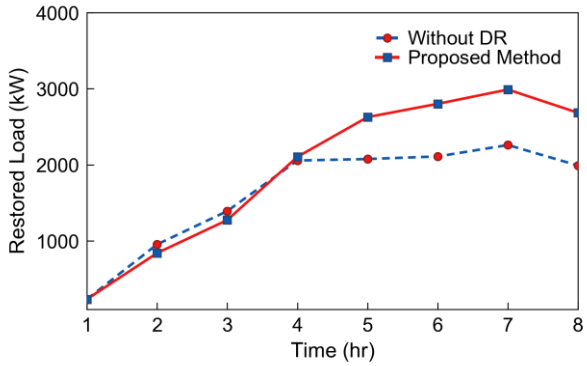

Figure 4.7. Comparison between load restoration at each hour interval without DR and DR based proposed method with 20 controllable buses.

4.4.3. Effect of Optimal Selection of Buses with DR Participation

Figure 4.8 shows the effects of random and optimal location selection of controllable buses. It illustrates that location selected using our proposed method ensures more energy restoration than random selection. It also reveals that with the increase in controllable buses, energy restoration increases. After a certain number of controllable buses, energy restoration becomes saturated. This saturation point can be considered as the 'optimal controllable bus number'. According to Figure 4.8, 'optimal controllable bus number' is 20 for the studied outage condition.

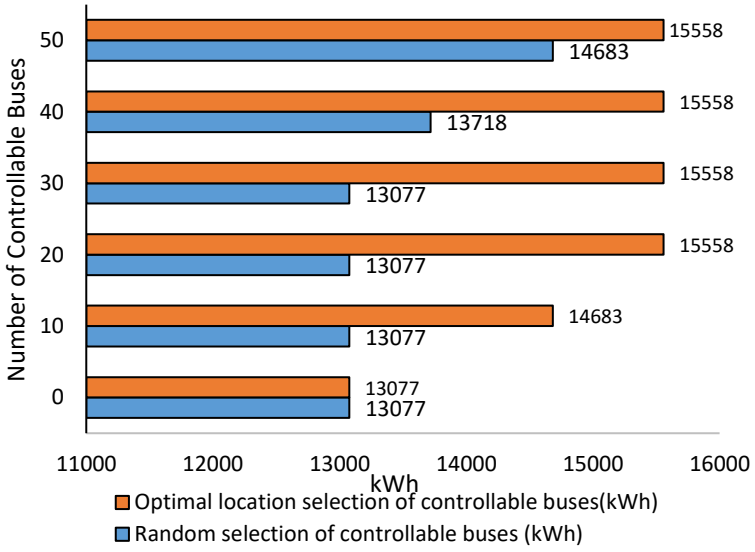

Figure 4.8. Restored energy comparison for optimal selection and random selection for different number of controllable buses.

4.4.4. Effect of Reduction Capacity of DG

If DG capacity decreases or some non-black start DGs are turned off, then the proposed method may need to enable DR on more buses through the optimal selection of controllable buses. In our case study, 2 non-black start DGs (DG3 and DG7) are turned off. According to the performed simulation for different numbers of controllable buses, as illustrated in Figure 4.9, the overall restored energy decreases due to the decrease in the amount of available generation, compared to Figure 4.8. To deal with this scenario where less generation is available, more flexible loads are needed to be controlled to reduce the load demand. Therefore, the optimal controllable bus number increases from 20 to 30 in comparison with Figure 4.8.

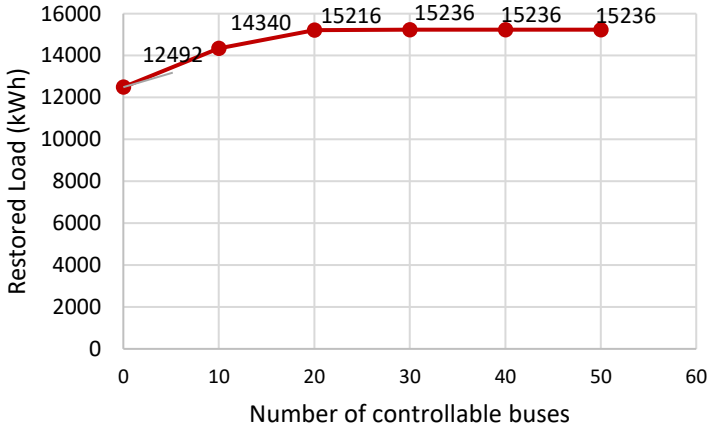

Figure 4.9. Energy restoration for non-black start generators turned off with different number of controllable buses.

4.4.5. Effect in Household Level Demand

The optimal load profiles defined from optimization problem 4.3.2 in a bus are divided among the assigned houses considering their fixed and flexible load demand according to the equation (4.29) and (4.30). Suppose after performing the optimization problem II, the target load at bus 16 are divided as local targets among 10 houses considering their flexible and fixed loads for each time. One household load in bus 16 is shown in Figure 4.10. It illustrates that target load

is increased with time as shown in Figure 4.7. It is also observed that the household load is reduced compared to the maximum load demand which is considered as fixed load for without DR method. It happens due to pick up the overall load in the system. To maintain this reduced load, the flexible appliances are controlled through HEM. Due to the space limitation, scheduled load profile of all appliances cannot be shown. Only indoor temperature control through HEM is shown in Figure 4.11. It shows that indoor temperature is increased from 72° F compared to the without DR method for the proposed method to maintain the target level. HEM maintains the comfortable temperature range which is up to 78° F.

Similarly, another household load of bus 87 can be considered. Based on Figure 4.5 and 4.6, bus 87 is not energized for without DR based method and is energized for proposed method, respectively. Therefore, the household load is restored after 3 hours based on our proposed method while it does not have any restored load for without DR method which is shown in Figure 4.12. Considering Figure 4.10 – 4.12, it can be said that our proposed approach helps to restore energy in one house by reducing flexible load demand from another house ensuring comfort level.

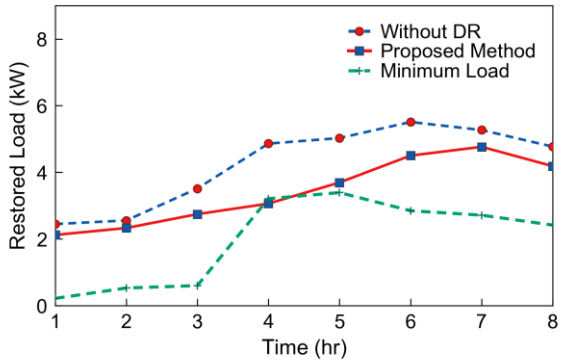

Figure 4.10. One household profile for without DR and proposed method at bus 16.

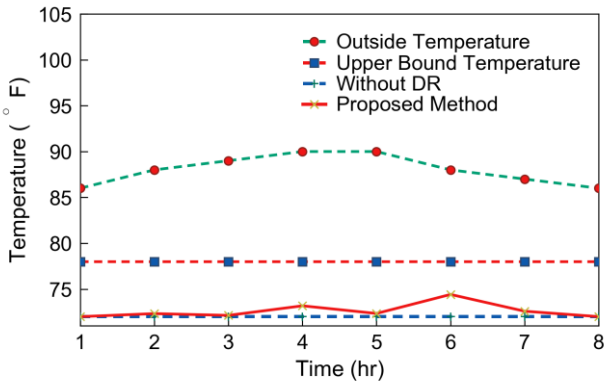

Figure 4.11. Outside and indoor temperature in a house at bus 16 for different control methods.

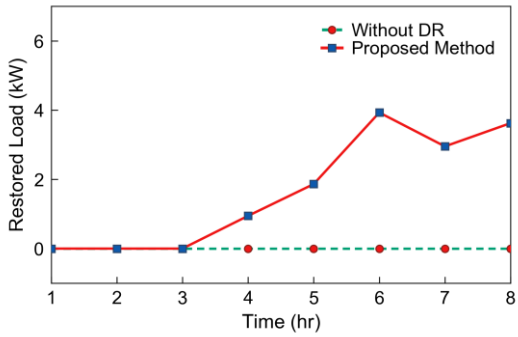

Figure 4.12. One household restored load profile for without DR and proposed method at bus 87.

4.4.6. Effect in HEM in System Resiliency

With the help of HEM, target loads in household to bus levels are maintained. Impact of changing preferable load demand in HEM will impact the DSR. For instance, if AC loads are preferred to be controlled between 72°F to 76°F instead of 72°F to 78°F, then load requirement will increase for each house. The minimum load requirement of the buses will also be changed. This impact can be observed in Table 4.3. If number of controllable buses are 10, then restored energy is only 13077 kWh for 72°F to 76°F preferable temperature range. It is 14683 kWh for 72°F to 78°F preferable temperature range according to Figure 4.8. Restored energy also reduces from 15558 kWh for 72°F to 78°F to 13718 kWh 72°F to 76°F for optimal 20 controllable buses.

Table 4.3. Restored energy comparison for different controllable buses with the change of loads.

Number of controllable buses	Restored energy (kWh)
0	13077
10	13077
20	13718
30	13718
40	13718
50	13718

4.5. Conclusion

In this work, an innovative DR based method is proposed for load restoration. The idea is

to improve grid resiliency by utilization of DR. The proposed method contains three level hierarchical methods following three optimization problems. Numerical results show that the load restoration performance can be significantly improved with the utilization of demand response in a distribution system with limited generation resources and microgrids facing multiple outages caused by natural disasters. Optimal allocation of controllable bus can further improve the restoration performance of the proposed method. Consideration of uncertainties in HEM system ensures maintaining the load level of the controlled buses. Overall, with the proposed method it is demonstrated that controlling the flexible loads in one house can help the DSR to pick up other fixed loads. Furthermore, the methods used here, such as assign time-varying load instead of spot load, define feasible controllable range of load demand on a distribution bus, and maintain target load considering uncertainties in load demand and solar generation through HEM, can provide guidance on market design for DR when resilience is considered.

CHAPTER 5

Real-time Energy Management in PV-Storage Hybrid Residential Unit

5.1. Introduction

Energy management for a PV-storage hybrid unit is typically formulated as an offline optimization problem for day-ahead scheduling, which is difficult to achieve in practice. On the other hand, existing online algorithms cannot ensure the maximum benefit to the homeowners. In this chapter, an integrated architecture is described where load and solar generation forecasting is performed in rolling horizon to predict the day-ahead profiles, use them to optimize the electricity purchase cost per day through SDDP algorithm in receding horizon, and utilize the optimal decision with rule-based control to implement a realistic control.

5.2. Motivation and System Overview

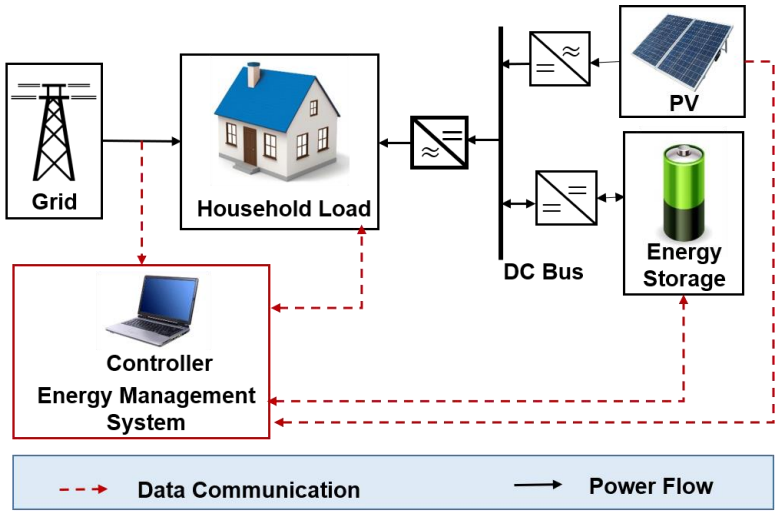

Figure 5.1. Overview of the PV-storage hybrid system.

The overview of the system is shown in Figure 5.1. A solar PV panel provides energy to a BESS and also delivers power to satisfy the household load demand through a DC bus. The energy storage is also connected to the DC bus and can store energy only from the PV panel or

discharge only to satisfy the household demand. The household load is mitigated through the grid, solar panels and/or BESS.

In the proposed integrated framework, three hierarchical steps are followed. In the first step, forecast of solar generation and load demand for next 24 hours with 15-minute resolution is performed. These updated forecasted profiles are utilized to calculate expected future costs in receding horizon to obtain optimal decision for next 15 minutes in second stage. Because of stochastic nature of cloud patterns, weather, user preference etc., solar generation and load demand do not remain exact to the forecasted profiles. Optimization is performed considering these uncertainties of load and solar generation in future. Utilizing the optimal decision from second stage, rule-based control is performed in the third step of the framework. Since the proposed rule-based control takes less time to take the decision, it is preferable to employ in real-time system. It also ensures proper utilization of solar generation by the owners.

In Figure 5.2, a protocol about how the proposed integrated system works is illustrated. At each 15 minute interval, forecast of solar generation and load demand is performed for next 24 hours that takes τ_1 time to calculate. These updated forecasted profiles are leveraged to perform SDDP optimization process considering the uncertainties in load and solar generation in receding horizon. Optimization requires τ_2 time period to update optimal decision. This optimal decision is updated on 15 minutes interval. The updated optimal decision is provided to the rule-based method to perform real-time dynamic control for BESS. For each τ_3 time interval, rule-based control is performed for the system. Details of these three steps are provided in the next section.

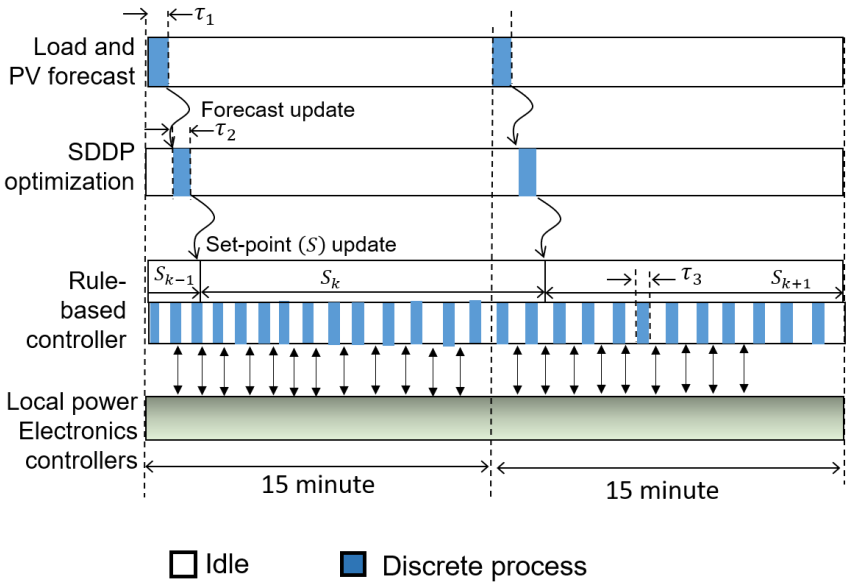

Figure 5.2. Three step protocol for the integrated proposed method.

5.3. Proposed Method

In this section, the proposed three-step method is described in three subsections. The load and solar generation forecast includes feature selection and forecasting algorithm. Second subsection consists of scenario generation, model formulation, and multi-stage stochastic programming methods. Finally, the rule-based control algorithm is demonstrated.

5.3.1. Load and Solar Forecasting

Inclusion of updated forecasted load and PV generation profiles improve the efficiency of energy management. In our proposed method, forecast is performed in each 15-minute interval considering previous stage historical values. To predict day-ahead profiles, our method forecasts next 96 values. The considered features and forecasted algorithm are described below.

A) Features Selection:

Feature selection reduces overfitting and increases accuracy of the predicted value. For household load prediction, characteristic features such as holiday versus working day, month of

the year, and day of the week are considered as features. These features are considered to help better understand the residents' habits and life patterns. Feature-extraction from household data at a very high resolution such as 1-minute interval, may lead to errors like over-fitting. Therefore, we choose a 15-minute interval for forecast update.

B) Forecasting Algorithm:

LSTM is one of the recurrent neural network (RNN) structures. In contrast to the standard RNN which has a series of repeating modules with relatively simple structure, the hidden layers of LSTM have a more complicated structure. Although a conventional feedforward neural network can learn sequences, LSTM is more powerful because it constrains a memory cell in its structure to remember important states in the past and has a forget-gate to learn to reset the memory cell from insignificant features during the learning process [161].

The simplest method to build up an LSTM model is to provide an input vector to the model for predicting the output. In this paper, the LSTM network models are trained with input vector of 17 (weekday stamp, month stamp and last 15 values of the time series) and output window size is 96 (next 96 values represent 24 hours at 15-minute interval). A way of training the LSTM models is to implement window-based learning. This method allows the LSTM model to directly deal with previous timestamp values (lagged values). After each prediction timestamp, LSTM window-based network model shifts both input and output windows by one step. In this way, the forecast method provides support for dynamic learning which is important for our proposed method.

5.3.2. Optimization Problem Formulation

A) Scenario Generation:

Similar scenario generation procedure considering the correlation between load and solar generation described in section 3.4.2 is followed.

B) Problem Formulation

Electricity purchase cost minimization of a household with optimal operation of the energy storage integrated PV system to benefit a customer is our objective. In this work, optimization cycle occurs from 0hr to 24hr period of a day with each 15-minute interval in receding horizon. The total left time for a day after each cycle is divided into *T* time periods based on resolution *Δt,* which is 15-minute in this work. Let C_t be the time-of-use (ToU) cost of electricity, $P_{L,t}^{\omega_{L,t}}$ and $P_{PV,t}^{\omega_t}$ are the generated load and solar profiles from the sets of all generated load and solar profiles $\Omega_{L,t}$ and $\Omega_{PV,t}$, correspondingly, and $P_{grid,t}$is the power demanded from grid at time *t;* the objective function *J* and constraints can then be written as -

$$\min J = \sum_{t=1}^{T} [C_t \cdot P_{grid,t}\,] \tag{5.1}$$

Subject to:

Power balance constraint:

$$P_{grid,t} - P_{b,t}^{ch} + P_{b,t}^{disch} - P_{def,t} = P_{L,t}^{\omega_{L,t}} - P_{PV,t}^{\omega_t} \tag{5.2}$$

Charge balance constraint:

$$SOC_{b,t} = SOC_{b,t-1} + \frac{P_{b,t}^{ch}\Delta t\, \eta_{b,ch,t}}{Q_b} - \frac{P_{b,t}^{disch}\,\Delta t}{Q_b\ \eta_{b,disch,t}}, \forall t \in T \tag{5.3}$$

Inequality constraints:

$$P_{b,t}^{ch} \le P_{PV,t}^{\omega_t}\,, \forall t \in T \tag{5.4}$$

$$P_{b,t}^{disch} \le P_{L,t}^{\omega_{L,t}}\,, \forall t \in T \tag{5.5}$$

$$P_{grid,t} \ge 0\,, \forall t \in T \tag{5.6}$$

Upper and lower bounds of the decision variables:

$$\underline{SOC_b} \le SOC_{b,t} \le \overline{SOC_b}\,, \forall t \in T \tag{5.7}$$

$$\underline{P_b^{ch}} \le P_{b,t}^{ch} \le \overline{P_b^{ch}}, \forall t \in T \tag{5.8}$$

$$\underline{P_b^{disch}} \leq P_{b,t}^{disch} \leq \overline{P_b^{disch}}, \forall t \in T \quad (5.9)$$

In this system according to figure 1, the PV generation does not provide power to the grid. During higher PV generation than the load demand if the storage is charged, then $P_{def,t}$ will take care of the excess generation as deferred energy. Equation (5.2) ensures the power balance of the whole system. Equation (5.3) calculates the SOC of storage, $SOC_{b,t}$ based on the instantaneous charging, $P_{b,t}^{ch}$ and discharging power, $P_{b,t}^{disch}$ of the storage device. Inequality constrains (5.4) maintains the condition that the storage will be charged only from the available PV generation, (5.5) maintains the condition of discharging of storage will only occur to mitigate the load demand. As back-feeding power to the grid is discouraged, we consider electricity purchase from grid will not be negative in (5.6). The lower and upper bounds of decision variables of the storage are defined in equation (5.7) – (5.9). If the household demand needs to be satisfied by both PV generation and battery discharge, then according to (5.1) and (5.3) it is less efficient to charge the battery with PV power, simultaneously. PV generation will satisfy the demand instead of storing energy into the battery. On the other hand, if PV generation is higher than the demand, the surplus will be stored in the battery based on available storage capacity and discharge of energy storage will not occur. Therefore, charging and discharging of the storage device simultaneously will not occur in this system.

C) Multi-stage Stochastic Optimization

The above-described optimization problem is solved with the method following section 3.2.2.

5.3.3. Rule-based Control

The optimization strategy for charging/discharging of the energy storage might not be always feasible for real application at a high time-resolution. For instance, we consider a

discharging command for the energy storage at an average rate of P_0 for the next 15-minute till the next update instant. However, in an event of a decrease in load demand, a constant discharge by the energy storage at the rate P_0 may lead to power injection into the grid incurring an effective loss to the customer. To prevent such scenarios, a rule-based control is integrated in our proposed method. The optimization decision, $P_{com,t}$ is calculated as follows in 15-minute interval-

$$P_{com,t} = P_{b,t}^{ch} - P_{b,t}^{disch} \tag{5.10}$$

Table 5.1. Rule-based algorithm.

Inputs	$SOC_{real,t}$ at time t
1	$P_{com,t} = P_{b,t}^{ch} - P_{b,t}^{disch}$
2	*if* $(P_{com,t} < 0)$ *and* $(P_{load,t} - P_{PV,t} > 0)$
3	*if* $(P_{com,t} \geq P_{PV,t} - P_{load,t})$: $P_{get} = P_{com,t}$
4	*else*: $P_{get} = P_{PV,t} - P_{load,t}$
5	*elseif* $(P_{com,t} < 0)$ *and* $(P_{load,t} - P_{PV,t} < 0)$:
6	$P_{get} = P_{PV,t} - P_{load,t}$
7	*elseif* $(P_{com,t} > 0)$ *and* $(P_{load,t} - P_{PV,t} \geq 0)$
8	*if* $(P_{com,t} \leq P_{PV,t})$: $P_{get} = P_{com,t}$
9	*else*: $P_{get} = P_{PV,t}$
10	*elseif* $(P_{com,t} > 0)$ *and* $(P_{load,t} - P_{PV,t} < 0)$
11	$P_{get} = P_{PV,t} - P_{load,t}$
12	*elseif* $(P_{com,t} == 0)$ *and* $(P_{load,t} - P_{PV,t} < 0)$
13	$P_{get} = P_{PV,t} - P_{load,t}$
14	*if* $(P_{com,t} \leq \overline{P_{b,t}^{ch}})$: $P_{get} = \overline{P_{b,t}^{ch}}$
15	*else:* $P_{get} = P_{com,t}$
16	*if* $(SOC_{real,t} \leq \underline{SOC_b})$:
17	*if* $P_{get} > 0$: $P_{rb,t} = P_{get}$
18	*else* $P_{rb,t} = 0$
19	*elseif* $(SOC_{real,t} \geq \overline{SOC_b})$:
20	*if* $P_{get} < 0$: $P_{rb,t} = P_{get}$
21	*else* $P_{rb,t} = 0$
22	*Else:* $P_{rb,t} = P_{get}$

If $P_{com,t}$ is negative, then energy storage is supposed to be discharged. But if the difference between the load demand, $P_{load,t}$ and PV generation, $P_{PV,t}$ in real-time is not higher as discharge power, $P_{b,t}^{disch}$; then battery should discharge only the difference. This rule is shown in Table 5.1, step 2-4. Here $P_{get}$is the energy storage charge/discharge command at a much higher time resolution. On the other hand, if there is a situation in real-time that solar generation is higher than load, but the optimization decision is giving the command to discharge the energy storage, then instead of discharging the energy storage, storing the excess solar generation will help to reduce deferral energy if there is available energy storage capacity. This rule is illustrated in step 5-6.

If $P_{com,t}$ is positive, then energy storage is supposed to be charged. But if there is not enough PV generation, $P_{PV,t}$ to charge the energy storage in real scenario, then according to the rule-based control $P_{b,t}^{ch}$ should be equal to available $P_{PV,t}$. If there is higher $P_{PV,t}$ than $P_{load,t}$ and $P_{b,t}^{ch}$; then excess generation is used to charge the energy storage to avoid deferral energy. The total charging energy should not go beyond the charger capacity. These rules are shown in Table 5.1, steps 7-11.

If $P_{com,t}$ becomes zero, but still there is excess PV generation than load, then the storage should store the excess generation till it is in the charger capacity and energy storage capacity bound. This is defined in state 12-14. After getting the command for energy storage charge/discharge, it is checked in real-time whether the storage goes beyond its upper and lower threshold or not. If lower threshold value is reached, then no discharge will occur. If upper threshold value is reached, then no charge will occur. These rules are maintained through step 16-22 in Table I. $P_{rb,t}$ will be sent to the energy storage from the controller.

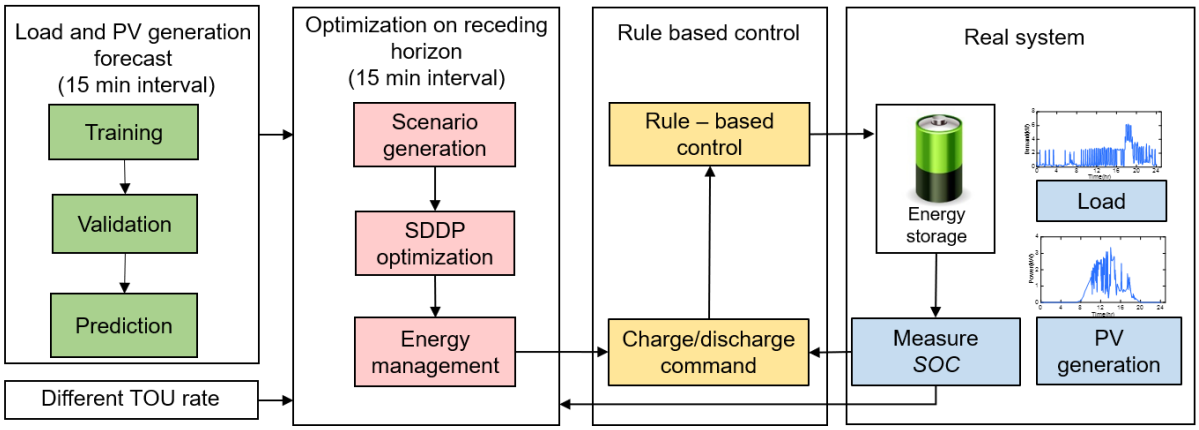

Figure 5.3. Integrated system overview.

The overall proposed system overview is shown in Figure 5.3. It is to be noted that in real-time operation $SOC_{real,t}$ is measured every 20μs and rule-based operation is performed within 20μs interval. But SDDP based optimization and forecasts are performed in 15-minute interval.

5.4. Simulation Set-up

The proposed method is validated using a real-time simulation platform based on Opal-RT. The simulation set-up is shown in Figure 5.4. The PV source, battery storage system, household load, and the power converters are modeled in real-time by Opal-RT system with a simulation time step of 20μs. Household load and corresponding solar generation profiles are obtained from PECAN Street data [157]. In Table 5.2, the test system parameters are shown. ToU rate is collected from [155] provided in Appendix A Table I. Forecast and optimization are performed in MATLAB in an Intel Core i5-4600U with a 1-GH CPU, 4 GB of RAM, and 64-bit operating system PC. Through a MODBUS communication interface, SOC feedback form the energy storage system is sent to the PC. Using the SOC feedback, forecast and optimization is performed and new power reference for the energy storage system is dispatched at a 15-minute interval. The rule-based controller is incorporated as a part of the local power electronic converter

controllers and therefore, is implemented in the real-time simulator. The following subsection describes the power converter models and the controllers used for voltage and current tracking.

Table 5.2. System parameters for hybrid residential unit.

Parameters	Values	Parameters	Values
Q_b	4 kWh	$\underline{SOC_t^B}, \overline{SOC_t^B}$	20%, 80%
η	92%	η	92%
$\underline{P_{b,t}^{ch}}, \overline{P_{b,t}^{ch}}$	0 kW, 3 kW	Forecast and optimization time interval, t	15 min
$\underline{P_{b,t}^{disch}}, \overline{P_{b,t}^{disch}}$	0 kW, 3 kW	Real-time simulation interval, τ	20 µsec
Initial SOC	20%	$\underline{SOC_t^B}, \overline{SOC_t^B}$	20%, 80%

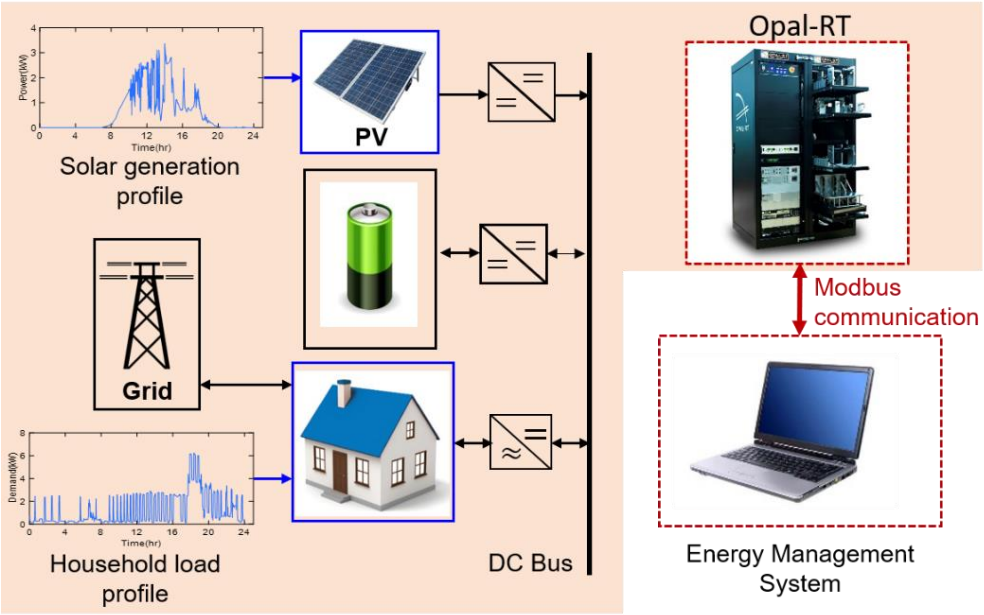

Figure 5.4. Simulation set-up.

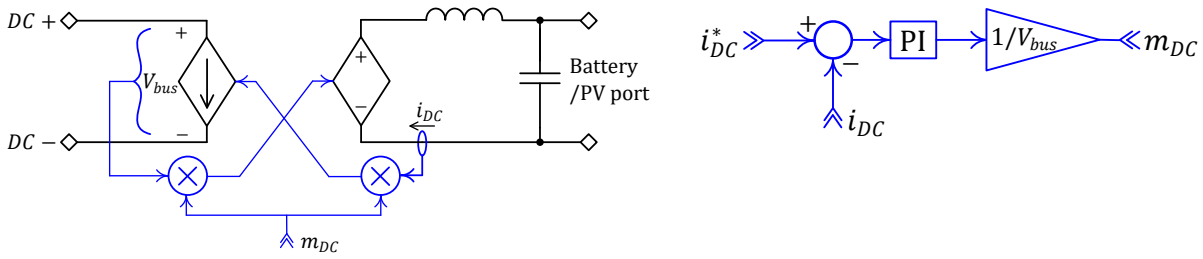

(a) (b)

Figure 5.5. (a) DC-DC converter model used for interfacing PV and battery and (b) Current controller for DC-DC converters.

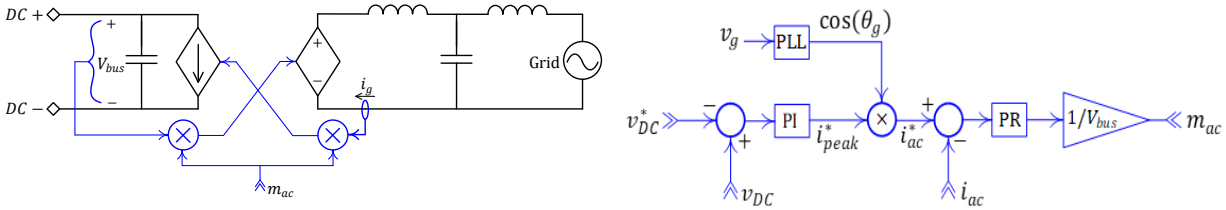

(a) (b)

Figure 5.6. (a) Rectifier model and (b) DC bus voltage and grid current controller used for the rectifier.

5.4.1. Power Electronic Converter Model:

To reduce simulation overhead, average models of the power converters are used. Figure 5.5 (a) shows the average model used for the DC-DC converters. Identical models have been used for the converters that interface the PV and the battery storage system. PV generation profile obtained from PECAN Street data was used to model the PV variation. Current reference tracking was achieved by a PI compensator, shown in Figure 5.5 (b). It is worth noting that the current reference $i^*_{DC} = i^*_{bat}$ for the DC-DC converter that interfaces the battery, is updated by the rule-based controller. For the PV converter, the current reference $i^*_{DC} = i^*_{PV}$ is updated by the rule-based controller; however, the reference is tracked when allowable by the PV generation profile and the extracted current is clamped at the maximum power point when $i^*_{PV} > i_{MPP}$, where i_{MPP} refers to the current at maximum power point.

A rectifier connects the household system with the grid. The average model is shown in Figure 5.6 (a). A cascaded control structure is used to maintain the desired voltage v_{DC}^{*} at the DC bus, shown in Figure 5.6 (b). An inner proportional-resonant (PR) compensator is used for current control and the current reference is dynamically generated by a PI compensator that tracks the DC bus voltage.

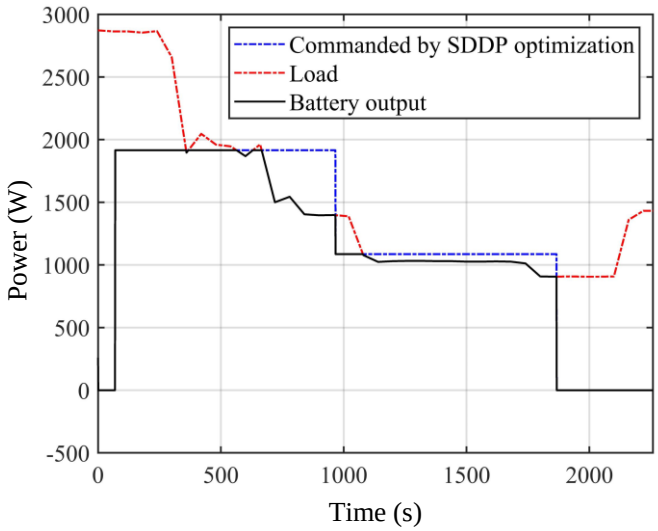

Figure 5.7. Real-time simulation of CHIL showing SDDP optimization command that updates in each 15 min interval and battery dispatch output following the proposed method with 1s interval.

5.4.2. Requirement of Real-time CHIL Simulation:

To evaluate the performance of any energy optimization algorithm, real-time control hardware in the loop (CHIL) simulation can facilitate a high fidelity emulation of the real system compared to an offline numerical simulation. This can be illustrated by a simple test case shown in Figure 5.7, where a snapshot of the real-time CHIL experiment result is considered. The red dashed curve denotes the load. the stochastic nature of the load is evident from the irregular variation of demand. Using our proposed SDDP optimization method, the battery power dispatch command is represented by the blue-dashed curve which is held constant between two update instants, i.e., 15 mins. It is worth noting that the load demand changes intermittently within that

15 min interval. The proposed rule based controller limits the battery output to the load demand when load demand falls below the commanded power reference for the battery by the energy optimization algorithm and ensures undesired discharge of the battery. The necessity of the rule-based controller thus becomes evident in this test case. Moreover, in an offline numerical simulator, energy consumption and net energy output are typically computed considering the average power flow over one optimization-update period, which obscures the effect of the intermittent mismatches between the commanded power reference and the varying loading conditions leading to inaccuracies in the estimation of net cost.

5.5. Results and Analysis

The simulation results for different steps and comparison analysis are illustrated below.

5.5.1. Load and Solar Generation Forecast

For residential load and solar generation forecasts, we use load and PV generation data of the previous one year period to train the model. The prediction is updated at 15-minute intervals in rolling horizon. Using the feedback of load and PV profiles in the current interval, prediction for the next 24 hours, i.e., 96 sets of values, are updated. We evaluate different machine learning algorithms in terms of forecast accuracy. In Figure 5.8, the forecasted solar profiles with different algorithms along with the real profiles are shown. It is to be noted that PV generation profile is subject to less variability compared to load profile over a 15-minute interval, which is reflected in the root mean square error (RMSE) shown in Table 5.3. Greater variability in household load demand is also evident in Figure 5.9. Regardless, RMSE is lower for LSTM compared to the other machine learning algorithms for both load demand and solar generation forecasts. Consequently, we chose LSTM as the preferred forecast algorithm for our proposed integrated energy management system. It was observed that for time resolutions less than 15-min, RMSE increases.

Therefore, to avoid higher RMSE 15-min- interval is chosen for forecast and optimization update.

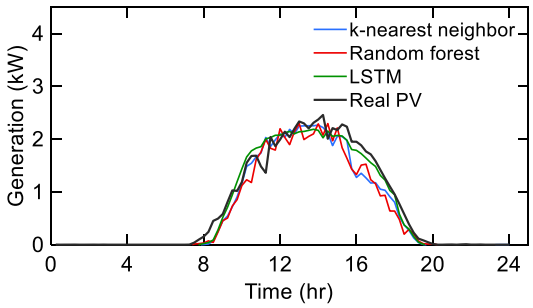

Figure 5.8. Forecasted solar generation with different methods and real solar generation.

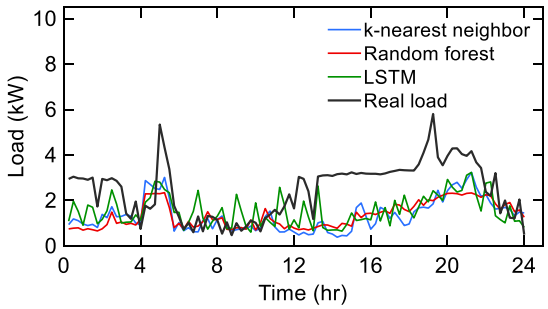

Figure 5.9. Forecasted load with different methods and real load.

Table 5.3. RMSE for load and solar forecasts.

Forecasting methods	Solar forecast		Load forecast	
	Summer	Winter	Summer	Winter
k-Nearest Neighbor	3%	5.8%	21%	12%
Random forest algorithm	3.3%	6.4%	20%	15%
LSTM	2%	5.6%	17%	11%

5.5.2. Reduction on Electricity Purchase from Grid

The load and PV models in Opal-RT real-time simulator are programmed to follow the profiles of a summer day (obtained from PECAN street data), shown in Figure 5.10. It is worth noting that the dataset used to train the forecast model does not include these profiles. The simulation results are recorded at one-minute interval for 24 hours. The BESS SOC for different control strategies are shown in Figure 5.11 and it can be seen that our proposed method prefers to charge during off-peak and partial-peak hours and discharge mostly at peak hours to reduce the electricity purchase cost. As a result, SOC of the storage increases during off-peak and partial-peak hour and it goes down during peak hours. On the other hand, for heuristic method, BESS is charged during excess generation and discharge occurs during higher load than generation which leads to underutilization of energy storage and higher electricity purchase cost.

Next, we evaluate the impact of the proposed rule-based with SDDP method. The BESS charging or discharging commands are updated at 15 min intervals. However, load and PV generation are subject to intermediate variability. For instance, we consider two specific operational cases- higher solar generation than the BESS charging command and lower load demand than the BESS discharging command. In the first case, solar energy is fed back to the grid which could be utilized to charge the BESS at a higher rate. In the later case, the BESS is discharged unnecessarily. Without the rule-based method, the mismatch at finer time resolution is not possible to correct; therefore, the waste of energy may persist as long as 15 minutes, in the worst case for SDDP application. The proposed inclusion of rule-based control with SDDP method resolves such intermittent mismatches at a finer time-resolution. The rule-based method is effectively actuated at the same time scale as the power electronics converter control. From Table 5.4, it is evident that our proposed method ensures greater reduction in electricity purchase cost in both summer and winter days compared to that of other methods. Due to the lower solar generation and lower difference between the peak and off-peak hour rates during winter days, electricity purchase cost saving is lower compared to summer days. Considering these electricity purchase costs ($/day), it can be expected that with our proposed method 8.4% savings annually.

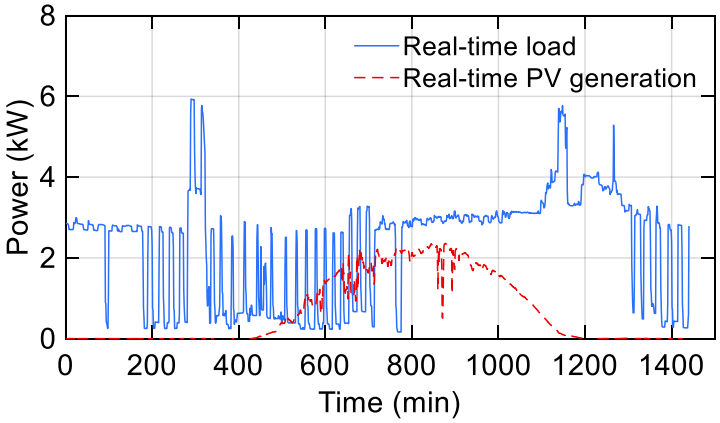

Figure 5.10. Real-time household and solar generation profiles.

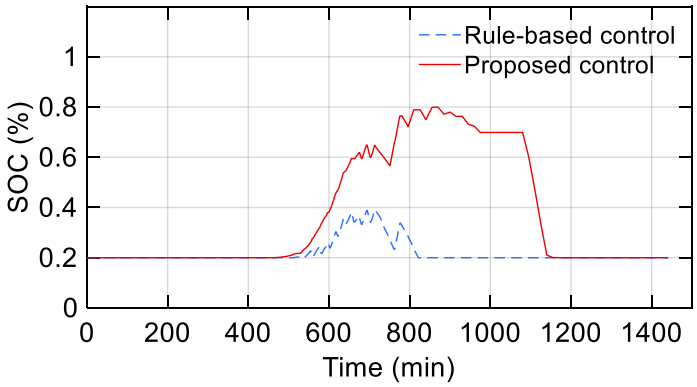

Figure 5.11. SOC of the energy storage in real-time for different control strategies for a summer day.

Table 5.4. Electricity purchase cost ($/day) comparison.

Methods	Summer	Winter
Electricity purchase cost without storage	8.9	3.2
Heuristic method	8.4	3
SDDP method	8.5	3
Proposed method	7.9	2.9

5.5.3. Improvement on Peak Hour Saving and Solar Energy Usage:

Peak hour saving not only helps the homeowners but also helps the utility companies. In our proposed method, peak hour saving is higher compared to the other methods for both in summer and winter days which is shown in the bar chart in Figure 5.12. Since SDDP method has proper estimation of expected future cost, it ensures higher peak saving compared to heuristic control method. But SDDP suffers from inefficient usage of solar energy due to the variability in real systems which is depicted in Figure 5.13 for both summer and winter days. Since we integrate SDDP for proper estimation of the expected future cost along with rule-based control for efficient use of energy, our proposed method outperforms both heuristic and SDDP based methods in terms of peak hour saving and solar energy usage.

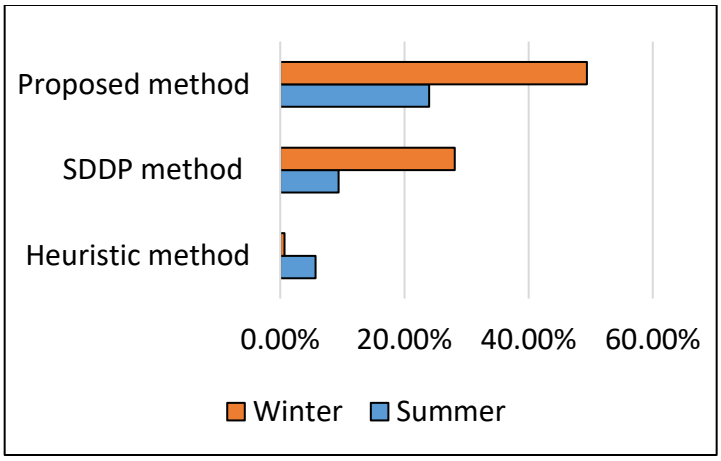

Figure 5.12. Comparison of peak hour saving in (%) for different control strategies.

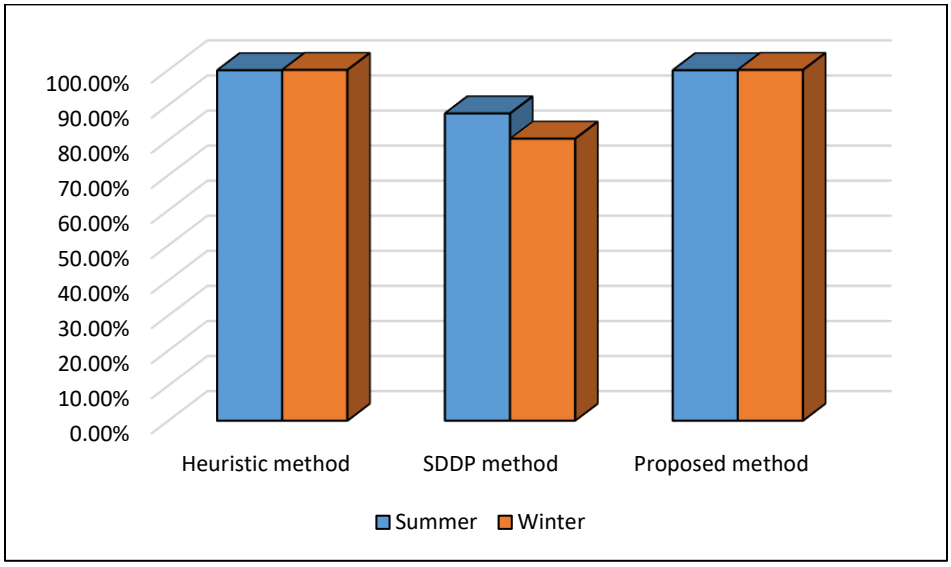

Figure 5.13. Comparison of solar generation usage in (%) for different control strategies.

5.6. Conclusion

In this work, a real-time residential BESS energy management method is proposed for daily electricity purchase cost minimization which is the primary concern of the users. Updated load and solar generation profiles through forecasting in rolling horizon, helps to improve the optimal decision-making process in the energy management algorithm. During optimization, consideration

of uncertain parameters and correlation between them increases the efficiency of the optimization. For application in real systems, integration of rule-based control reduces deferred solar energy as well as ensures proper utilization of the energy storage. Real-time control hardware-in-the-loop experiments validate the superior performance of the proposed method in comparison with existing energy management algorithms in terms of electricity purchase cost, peak hour savings and solar energy usage.

CHAPTER 6

Contributions and Future Works

6.1. Contributions

This dissertation presented and discussed a new method for PV-panel and energy storage sizing. It showed that the consideration of deterministic model-based energy management and NPV analysis ensures economic benefit to obtain the optimal PV-panel and storage capacity sizes to the owner. Another unique contribution of this dissertation is to integrate solar generation with storage and PEV on a residential system to control their charge/discharge profile to achieve minimum load variance. Load variance control from residential level helps electric service providers to get rid of the problem like "duck-belly" curve or over voltage. Since the control is performed in residential level, electricity service providers do not require to control each individual house through a centralized control system that requires a lot of computation and effective communication system.

The models formulated in consideration of uncertainties in solar generation and load demand in this dissertation, showed the importance of considering proper models and algorithms. The results obtained from applying the SDDP for optimal state of charge and control trajectories analyze that by controlling the charging/discharging schedule of the PV-based storage/PEV storage, it is possible to minimize the household cost of purchasing power from the grid. The importance of coordinated control between PV based storage and the PEV storage illustrated in this dissertation for a household system to minimize the overall electricity purchase costs from the grid. The correlation consideration between load demand and solar generation helps to avoid unrealistic scenario generation (e. g. lower load demand with higher solar generation during hot summer days). The simulation results validated that the coordinated control scheme achieved

higher economic benefit to the owner with respect to heuristic control, standalone application of SDDP to PV based storage and standalone application of SDDP to PEV storage. Performed simulations for these models, show that the electricity purchase cost reduces for the stochastic optimization compared to the deterministic optimization method.

A novel framework for energy management in a system composed by renewable energy and storage devices for a community was presented in the later part of chapter 3. The proposed approach can be an enabler for the future shared community generation- storage designs in the smart grid environment providing a technical decision-making framework for storage addition, and capacity sizing of storage devices, that allows planners to perform comparisons between the optimal capacity sizing of shared versus individually controlled and owned devices based on NPV calculations. The results obtained from the SEM control strategy suggested that by controlling the energy storage devices and the solar PV generation power flow, it is possible not only to improve critical parameters such as electricity purchase costs, electricity peak shaving and solar PV usage on a daily basis, but also to reduce the storage capacity requirement. As a result, this tool is beneficial to the homeowners in terms of reducing the electricity purchases from the grid and the energy storage installation costs.

An innovative DR-based method for load restoration service was proposed in chapter 4. The idea is to improve grid resiliency using DR. Numerical results showed notable improvement on load restoration in a distribution system with limited generation resources and microgrids. This proposed framework can be employed for various operations, such as voltage violation control and frequency regulation in distribution systems. Furthermore, the methods used to assign time-varying load instead of spot load in a distribution test system, define feasible controllable range of load demand in a distribution bus, and maintain target load considering uncertainties in load

demand and solar generation through HEM can provide guidance on market design for DR when resilience is considered.

To advance the SDDP based energy management strategy one step further, a real-time based residential PV-storage control method was developed for daily electricity purchase cost minimization in chapter 5. A real-time residential energy storage control method is proposed for electricity purchase minimization which is the primary concern of the users. Updated load and solar generation profiles in rolling horizon helps to improve the optimal decision-making process in the energy management algorithm. During optimization, consideration of uncertain parameters and correlation between them increases the efficiency of the optimization. For application in real systems, integration of rule-based control ensures the reduction of deferral solar energy and proper utilization of the energy storage. Real-time simulation results validate the superior performance of the proposed method over existing methods. The proposed methodology can be extended for distribution, transmission and generation level energy storage management.

6.2. Future Works

The following future works are suggested for further improvement of the dissertation:

- For PV-panel and storage sizing, the impact of storage cost and ToU rate are considered. Other parameters like the presence of DR, PEV, energy storage degradation model can be considered for sensitivity analysis.
- For community level, inclusion of PEVs can be considered for energy management and capacity sizing of energy storages.
- Impact of deterministic and stochastic methods for capacity sizing method can be analyzed for capacity sizing of storage.

- DR based method for DSR can be utilized to control other parameters like voltage and frequency regulation.

REFERENCES

[1] P. Gagnon, R. Margolis, J. Melius, and C. Philips, "Rooftop Solar Photovoltaic Technical Potential in the United States: A Detailed Assesment," *Natl. Renew. Energy Lab.*, pp. 1–82.

[2] Y. T. Tan and D. S. Kirschen, "Impact on the power system of a large penetration of photovoltaic generation," in Proc. *2007 IEEE Power Engineering Society General Meeting*, Jul. 2007.

[3] S. R. Deeba, R. Sharma, T. K. Saha, and A. Thomas, "Investigation of voltage performance of an LV distribution network for improving rooftop photovoltaic uptake in Australia," in *IEEE Power and Energy Society General Meeting*, Jul. 2016.

[4] J. V. Paatero and P. D. Lund, "Effects of large-scale photovoltaic power integration on electricity distribution networks," *Renew. Energy*, vol. 32, no. 2, pp. 216–234, 2007.

[5] F. Sayadi, S. Esmaeili, and F. Keynia, "Two-layer volt/var/total harmonic distortion control in distribution network based on PVs output and load forecast errors," *IET Gener. Transm. Distrib.*, vol. 11, no. 8, pp. 2130–2137, 2017.

[6] P. K. Bhatt and S. Y. Kumar, "Impact of Solar PV Inverters on the Power Quality of Smart Urban Distribution Grid," *Int. J. Electr. Eng. Technol.*, vol. 8, no. 2, pp. 18–24, 2017.

[7] S. Eftekharnejad, V. Vittal, G. T. Heydt, B. Keel, and J. Loehr, "Impact of Increased Penetration of Photovoltaic Generation on Power Systems," *Power Syst. IEEE Trans.*, vol. 28, no. 2, pp. 893–901, 2013.

[8] H. Liu, L. Jin, D. Le, and A. A. Chowdhury, "Impact of high penetration of solar photovoltaic generation on power system small signal stability," *2010 Int. Conf. Power Syst. Technol.*, pp. 1–7, 2010.

[9] D. Schwanz, F. Moller, S. K. Ronnberg, J. Meyer, and M. H. J. Bollen, "Stochastic

Assessment of Voltage Unbalance Due to Single-Phase-Connected Solar Power," *IEEE Trans. Power Deliv.*, vol. 32, no. 2, pp. 852–861, 2017.

[10] U. Jayatunga, S. Perera, P. Ciufo, and A. P. Agalgaonkar, "Voltage unbalance emission assessment in interconnected power systems," *IEEE Trans. Power Deliv.*, vol. 28, no. 4, pp. 2383–2393, 2013.

[11] V. H. M, Quezada, J. R. Abbad, and T. G. S. Roman, "Assessment of energy distribution losses for increasing penetration of distributed generation," *IEEE Trans. Power Syst.*, vol. 21, no. 2, pp. 533–540, 2006.

[12] R. Seguin, J. Woyak, D. Costyk, J. Hambrick, B. Mather, "High-Penetration PV Integration Handbook for Distribution Engineers," *Natl. Renew. Energy Lab. (NREL), Tech. Rep.*, 2016.

[13] A. Alkuhayli, F. Hafiz, and I. Husain, "Volt / Var Control in Distribution Networks with High Penetration of PV Considering Inverter Utilization," *in Proc. IEEE Power and Energy Society General Meeting*, Jul. 2017.

[14] P. Denholm, M. O'Connell, G. Brinkman, and J. Jorgenson, "Overgeneration from Solar Energy in California: A Field Guide to the Duck Chart (NREL/TP-6A20-65023)," *T Natl. Renew. Energy Lab. (NREL), Tech. Rep*, 2015.

[15] M. M. J. Cochran, P. Danholm, and B. Speer, "Grid Integration and the Carrying Capacity of the U . S . Grid to Incorporate Variable Renewable Energy," *Natl. Renew. Energy Lab.*, pp. 1–30, 2015.

[16] D. L. L. Bird, M. Miligan, "Integrating Variable Renewable Energy : Challenges and Solutions Integrating Variable Renewable Energy : Challenges and Solutions," *Natl. Renew. Energy Lab. (NREL), Tech. Rep.*, pp. 1–14, 2013.

[17] R. Tonkoski, L. A. C. Lopes, and T. H. M. El-Fouly, “Coordinated active power curtailment of grid connected PV inverters for overvoltage prevention,” *IEEE Trans. Sustain. Energy*, vol. 2, no. 2, pp. 139–147, 2011.

[18] W. J. Cole, C. Marcy, V. K. Krishnan, and R. Margolis, “Utility-scale lithium-ion storage cost projections for use in capacity expansion models,” *NAPS 2016 - 48th North Am. Power Symp. Proc.*, 2016.

[19] X. Li, D. Hui, and X. Lai, “Battery energy storage station (BESS)-based smoothing control of photovoltaic (PV) and wind power generation fluctuations,” *IEEE Trans. Sustain. Energy*, vol. 4, no. 2, pp. 464–473, 2013.

[20] C. Noce, S. Riva, G. Sapienza, and M. Brenna, “Electrical energy storage in Smart Grid: Black-start study using a real-time digital simulator,” *2012 3rd IEEE Int. Symp. Power Electron. Distrib. Gener. Syst.*, pp. 216–220, 2012.

[21] F. A. Bhuiyan and A. Yazdani, “Energy storage technologies for grid-connected and off-grid power system applications,” *2012 IEEE Electr. Power Energy Conf. EPEC 2012*, pp. 303–310, 2012.

[22] B. Zhao, Y. Shi, X. Dong, W. Luan, and J. Bornemann, “Short-term operation scheduling in renewable-powered microgrids: A duality-based approach,” *IEEE Trans. Sustain. Energy*, vol. 5, no. 1, pp. 209–217, 2014.

[23] R. Hemmati and H. Saboori, “Short-term bulk energy storage system scheduling for load leveling in unit commitment: Modeling, optimization, and sensitivity analysis,” *J. Adv. Res.*, vol. 7, no. 3, pp. 360–372, 2016.

[24] A. S. A. Awad, J. D. Fuller, T. H. M. El-Fouly, and M. M. A. Salama, “Impact of energy storage systems on electricity market equilibrium,” *IEEE Trans. Sustain. Energy*, vol. 5, no.

3, pp. 875–885, 2014.

[25] P. Denholm *et al.*, “The Value of Energy Storage for Grid Applications,” *Natl. Renew. Energy Lab. (NREL), Tech. Rep.*, 2013.

[26] C. R. Vergara, “Parametric interface for Battery Energy Storage Systems providing ancillary services,” *IEEE PES Innov. Smart Grid Technol. Conf. Eur.*, pp. 1–7, 2012.

[27] J. Eyer, “Electric Utility Transmission and Distribution Upgrade Deferral Benefits from Modular Electricity Storage,” *Sandia Natl. Lab.*, 2009.

[28] C. Sabillon, O. Melgar Dominguez, J. Franco, M. Lavorato, and M. J. Rider, “Volt-VAr Control and Energy Storage Device Operation to Improve the Electric Vehicle Charging Coordination in Unbalanced Distribution Networks,” *IEEE Trans. Sustain. Energy*, vol. 3029, no. 2, pp. 1–1, 2017.

[29] V. Knap, S. K. Chaudhary, D. I. Stroe, M. Swierczynski, B. I. Craciun, and R. Teodorescu, “Sizing of an energy storage system for grid inertial response and primary frequency reserve,” *IEEE Trans. Power Syst.*, vol. 31, no. 5, pp. 3447–3456, 2016.

[30] A. D. Del Rosso and S. W. Eckroad, “Energy storage for relief of transmission congestion,” *IEEE Trans. Smart Grid*, vol. 5, no. 2, pp. 1138–1146, 2014.

[31] S. Agnew and P. Dargusch, “Consumer preferences for household-level battery energy storage,” *Renew. Sustain. Energy Rev.*, vol. 75, pp. 609–617, 2017.

[32] S. Hambridge, A. Q. Huang, and N. Lu, “Proposing a Frequency Based Real-Time Energy Market and Economic Dispatch Strategy,” *IEEE Power Energy Soc. Gen. Meet.*, pp. 1–5, 2016.

[33] S. Hambridge, A. Q. Huang, and R. Yu, “Solid State Transformer (SST) as an energy router: Economic dispatch based energy routing strategy,” *2015 IEEE Energy Convers. Congr.*

Expo., pp. 2355–2360, 2015.

[34] K. Huq and M. Baran, "An Energy Management System for a community energy storage system," *2012 IEEE Energy Convers. Congr. Expo*, pp. 2759–2763, 2012.

[35] X. Zhu, J. Yan, and N. Lu, "A Graphical Performance-Based Energy Storage Capacity Sizing Method for High Solar Penetration Residential Feeders," *IEEE Trans. Smart Grid*, vol. 8, no. 1, pp. 3–12, 2017.

[36] M. B. Shadmand, S. Member, R. S. Balog, and S. Member, "Multi-Objective Optimization and Design of Photovoltaic-Wind Hybrid System for Community Smart DC Microgrid," *IEEE Trans. Smart Grid*, vol. 5, no. 5, pp. 2635–2643, 2014.

[37] J. K. Kaldellis, D. Zafirakis, and E. Kondili, "Optimum sizing of photovoltaic-energy storage systems for autonomous small islands," *Int. J. Electr. Power Energy Syst.*, vol. 32, no. 1, pp. 24–36, 2010.

[38] Y. V. Makarov, P. Du, M. C. W. Kintner-Meyer, C. Jin, and H. F. Illian, "Sizing energy storage to accommodate high penetration of variable energy resources," *IEEE Trans. Sustain. Energy*, vol. 3, no. 1, pp. 34–40, 2012.

[39] I. A. G. Wilson, P. G. McGregor, D. G. Infield, and P. J. Hall, "Grid-connected renewables, storage and the UK electricity market," *Renew. Energy*, vol. 36, no. 8, pp. 2166–2170, 2011.

[40] D. T. Swift-Hook, "Grid-connected intermittent renewables are the last to be stored," *Renew. Energy*, vol. 35, no. 9, pp. 1967–1969, 2010.

[41] J. K. Kaldellis, D. Zafirakis, and E. Kondili, "Optimum sizing of photovoltaic-energy storage systems for autonomous small islands," *Int. J. Electr. Power Energy Syst.*, vol. 32, no. 1, pp. 24–36, 2010.

[42] J. Mitra, "Reliability-based sizing of backup storage," *IEEE Trans. Power Syst.*, vol. 25, no.

2, pp. 1198–1199, 2010.

[43] E. Telaretti and L. Dusonchet, “Battery storage systems for peak load shaving applications: Part 1: Operating strategy and modification of the power diagram,” *EEEIC 2016 - Int. Conf. Environ. Electr. Eng.*, 2016.

[44] J. Mitra and M. R. Vallem, “Determination of storage required to meet reliability guarantees on island-capable microgrids with intermittent sources,” *IEEE Trans. Power Syst.*, vol. 27, no. 4, pp. 2360–2367, 2012.

[45] P. D. Brown, J. A. Peças Lopes, and M. A. Matos, “Optimization of pumped storage capacity in an isolated power system with large renewable penetration,” *IEEE Trans. Power Syst.*, vol. 23, no. 2, pp. 523–531, 2008.

[46] A. W. T. Simpkins, D. Cutler, K. Andersion, D. Olis, E. Elgqvist, M. Callahan, “REopt: A Platform for Energy System Integration and Optimization,” *Natl. Renew. Energy Lab.*, pp. 1–10, 2014.

[47] Y. M. Atwa and E. F. El-Saadany, “Optimal allocation of ESS in distribution systems with a high penetration of wind energy,” *IEEE Trans. Power Syst.*, vol. 25, no. 4, pp. 1815–1822, 2010.

[48] F. Marra, G. Yang, C. Træholt, J. Østergaard, and E. Larsen, “A decentralized storage strategy for residential feeders with photovoltaics,” *IEEE Trans. Smart Grid*, vol. 5, no. 2, pp. 974–981, 2014.

[49] Y. Wang, X. Lin, and M. Pedram, “Adaptive control for energy storage systems in households with photovoltaic modules,” *IEEE Trans. Smart Grid*, vol. 5, no. 2, pp. 992–1001, 2014.

[50] Y. Wang, S. Member, X. Lin, S. Member, M. Pedram, and A. Integrating, “A Near-Optimal

Model-Based Control Algorithm for Households Equipped With Residential Photovoltaic Power Generation and Energy Storage Systems," *IEEE Trans. Sustain. Energy*, vol. 7, no. 1, pp. 1–10, 2015.

[51] R. Sioshansi, S. H. Madaeni, and P. Denholm, "A dynamic programming approach to estimate the capacity value of energy storage," *IEEE Trans. Power Syst.*, vol. 29, no. 1, pp. 395–403, 2014.

[52] D. K. Maly, "Optimal battery energy storage system (BESS) charge scheduling with dynamic programming," *IEE Proc. Sci. Meas. Technol.*, vol. 142, no. 6, p. 453, 1995.

[53] C. H. Lo and M. D. Anderson, "Economic dispatch and optimal sizing of battery energy storage systems in utility load-leveling operations," *IEEE Trans. Energy Convers.*, vol. 14, no. 3, pp. 824–829, 1999.

[54] H. Oh, "Optimal planning to include storage devices in power systems," *IEEE Trans. Power Syst.*, vol. 26, no. 3, pp. 1118–1128, 2011.

[55] D. P. Bertsekas, Dynamic Programming and Optimal Control, vol. I. 2007.

[56] D. P. Bertsekas, "Dynamic Programming and Optimal Control 3rd Edition , Volume II by Chapter 6 Approximate Dynamic Programming Approximate Dynamic Programming," *Control*, vol. II, pp. 1–200, 2010.

[57] Q. Wei, G. Shi, R. Song, and Y. Liu, "Adaptive Dynamic Programming-Based Optima Control Scheme for Energy Storage Systems With Solar Renewable Energy," *IEEE Trans. Ind. Electron.*, vol. 64, no. 7, pp. 1–1, 2017.

[58] R. M. Vignali, F. Borghesan, L. Piroddi, M. Strelec, and M. Prandini, "Energy Management of a Building Cooling System With Thermal Storage: An Approximate Dynamic Programming Solution," *IEEE Trans. Autom. Sci. Eng.*, vol. 14, no. 2, pp. 619–633, 2017.

[59] G. Carpinelli and F. Mottola, “Optimal allocation of dispersed generators, capacitors and distributed energy storage systems in distribution networks,” *Mod. Electr. Power Syst. (MEPS), 2010 Proc. Int. Symp.*, pp. 1–6, 2010.

[60] S. Kahrobaee, S. Asgarpoor, and W. Qiao, “Optimum Sizing of Distributed Generation and Storage Capacity in Smart Households,” *IEEE Trans. Smart Grid*, vol. 4, no. 4, pp. 1791–1801, 2013.

[61] Y. Zheng, Z. Y. Dong, F. J. Luo, K. Meng, J. Qiu, and K. P. Wong, “Optimal allocation of energy storage system for risk mitigation of discos with high renewable penetrations,” *IEEE Trans. Power Syst.*, vol. 29, no. 1, pp. 212–220, 2014.

[62] B. J. Donnellan, D. J. Vowles, and W. L. Soong, “A Review of Energy Storage and its Application in Power Systems,” *Aust. Univrtsities Power Eng. Conf.*, 2015.

[63] R. H. Byrne, T. A. Nguyen, D. A. Copp, B. R. Chalamala, and I. Gyuk, “Energy Management and Optimization Methods for Grid Energy Storage Systems,” *IEEE Access*, vol. 6, pp. 13231–13260, 2017.

[64] W. Su, S. Member, H. R. Eichi, and S. Member, “A Survey on the Electrification of Transportation in a Smart Grid Environment,” *IEEE Trans. Ind. Electron.*, vol. 8, no. 1, pp. 1–10, 2012.

[65] M. Muratori, “Impact of uncoordinated plug-in electric vehicle charging on residential power demand,” *Nat. Energy*, vol. 3, no. 3, pp. 193–201, 2018.

[66] U.S. Department of Energy, “Plug-In Electric Vehicle Handbook for Workplace Charging Hosts,” pp. 1–20, 2013.

[67] L. Liu, F. Kong, X. Liu, Y. Peng, and Q. Wang, “A review on electric vehicles interacting with renewable energy in smart grid,” *Renew. Sustain. Energy Rev.*, vol. 51, pp. 648–661,

2015.

[68] T. Bhattacharya, V. S. Giri, K. Mathew, and L. Umanand, “Multiphase Bidirectional Flyback Converter Topology for Hybrid Electric Vehicles,” *IEEE Trans. Ind. Electron.*, vol. 56, no. 1, pp. 78–84, 2009.

[69] R. Patil, J. Kelly, H. Fathy, and Z. Filipi, “Plug-in HEV charging for maximum impact of wind energy on reduction of CO2 emissions in propulsion,” *2012 IEEE Int. Electr. Veh. Conf. IEVC 2012*, 2012.

[70] E. Sortomme *et al.*, “Coordinated Charging of Plug-In Hybrid Electric Vehicles to Minimize Distribution System Losses,” *IEEE Trans. Smart Grid*, vol. 2, no. 1, pp. 198–205, 2011.

[71] C. Sabillon, O. Melgar Dominguez, J. Franco, M. Lavorato, and M. J. Rider, “Volt-VAr Control and Energy Storage Device Operation to Improve the Electric Vehicle Charging Coordination in Unbalanced Distribution Networks,” *IEEE Trans. Sustain. Energy*, vol. 3029, no. 2, pp. 1–1, 2017.

[72] W. Su, S. Member, and M. Chow, “An Intelligent Energy Management System for PHEVs Considering Demand Response,” *FREEDM Annual. Conf.*, pp. 1–6.

[73] F. Hafiz, P. Fajri, and I. Husain, “Effect of brake power distribution on dynamic programming technique in plug-in series hybrid electric vehicle control strategy,” *2015 IEEE Energy Convers. Congr. Expo.(ECCE), 2015*, pp. 100–105, 2015.

[74] M. O. Badawy, “Power Flow Management of a Grid Tied PV-Battery Powered Fast Electric Vehicle Charging Station,” pp. 4959–4966, 2015.

[75] M. Zeraati, M. E. H. Golshan, and J. M. Guerrero, “A Consensus-Based Cooperative Control of PEV Battery and PV Active Power Curtailment for Voltage Regulation in Distribution Networks,” *IEEE Trans. Smart Grid*, 2017.

[76] A. S. A. Awad, M. F. Shaaban, T. H. M. El-Fouly, E. F. El-Saadany, and M. M. A. Salama, "Optimal Resource Allocation and Charging Prices for Benefit Maximization in Smart PEV-Parking Lots," *IEEE Trans. Sustain. Energy*, vol. 8, no. 3, pp. 906–915, 2017.

[77] E. Ela *et al.*, "Impacts of Variability and Uncertainty in Solar Photovoltaic Generation at Multiple Timescales Impacts of Variability and Uncertainty in Solar Photovoltaic Generation at Multiple Timescales," *Natl. Renew. Energy Lab.*

[78] P. Kou, D. Liang, L. Gao, and F. Gao, "Stochastic Coordination of Plug-In Electric Vehicles and Wind Turbines in Microgrid: A Model Predictive Control Approach," *IEEE Trans. Smart Grid*, vol. 7, no. 3, pp. 1537–1551, 2016.

[79] D. T. Nguyen and L. B. Le, "Joint optimization of electric vehicle and home energy scheduling considering user comfort preference," *IEEE Trans. Smart Grid*, vol. 5, no. 1, pp. 188–199, 2014.

[80] L. Jian, H. Xue, G. Xu, X. Zhu, D. Zhao, and Z. Y. Shao, "Regulated charging of plug-in hybrid electric vehicles for minimizing load variance in household smart microgrid," *IEEE Trans. Ind. Electron.*, vol. 60, no. 8, pp. 3218–3226, 2013.

[81] A. Alahyari, M. Fotuhi-Firuzabad, and M. Rastegar, "Incorporating Customer Reliability Cost in PEV Charge Scheduling Schemes Considering Vehicle-to-Home Capability," *IEEE Trans. Veh. Technol.*, vol. 64, no. 7, pp. 2783–2791, 2015.

[82] X. Wang and Q. Liang, "Energy Management Strategy for Plug-In Hybrid Electric Vehicles via Bidirectional Vehicle-to-Grid," *IEEE Syst. J.*, vol. PP, no. 99, pp. 1–10, 2015.

[83] F. Hafiz, A. R. Queiroz, and I. Husain, "Solar Generation, Storage, and Plug-in Electric Vehicles in Power Grids: Challenges and Solutions with Coordinated Control at the Residential Level," *IEEE Electrification Magazine*, vol. 6, no. 4, pp. 83-90, Dec. 2018.

[84] F. Khoucha *et al.*, "Integrated Energy Management of a Plug-in Electric Vehicle in Residential Distribution Systems with Renewables Integrated Energy Management of a Plug-in Electric Vehicle in Residential Distribution Systems with Renewables," *2015 IEEE 24th Int. Symp. Ind. Electron.*, pp. 717–722, 2015.

[85] A. Bedir, B. Ozpineci, and J. E. Christian, "The impact of plug-in hybrid electric vehicle interaction with energy storage and solar panels on the grid for a zero energy house," *Transm. Distrib. Conf. Expo. 2010 IEEE PES*, pp. 7–12, 2010.

[86] X. Wu, X. Hu, S. Moura, X. Yin, and V. Pickert, "Stochastic control of smart home energy management with plug-in electric vehicle battery energy storage and photovoltaic array," *J. Power Sources*, vol. 333, pp. 203–212, 2016.

[87] J. Soares, B. Canizes, M. A. F. Ghazvini, Z. Vale, and G. K. Venayagamoorthy, "Two-Stage Stochastic Model Using Benders' Decomposition for Large-Scale Energy Resource Management in Smart Grids," *IEEE Trans. Ind. Appl.*, vol. 53, no. 6, pp. 5905–5914, 2017.

[88] A. Kavousi-Fard, T. Niknam, and M. Fotuhi-Firuzabad, "Stochastic Reconfiguration and Optimal Coordination of V2G Plug-in Electric Vehicles Considering Correlated Wind Power Generation," *IEEE Trans. Sustain. Energy*, vol. 6, no. 3, pp. 822–830, 2015.

[89] P. Tian, X. Xiao, K. Wang, and R. Ding, "A Hierarchical Energy Management System Based on Hierarchical Optimization for Microgrid Community Economic Operation," *IEEE Trans. Smart Grid*, vol. 7, no. 5, pp. 2230–2241, 2016.

[90] W. Tushar *et al.*, "Energy Storage Sharing in Smart Grid: A Modified Auction Based Approach," *IEEE Trans. Smart Grid*, vol. 7, no. 3, pp. 1462–1475, 2016.

[91] C. P. Mediwaththe, S. Member, E. R. Stephens, and D. B. Smith, "A Dynamic Game for Electricity Load Management in Neighborhood Area Networks," *IEEE Trans. Smart Grid*,

vol. 7, no. 3, pp. 1–8, 2016.

[92] M. J. E. Alam, K. M. Muttaqi, and D. Sutanto, “Community Energy Storage for Neutral Voltage Rise Mitigation in Four-Wire Multigrounded LV Feeders with Unbalanced Solar PV Allocation,” *IEEE Trans. Smart Grid*, vol. 6, no. 6, pp. 2845–2855, 2015.

[93] G. Ye, G. Li, D. Wu, X. Chen, and Y. Zhou, “Towards Cost Minimization with Renewable Energy Sharing in Cooperative Residential Communities,” *IEEE Access*, vol. 5, 2017.

[94] D. Kalathil, C. Wu, K. Poolla, and P. Varaiya, “The Sharing Economy for the Electricity Storage,” *IEEE Trans. Smart Grid*, 2017.

[95] I. S. Bayram, M. Abdallah, S. Member, A. Tajer, and K. A. Qaraqe, “A Stochastic Sizing Approach for Sharing-Based Energy Storage Applications,” *IEEE Trans. Smart Grid*, vol. 8, no. 3, pp. 1075–1084, 2017.

[96] S. El-batway, S. Member, W. G. Morsi, and S. Member, “Optimal Design of Community Battery Energy Storage Systems with Prosumers Owning Electric Vehicles,” *IEEE Trans. Ind. Informatics*, 2017.

[97] N. Good and P. Mancarella, “Flexibility in multi-energy communities with electrical and thermal storage: A stochastic, robust approach for multi-service demand response,” *IEEE Trans. Smart Grid*, vol. In Press, 2017.

[98] S. Hashemi, J. Ostergaard, and G. Yang, “A scenario-based approach for energy storage capacity determination in LV grids with high PV penetration,” *IEEE Trans. Smart Grid*, vol. 5, no. 3, pp. 1514–1522, 2014.

[99] K. Baker, G. Hug, and X. Li, “Energy Storage Sizing Taking Into Account Forecast Uncertainties and Receding Horizon Operation,” *IEEE Trans. Sustain. Energy*, vol. 8, no. 1, pp. 331–340, 2017.

[100] H. Shareef, M. S. Ahmed, A. Mohamed, and E. Al Hassan, “Review on Home Energy Management System Considering Demand Responses, Smart Technologies, and Intelligent Controllers,” *IEEE Access*, vol. 6, pp. 24498–24509, 2018.

[101] S. L. Arun and M. P. Selvan, “Dynamic demand response in smart buildings using an intelligent residential load management system,” *IET Gener. Transm. Distrib.*, vol. 11, no. 17, pp. 4348–4357, 2017.

[102] D. Jay and K. S. Swarup, “Price Based Demand Response of Aggregated Thermostatically Controlled Loads For Load Frequency Control,” vol. 2, no. 1, pp. 2–6.

[103] D. Wang *et al.*, “A demand response and battery storage coordination algorithm for providing microgrid Tie-Line smoothing services,” *IEEE Trans. Sustain. Energy*, vol. 5, no. 2, pp. 476–486, 2014.

[104] F. Wang, L. Zhou, H. Ren, X. Liu, M. Shafie-khah, and J. P. S. Catalão, “Multi-objective optimization model of source-load-storage synergetic dispatch for building energy system based on tou price demand response,” *2017 IEEE Ind. Appl. Soc. Annu. Meet. IAS 2017*, vol. 2017–Janua, no. 2, pp. 1–10, 2017.

[105] H. Huang, F. Li, and Y. Mishra, “Modeling Dynamic Demand Response Using Monte Carlo Simulation and Interval Mathematics for Boundary Estimation,” *IEEE Trans. Smart Grid*, vol. 6, no. 6, pp. 2704–2713, 2015.

[106] S. R. Konda, B. Mukkapati, L. K. Panwar, B. K. Panigrahi, and R. Kumar, “Dynamic Energy Balancing Cost Model for Day Ahead Markets with Uncertain Wind Energy and Generation Contingency under Demand Response,” *IEEE Trans. Ind. Appl.*, vol. 54, no. 5, pp. 4908–4916, 2018.

[107] C. Chen, J. Wang, and S. Kishore, “A distributed direct load control approach for large-

scale residential demand response," *IEEE Trans. Power Syst.*, vol. 29, no. 5, pp. 2219–2228, 2014.

[108] J. Medina, N. Muller, and I. Roytelman, "Demand response and distribution grid operations: Opportunities and challenges," *IEEE Trans. Smart Grid*, vol. 1, no. 2, pp. 193–198, 2010.

[109] W. Zheng, W. Wu, B. Zhang, and W. Sheng, "Distributed Optimal residential demand response considering the operational constraints of unbalanced distribution networks," *IET Gener. Transm. Distrib.*, vol. 12, no. 9, pp. 1970–1979, 2018.

[110] A. L. A. Syrri and P. Mancarella, "Reliability and risk assessment of post-contingency demand response in smart distribution networks," *Sustain. Energy, Grids Networks*, vol. 7, pp. 1–12, 2016.

[111] D. T. Ton and W.-T. P. Wang, "A More Resilient Grid," *IEEE Power Energy Mag.*, vol. 13, no. 3, pp. 26–34, 2015.

[112] A. Gholami and F. Aminifar, "A Hierarchical Response-Based Approach to the Load Restoration Problem," *IEEE Trans. Smart Grid*, vol. 8, no. 4, pp. 1700–1709, 2017.

[113] F. Wang *et al.*, "A multi-stage restoration method for medium-voltage distribution system with DGs," *IEEE Trans. Smart Grid*, vol. 8, no. 6, pp. 2627–2636, 2017.

[114] C. P. Nguyen and A. J. Flueck, "Agent based restoration with distributed energy storage support in smart grids," *IEEE Trans. Smart Grid*, vol. 3, no. 2, pp. 1029–1038, 2012.

[115] Y. J. Kim, J. Wang, and X. Lu, "A Framework for Load Service Restoration Using Dynamic Change in Boundaries of Advanced Microgrids with Synchronous-Machine DGs," *IEEE Trans. Smart Grid*, vol. 9, no. 4, pp. 3676–3690, 2018.

[116] M. R. Kleinberg, K. Miu, and H. D. Chiang, "Improving service restoration of power distribution systems through load curtailment of in-service customers," *IEEE Trans. Power*

Syst., vol. 26, no. 3, pp. 1110–1117, 2011.

[117] S. Lei, J. Wang, C. Chen, and Y. Hou, "Mobile Emergency Generator Pre-Positioning and Real-Time Allocation for Resilient Response to Natural Disasters," *IEEE Trans. Smart Grid*, vol. 9, no. 3, pp. 2030–2041, 2018.

[118] Y. Xu, C. C. Liu, K. P. Schneider, F. K. Tuffner, and D. T. Ton, "Microgrids for service restoration to critical load in a resilient distribution system," *IEEE Trans. Smart Grid*, vol. 9, no. 1, pp. 426–437, 2018.

[119] S. Ma, L. Su, Z. Wang, F. Qiu, and G. Guo, "Resilience enhancement of distribution grids against extreme weather events," *IEEE Trans. Power Syst.*, vol. 33, no. 5, pp. 4842–4853, 2018.

[120] A. Sharma, D. Kiran, and B. K. Panigrahi, "Planning the coordination of overcurrent relays for distribution systems considering network reconfiguration and load restoration," *IET Gener. Transm. Distrib.*, 2017.

[121] B. Chen, C. Chen, J. Wang, and K. L. Butler-Purry, "Sequential Service Restoration for Unbalanced Distribution Systems and Microgrids," *IEEE Trans. Power Syst.*, vol. 33, no. 2, pp. 1507–1520, 2018.

[122] W. C. Hong, Y. Dong, W. Y. Zhang, L. Y. Chen, and B. K. Panigrahi, "Cyclic electric load forecasting by seasonal SVR with chaotic genetic algorithm," *Int. J. Electr. Power Energy Syst.*, vol. 44, no. 1, pp. 604–614, 2013.

[123] Y. H. Chen, W. C. Hong, W. Shen, and N. N. Huang, "Electric load forecasting based on a least squares support vector machine with fuzzy time series and global harmony search algorithm," *Energies*, vol. 9, no. 2, pp. 1–13, 2016.

[124] G. Dudek, "Short-term load forecasting using random forests," *Adv. Intell. Syst. Comput.*,

vol. 323, pp. 821–828, 2015.

[125] A. S. Ahmad *et al.*, “A review on applications of ANN and SVM for building electrical energy consumption forecasting,” *Renew. Sustain. Energy Rev.*, vol. 33, pp. 102–109, 2014.

[126] W. Kong, Z. Y. Dong, D. J. Hill, F. Luo, and Y. Xu, “Short-Term Residential Load Forecasting based on Resident Behaviour Learning,” *IEEE Trans. Power Syst.*, vol. 33, no. 1, pp. 1–1, 2017.

[127] J. Bedi and D. Toshniwal, “Empirical Mode Decomposition Based Deep Learning for Electricity Demand Forecasting,” *IEEE Access*, vol. 6, pp. 49144–49156, 2018.

[128] F. Conte, S. Massucco, M. Saviozzi, and F. Silvestro, “A Stochastic Optimization Method for Planning and Real-Time Control of Integrated PV-Storage Systems: Design and Experimental Validation,” *IEEE Trans. Sustain. Energy*, vol. 9, no. 3, pp. 1188–1197, 2018.

[129] H. Geramifar, M. Shahabi, and T. Barforoshi, “Coordination of energy storage systems and DR resources for optimal scheduling of microgrids under uncertainties,” *IET Renew. Power Gener.*, vol. 11, no. 2, pp. 378–388, 2017.

[130] M. Nistor and C. H. Antunes, “Integrated management of energy resources in residential buildings — A Markovian approach,” *IEEE Trans. Smart Grid*, vol. 9, no. 1, pp. 240–251, 2018.

[131] T. Li and M. Dong, “Real-time energy storage management: Finite-time horizon approach,” *IEEE J. Sel. Areas Commun.*, vol. 33, no. 12, pp. 2524–2539, 2015.

[132] T. Li and M. Dong, “Real-Time Joint Energy Storage Management and Load Scheduling with Renewable Intigration,” *IEEE Trans. Smart Grid*, vol. 9, no. 1, pp. 283–298, 2016.

[133] C. K. Chau, G. Zhang, and M. Chen, “Cost Minimizing Online Algorithms for Energy Storage Management With Worst-Case Guarantee,” *IEEE Trans. Smart Grid*, vol. 7, no. 6,

pp. 2691–2702, 2016.

[134] K. Rahbar, J. Xu, and R. Zhang, "Real-time energy storage management for renewable integration in microgrid: An off-line optimization approach," *IEEE Trans. Smart Grid*, vol. 6, no. 1, pp. 124–134, 2015.

[135] K. Rahbar, C. C. Chai, R. Zhang, and S. Member, "Energy Cooperation Optimization in Microgrids with Renewable Energy Integration," *IEEE Trans. Smart Grid*, vol. 9, no. 2, pp. 1482–1493, 2016.

[136] W. Wetekamp, "Net present value (NPV) as a tool supporting effective project management," in *Proc. o 6th IEEE International Conference on Intelligent Data Acquisition and Advanced Computing Systems: Technology and Applications, IDAACS'2011*, 2011, vol. 2, no. September, pp. 898–900.

[137] F. Hafiz, D. Lubkeman, and I. Husain, "Energy Storage Management Strategy Based on Dynamic Programming and Optimal Sizing of PV Panel-Storage Capacity for a Residential System," in *IEEE Transmission and Distribution Symposium*, 2018.

[138] F. Hafiz, P. Fajri, and I. Husain, "Load regulation of a smart household with PV-storage and electric vehicle by dynamic programming successive algorithm technique," *IEEE Power Energy Soc. Gen. Meet.*, vol. 2016–Novem, 2016.

[139] F. Hafiz, A. R. De Queiroz, and I. Husain, "Multi-stage Stochastic Optimization for a PV-Storage Hybrid Unit in a Household," in Proc. *IEEE Industrial Application Society Annual Meeting*, 2017.

[140] M. V. F. Pereira and L. M. V. G. Pinto, "Multi-stage stochastic optimization applied to energy planning," *Math. Program.*, vol. 52, no. 1–3, pp. 359–375, 1991.

[141] F. Hafiz, A. R. De Quieroz, and I. Husain, "Charge Scheduling of a Plug-in Electric Vehicle

Considering Load Demand Uncertainty based on Multi-stage Stochastic Optimization," in *North American Power Symposium 2017, NAPS*, 2017.

[142] D. Srinivasan and S. Gundam, "Correlation analysis of solar power and electric demand," *2013 Int. Conf. Renew. Energy Sustain. Energy*, pp. 221–226, 2013.

[143] F. Hafiz, A. R. De Queiroz, and I. Husain, "Co-ordinated Control of PEV and PV-based Storage System under PV generation and Load Uncertainty," *in Proc. IEEE Industrial Application Society Annual Meeting*, 2018.

[144] F. Hafiz, A. R. De Queiroz, I. Husain, and P. Fajri, "Energy Management For a Community Storage System : A Multi-stage Stochastic Optimization Approach," *Applied Energy*, vol. 236, pp. 42-54, Feb. 2019

[145] F. Hafiz, B. Chen, C. Chen, A. R. De Queiroz, and I. Husain, "Utilizing Demand Response for Distribution Service Restoration to Achieve Grid Resiliency against Natural Disasters," *submitted*, pp. 1–10, 2018.

[146] F. Hafiz, MA Awal, A. R. Queiroz, and I. Husain, "Real-Time Energy Management in Hybrid Residential Unit Considering the Uncertainties of Load and Solar Generation on Forecast," *submitted*, pp. 1–10, 2018.

[147] "Household load profile." [Online]. Available: https://www.pge.com/.

[148] "Solar Resource & Meteorological Assessment Project (SOLRMAP)." [Online]. Available: www.nrel.gov/midc/lmu/.

[149] N. S. Jayalakshmi, D. N. Gaonkar, S. Adarsh, and S. Sunil, "A control strategy for power management in a PV-battery hybrid system with MPPT," in *1st IEEE International Conference on Power Electronics, Intelligent Control and Energy Systems, ICPEICES* 2017, pp. 1–6.

[150] “Institute of Renewable Energy Agency (IRENA).” [Online]. Available: www.irena.org/documentdownloads/publications/irena_battery_storage_report_2015.pdf.

[151] “U.S. solar market insight 2017 report (SEIA).” [Online]. Available: www.seia.org/research-resources/solar-market-insight-report-2017-q2.

[152] A. M. Law and W. D. Kelton, “Simulation Modeling and Analysis,” *Acm Trans. Model. Comput. Simul.*, vol. 2, no. 2, pp. 1370–1375, 2000.

[153] A. R. De Queiroz, “Stochastic hydro-thermal scheduling optimization: An overview,” *Renew. Sustain. Energy Rev.*, vol. 62, pp. 382–395, 2016.

[154] A. R. De Queiroz and D. P. Morton, “Sharing cuts under aggregated forecasts when decomposing multi-stage stochastic programs,” *Oper. Res. Lett.*, vol. 41, no. 3, pp. 311–316, 2013.

[155] “ToU Rate.” [Online]. Available: www.pge.com.

[156] S. R. Silva, A. R. De Queiroz, L. M. M. Lima, and J. W. M. Lima, “Effects of wind penetration in the scheduling of a hydro-dominant power system,” *IEEE Power Energy Soc. Gen. Meet.*, vol. 2014–Octob, no. October, 2014.

[157] “Load Profiles.” [Online]. Available: www.pecanstreet.org.

[158] B. Wang, M. Sechilariu, and F. Locment, “Intelligent DC microgrid with smart grid communications: Control strategy consideration and design,” *IEEE Trans. Smart Grid*, vol. 3, no. 4, pp. 2148–2156, 2012.

[159] J. Coughlin *et al.*, “A Guide to Community Shared Solar: Utility , Private , and Nonprofit Project Development,” *Natl. Renew. Energy Lab. (NREL), Tech. Rep.*, pp. 1–68, 2012.

[160] “IEEE PES Distribution Test Feeders.” [Online]. Available: www.ewh.ieee.org/soc/pes/dsacom/testfeeders/index.html.

[161] F. A. Gers, N. N. Schraudolph, and J. Schmidhuber, “Learning Precise Timing with LSTM Recurrent Network,” *J. Mach. Learn. Res.*, vol. 3, pp. 115–143, 2002.

APPENDIX

Appendix A

TABLE I
TOU RATE 1

Season	Load Type	Period	*ToU* Rate ($/kWh)
Summer (June-September)	Off-Peak	9:00 PM-9:00 AM	0.15
	Partial Peak	10:00 AM-1:00 PM & 7:00 PM-9:00PM	0.226
	Peak	1:00 PM- 7:00 PM	0.342
Winter (October-May)	Off-Peak	8:00 PM-5:00 PM	0.15
	Peak	5:00 PM – 8:00 PM	0.171

TABLE II
TOU RATE 2

Season	Load Type	Period	*ToU* Rate ($/kWh)
Summer (June-September)	Off-Peak	10:00PM-11:00 AM	0.009
	Peak	11:00 AM-10:00 PM	0.0927
Winter (October-May)	Off-Peak	11:00 AM-5:00 PM & 10:00 PM-7:00AM	0.009
	Peak	7:00 AM–11:00 AM & 5:00 PM – 9:00 PM	0.0927